Toward incorporating organized eddy structures in the modelling of wall-bounded turbulence

Ivan Marusic

Department of Mechanical Engineering
University of Melbourne, Australia

Outline

- Introduction
- Review of Townsend/Perry view of eddies and turbulence
- Approaches for using organized eddy concepts for modelling
- Inner and outer region interactions - prospects for modelling

Turbulent Boundary Layer

(Flow visualization using *Al* flakes in water channel: Cantwell *et al*)

Flow direction

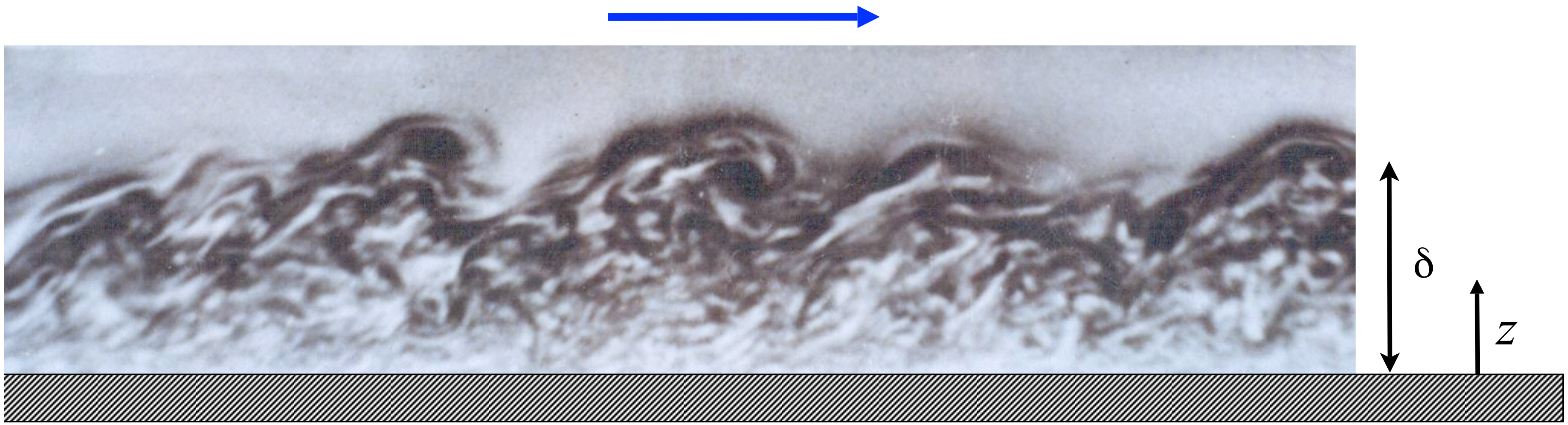

$$U^+ = U/U_\tau\,;\; z^+ = zU_\tau/\nu$$

$$\frac{\partial U}{\partial x} + \frac{\partial W}{\partial z} = 0$$

$$U\frac{\partial U}{\partial x} + W\frac{\partial U}{\partial z} = -\frac{1}{\rho}\frac{\mathrm{d}p_1}{\mathrm{d}x} + \frac{1}{\rho}\frac{\partial \tau}{\partial z},$$

$$\frac{\tau}{\rho} = -\overline{u_1 u_3} + \nu\frac{\partial U}{\partial z}, \qquad \frac{\tau}{\rho} = (\nu_T + \nu)\,\frac{\partial U}{\partial z}$$

$$\nu_T = -\overline{u_1 u_3}\left(\frac{\partial U}{\partial z}\right)^{-1}$$

$$\nu_T = -\overline{u_1 u_3}\left(\frac{\partial U}{\partial z}\right)^{-1} \qquad\qquad \nu = \frac{\tau_L}{\rho}\left(\frac{\partial U}{\partial z}\right)^{-1}$$

$$\nu_T = -\overline{u_1 u_3}\left(\frac{\partial U}{\partial z}\right)^{-1} \qquad \nu = \frac{\tau_L}{\rho}\left(\frac{\partial U}{\partial z}\right)^{-1}$$

$$\frac{\nu_T}{(\delta U_\tau)} = \text{constant}$$

$$\nu_T = -\overline{u_1 u_3}\left(\frac{\partial U}{\partial z}\right)^{-1} \qquad \nu = \frac{\tau_L}{\rho}\left(\frac{\partial U}{\partial z}\right)^{-1}$$

$$\frac{\nu_T}{(\delta U_\tau)} = \text{constant}$$

$$\frac{\nu_T}{(\delta U_\tau)} = \phi\left(z/\delta\right)$$

$$\nu_T = -\overline{u_1 u_3}\left(\frac{\partial U}{\partial z}\right)^{-1} \qquad \nu = \frac{\tau_L}{\rho}\left(\frac{\partial U}{\partial z}\right)^{-1}$$

$$\frac{\nu_T}{(\delta U_\tau)} = \mathrm{constant}$$

$$\frac{\nu_T}{(\delta U_\tau)} = \phi\left(z/\delta\right)$$

$$\frac{\nu_T}{(\delta U_\tau)} = \phi\left(z/\delta, \Pi\right)$$

$$\nu_T = -\overline{u_1 u_3} \left(\frac{\partial U}{\partial z} \right)^{-1} \qquad \nu = \frac{\tau_L}{\rho} \left(\frac{\partial U}{\partial z} \right)^{-1}$$

$$\frac{\nu_T}{(\delta U_\tau)} = \phi\left(z/\delta, \Pi\right)$$

$$U^+ = f(z^+) + \Pi \; g(z/\delta)$$

$$\nu_T = -\overline{u_1 u_3}\left(\frac{\partial U}{\partial z}\right)^{-1} \qquad \nu = \frac{\tau_L}{\rho}\left(\frac{\partial U}{\partial z}\right)^{-1}$$

$$\frac{\nu_T}{(\delta U_\tau)} = \phi\left(z/\delta, \Pi\right)$$

$$(U_1 - U)^+ = f(z/\delta, \Pi)$$

$$\nu_T = -\overline{u_1 u_3}\left(\frac{\partial U}{\partial z}\right)^{-1} \qquad\qquad \nu = \frac{\tau_L}{\rho}\left(\frac{\partial U}{\partial z}\right)^{-1}$$

$$\frac{\nu_T}{(\delta U_\tau)} = \phi\left(z/\delta, \Pi\right)$$

$$(U_1 - U)^+ = f(z/\delta, \Pi)$$

$$\frac{\nu_T}{(\delta U_\tau)} = \phi\left(z/\delta, \Pi, ?\right)$$

$$U\frac{\partial U}{\partial x} + W\frac{\partial U}{\partial z} = -\frac{1}{\rho}\frac{\mathrm{d}p_1}{\mathrm{d}x} + \frac{1}{\rho}\frac{\partial \tau}{\partial z},$$

$$\frac{\partial U}{\partial x} + \frac{\partial W}{\partial z} = 0$$

$$\frac{\tau}{\rho} = -\overline{u_1 u_3} + \nu\frac{\partial U}{\partial z}$$

$$(U_1 - U)^+ = f(z/\delta, \Pi)$$

$$\boxed{\frac{\tau}{\tau_0} = f_1[\eta, \Pi, S] + g_1[\eta, \Pi, S]\zeta + g_2[\eta, \Pi, S]\beta}$$

$$\Pi, \quad S = \frac{U_1}{U_\tau}, \quad \beta = \frac{\delta^*}{\tau_0}\frac{\mathrm{d}p}{\mathrm{d}x}, \quad \zeta = S\delta\frac{\mathrm{d}\Pi}{\mathrm{d}x}.$$

$$\nu_T = -\overline{u_1 u_3} \left(\frac{\partial U}{\partial z} \right)^{-1} \qquad \nu = \frac{\tau_L}{\rho} \left(\frac{\partial U}{\partial z} \right)^{-1}$$

$$(U_1 - U)^+ = f(z/\delta, \Pi)$$

$$\frac{\nu_T}{(\delta U_\tau)} = \phi\left(z/\delta, \Pi, \beta, S, \zeta\right)$$

Non-local effects important

R_{uu}

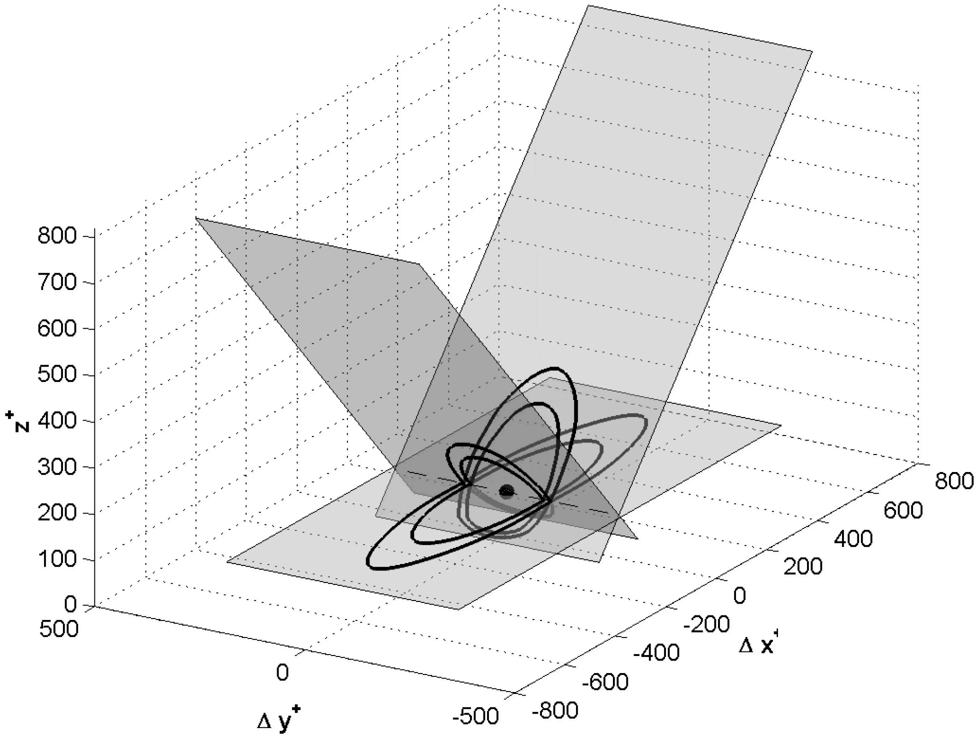

$\mathbf{z^+ = 92}$

Log region

Outer wake region

$\mathbf{z/\delta = 0.5}$

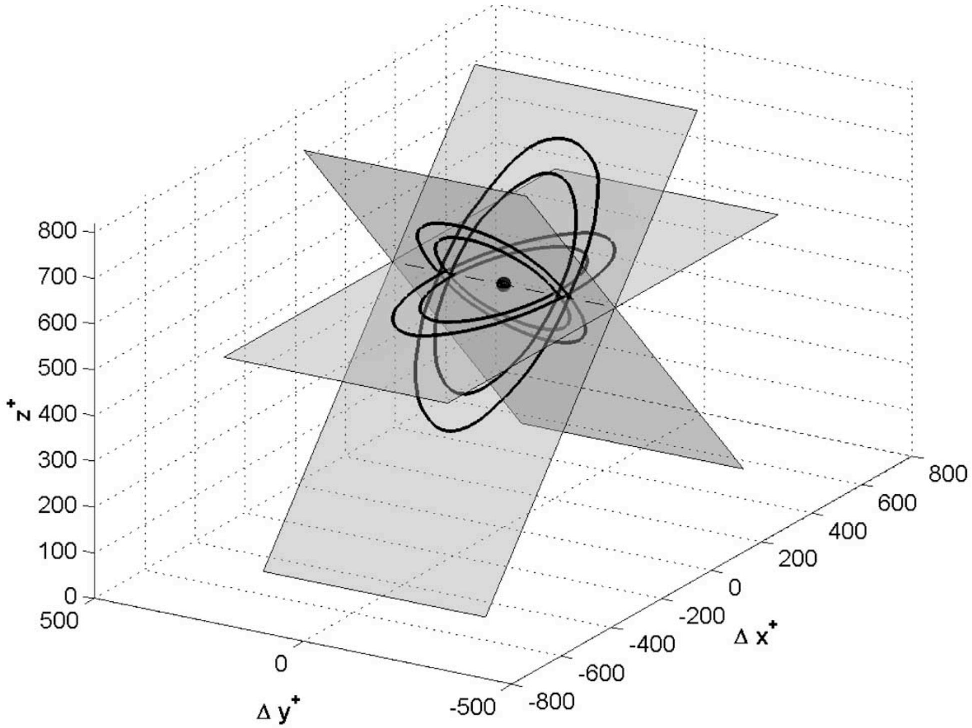

Ganapathisubramani et al (2005)

Organized Eddies/Coherent Structures and Turbulence Modelling

Alan Townsend

Tony Perry

Townsend (1987):

“Local” descriptions of turbulent flows are conceptually unsatisfactory when eddies controlling levels of transport extend over the entire flow width.

Perry et al (1994):

Rather than using exchange coefficients related to local flow variables, the layers should be looked at as an “integrated whole” with the transport properties at one point being related to motions in regions remote from the point of interest.

Townsend (1987):

Instead of assuming some form of similarity of the turbulent motion - eg. constancy of stress-intensity ratio - in all flows, the additional and varying contributions to Reynolds stresses from the organized eddies could be included and lead to better description.

Improvements in the performance of schemes for flow calculation can be made in a more rational manner from a knowledge of the organized eddies that control the flow than from empirical adjustments based on comparison of predicted and observed values of the flow parameters.

An appreciation of the mechanisms that lead to the differences in form and function of the organized eddies suggest limits to the applicability of a particular scheme to flows outside its design range.

Case study: Attached eddy model

Aim: Construct turbulence statistics given the mean-velocity field

Perry & Marusic (1995)

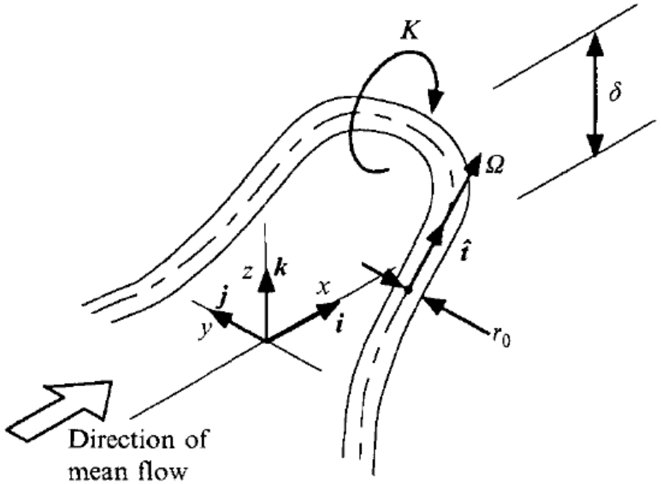

FIGURE 2. Sketch of a representative attached eddy.

$$\frac{U_0}{\delta} = \frac{K}{2\pi\delta^2} = \frac{\pi r_0^2 \Omega_0}{2\pi\delta^2} = \tfrac{1}{2} q^2 \Omega_0$$

Applying Biot-Savart integral for representative eddy (with image in wall), and using Campbell's theorem:

$$f[z/\delta] = \frac{2}{q^2}\int_{-\infty}^{\infty}\int_{-\infty}^{\infty}\frac{\Omega}{\Omega_0}\,(\hat{\boldsymbol{t}}\cdot\boldsymbol{j})\,\mathrm{d}(x/\delta)\,\mathrm{d}(y/\delta)$$

Representative eddy cross-stream vorticity distribution

$$I_{ij}[\tfrac{z}{\delta}] = \int_{-\infty}^{\infty}\int_{-\infty}^{\infty}\frac{V_i V_j}{U_0^2}\,\mathrm{d}(x/\delta)\,\mathrm{d}(y/\delta)$$

Townsend eddy intensity functions

Hierarchy of eddy scales

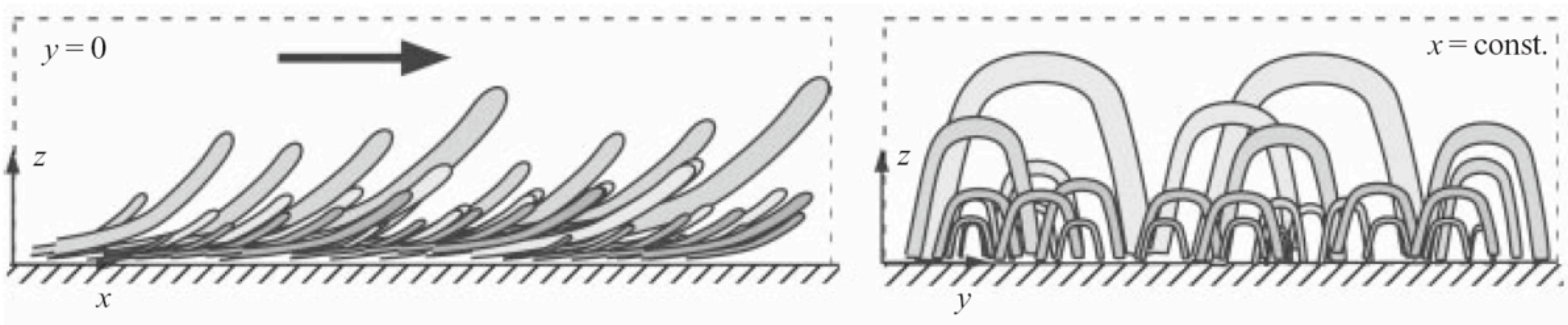

$$\frac{\mathrm{d}U/U_\tau}{\mathrm{d}z} = \int_{\delta_1}^{\delta_c} f[z/\delta]\, Q[\delta/\delta_c]\, D[\delta/\delta_c]\, \frac{1}{\delta^2}\, \mathrm{d}\delta$$

$$\frac{\overline{u_i u_j}}{U_\tau^2} = \int_{\delta_1}^{\delta_c} I_{ij}[z/\delta]\, Q^2[\delta/\delta_c]\, D[\delta/\delta_c]\, \frac{1}{\delta}\, \mathrm{d}\delta$$

$D[\delta/\delta_c]$: Measure of how the p.d.f. of eddy scales departs from a -1 power law (geometric progression)

$Q[\delta/\delta_c]$: Measure of velocity scale variation across hierarchies

$$\boxed{\begin{aligned} \frac{\mathrm{d}U_D^*}{\mathrm{d}\lambda_E} &= \int_{-\infty}^{\infty} h[\lambda]\mathrm{e}^{-\lambda}\, T[\lambda-\lambda_E]\, w[\lambda-\lambda_E]\, \mathrm{d}\lambda \\ \frac{\overline{u_i u_j}}{U_\tau^2} &= \int_{-\infty}^{\infty} J_{ij}[\lambda]\, T^2[\lambda-\lambda_E]\, w[\lambda-\lambda_E]\, \mathrm{d}\lambda \end{aligned}}$$

$$\lambda = \log[\delta/z], \quad \lambda_E = \log[\delta_c/z], \quad \lambda_1 = \log[\delta_1/z]$$

$$w[\lambda-\lambda_E] = D[\delta/\delta_c], \quad T[\lambda-\lambda_E] = Q[\delta/\delta_c], \quad h[\lambda] = f[z/\delta]$$

$$J_{ij}[\lambda] = I_{ij}[z/\delta]$$

Similarly for spectra:

$$\frac{\Phi_{ij}[k_1 z, z/\delta_c, z/\delta_1]}{U_\tau^2} = \int_{\delta_1}^{\delta_c} G_{ij}[k_1 z, z/\delta]\, Q^2[\delta/\delta_c]\, D[\delta/\delta_c] \frac{1}{\delta}\, \mathrm{d}\delta$$

$$\frac{\Psi_{ij}[\alpha_z, \lambda_E, \lambda_1]}{U_\tau^2} = \int_{-\infty}^{\infty} g_{ij}[\alpha_z, \lambda]\, T^2[\lambda - \lambda_E]\, w[\lambda - \lambda_E]\, \mathrm{d}\lambda,$$

$$\Psi_{ij}[\alpha_z, \lambda_E, \lambda_1] = k_1 z\, \Phi_{ij}[k_1 z, z/\delta_c, z/\delta_1],$$

$$g_{ij}[\alpha_z, \lambda] = k_1 z\, G_{ij}[k_1 z, z/\delta]$$

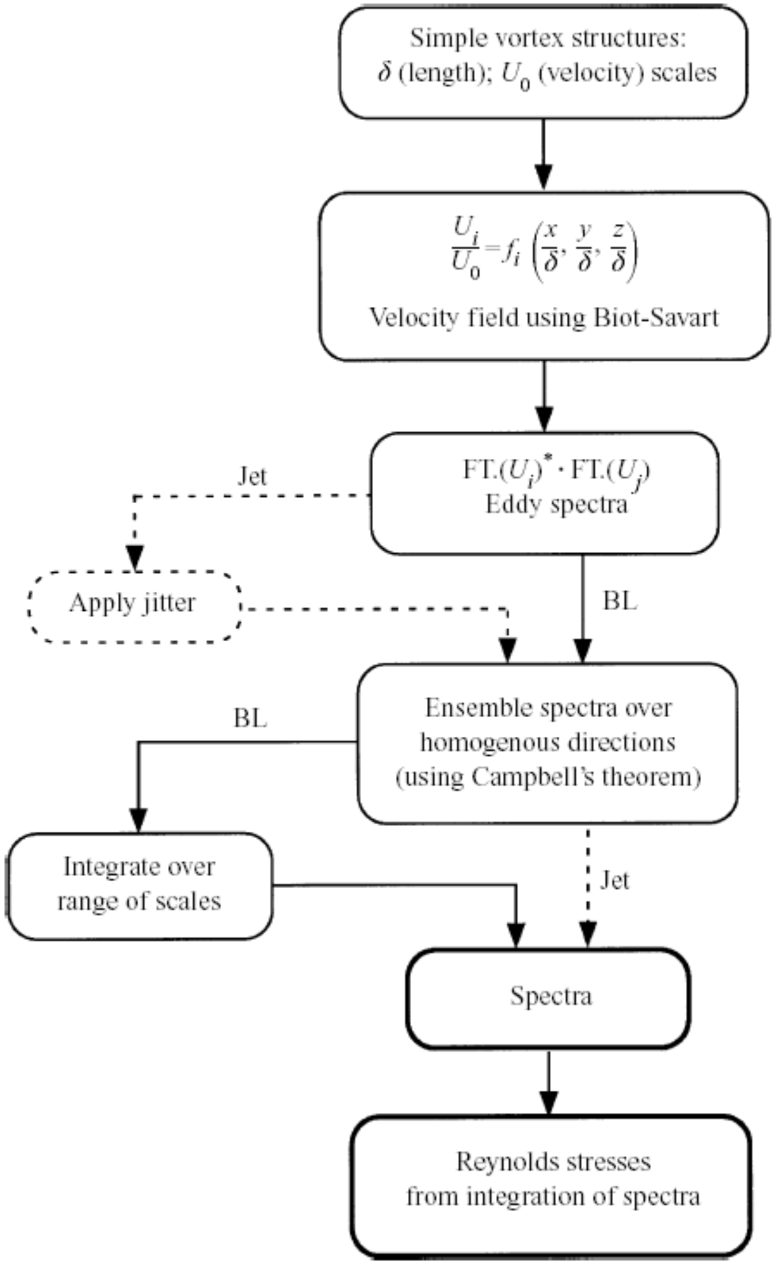

- Compute turbulence statistics (Reynolds stresses, spectra etc), given
  - – Mean-velocity flow field
  - – Equations of motion

$$\frac{\nu_T}{(\delta U_\tau)} = \frac{\int_{-\infty}^{\infty} J_{13}(\lambda)\ T^2(\lambda-\lambda_E)w(\lambda-\lambda_E)\ d\lambda}{\int_{-\infty}^{\infty} h(\lambda)e^{-\lambda}\ T(\lambda-\lambda_E)w(\lambda-\lambda_E)\ d\lambda}$$

$$\frac{\nu_T}{(\delta U_\tau)} = \frac{\int_{-\infty}^{\infty} J_{13}(\lambda)\ T^2(\lambda-\lambda_E) w(\lambda-\lambda_E)\ d\lambda}{\int_{-\infty}^{\infty} h(\lambda) e^{-\lambda}\ T(\lambda-\lambda_E) w(\lambda-\lambda_E)\ d\lambda}$$

Π*, *S*, *ζ*, *β
from experiment

$$\longrightarrow \boxed{-\frac{\overline{u_1 u_3}}{U_\tau^2} = f_1[\eta, \Pi, S] + g_1[\eta, \Pi, S]\,\zeta + g_2[\eta, \Pi, S]\,\beta}$$

$$\downarrow$$

$$\boxed{\frac{\overline{u_1 u_3}}{U_\tau^2} = \int_{-\infty}^{\infty} J_{13}[\lambda]\ T^2[\lambda-\lambda_E]\omega[\lambda-\lambda_E]\ \mathrm{d}\lambda} \longrightarrow T^2\omega$$

$$\Pi \longrightarrow \boxed{\frac{\mathrm{d}U_D^*}{\mathrm{d}\lambda_E} = \int_{-\infty}^{\infty} h[\lambda]\mathrm{e}^{-\lambda}\ T[\lambda-\lambda_E]\ w[\lambda-\lambda_E]\ \mathrm{d}\lambda,} \longrightarrow T\omega$$

$$\frac{\nu_T}{(\delta U_\tau)} = \frac{\int_{-\infty}^{\infty} J_{13}(\lambda)\ T^2(\lambda - \lambda_E) w(\lambda - \lambda_E)\ d\lambda}{\int_{-\infty}^{\infty} h(\lambda) e^{-\lambda}\ T(\lambda - \lambda_E) w(\lambda - \lambda_E)\ d\lambda}$$

Require T=1 (same velocity scale for each hierarchy) for

$$(U_1 - U)^+ = f(z/\delta, \Pi), \qquad \frac{\nu_T}{(\delta U_\tau)} = \phi\,(z/\delta, \Pi)$$

$\Rightarrow$ works for quasi-equilibrium boundary layers, self-similar jets etc

Coflowing jets

T. B. Nickels and A. E. Perry

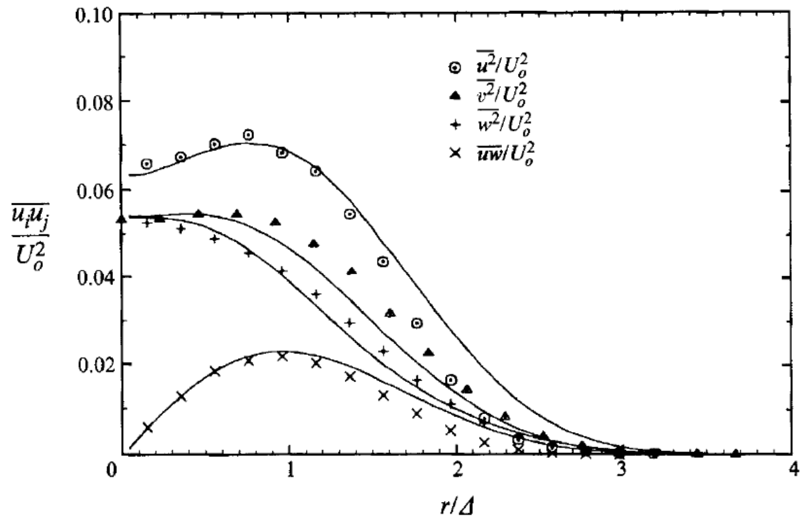

FIGURE 20. Reynolds stresses from experiment ($x/D = 30$, $\lambda_J = 2$) compared wit (solid lines).

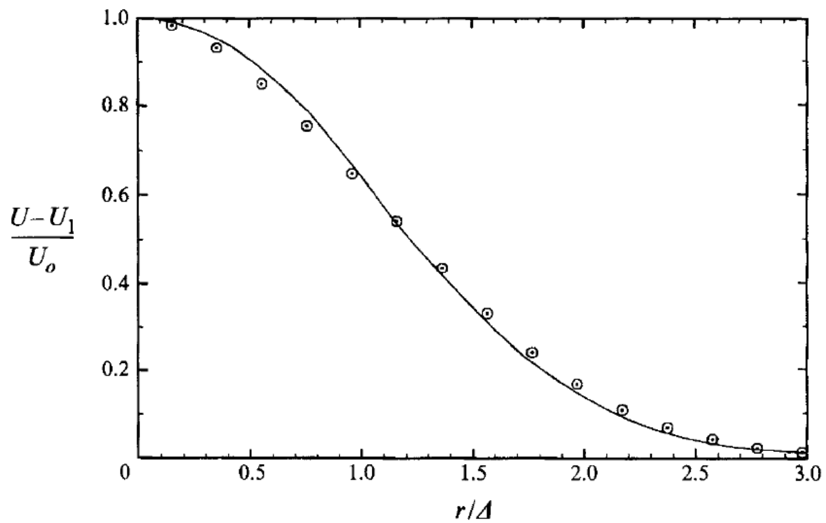

T. B. Nickels and I. Marusic

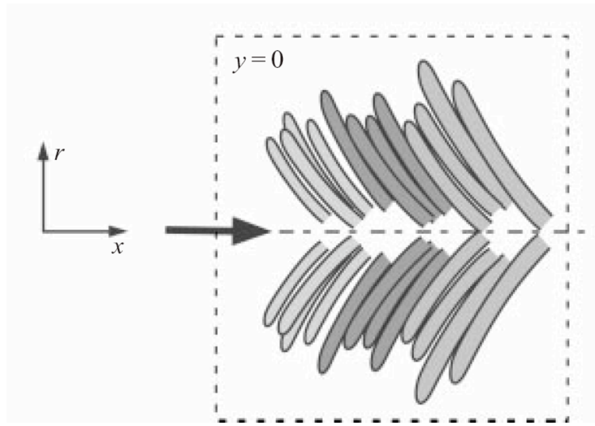

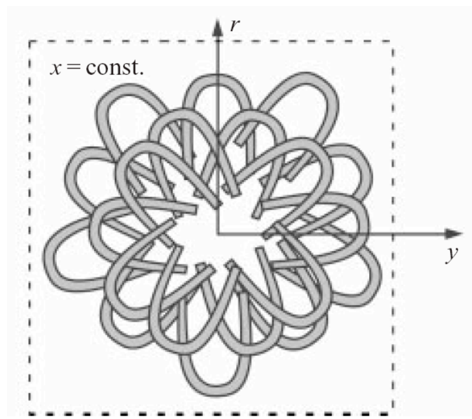

Attached eddy model calculation road map

Π, S, ζ, β
from experiment

$$-\frac{\overline{u_1 u_3}}{U_\tau^2} = f_1[\eta, \Pi, S] + g_1[\eta, \Pi, S]\,\zeta + g_2[\eta, \Pi, S]\,\beta$$

$$\frac{\overline{u_1 u_3}}{U_\tau^2} = \int_{-\infty}^{\infty} J_{13}[\lambda]\; T^2[\lambda-\lambda_E]\,\omega[\lambda-\lambda_E]\;\mathrm{d}\lambda$$

$T^2\omega$ by deconvolution

$$\frac{\overline{u_1^2}}{U_\tau^2} = \int_{-\infty}^{\infty} J_{11}[\lambda]\; T^2[\lambda-\lambda_E]\,\omega[\lambda-\lambda_E]\;\mathrm{d}\lambda$$

$\frac{\overline{u_1^2}}{U_\tau^2}$ and similarly $\frac{\overline{u_2^2}}{U_\tau^2}$ and $\frac{\overline{u_3^2}}{U_\tau^2}$ by convolution

<u>Wall-wake attached eddy model of wall turbulence</u>
- with and without pressure gradients

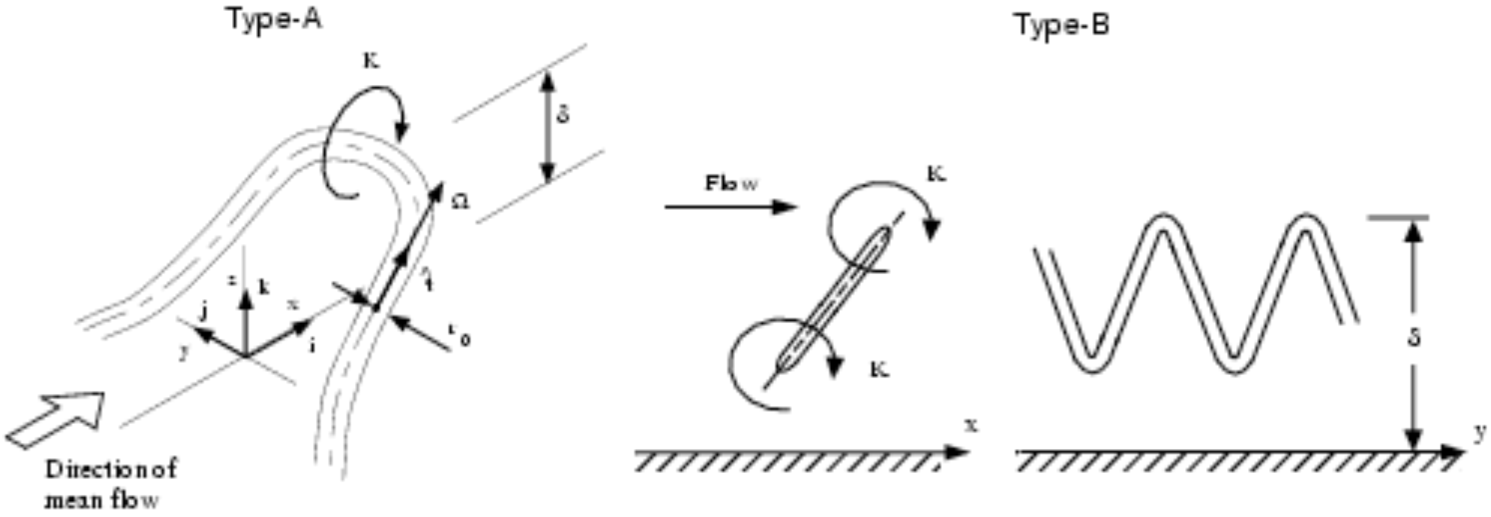

cf. Coles' law of the wall, law of the wake

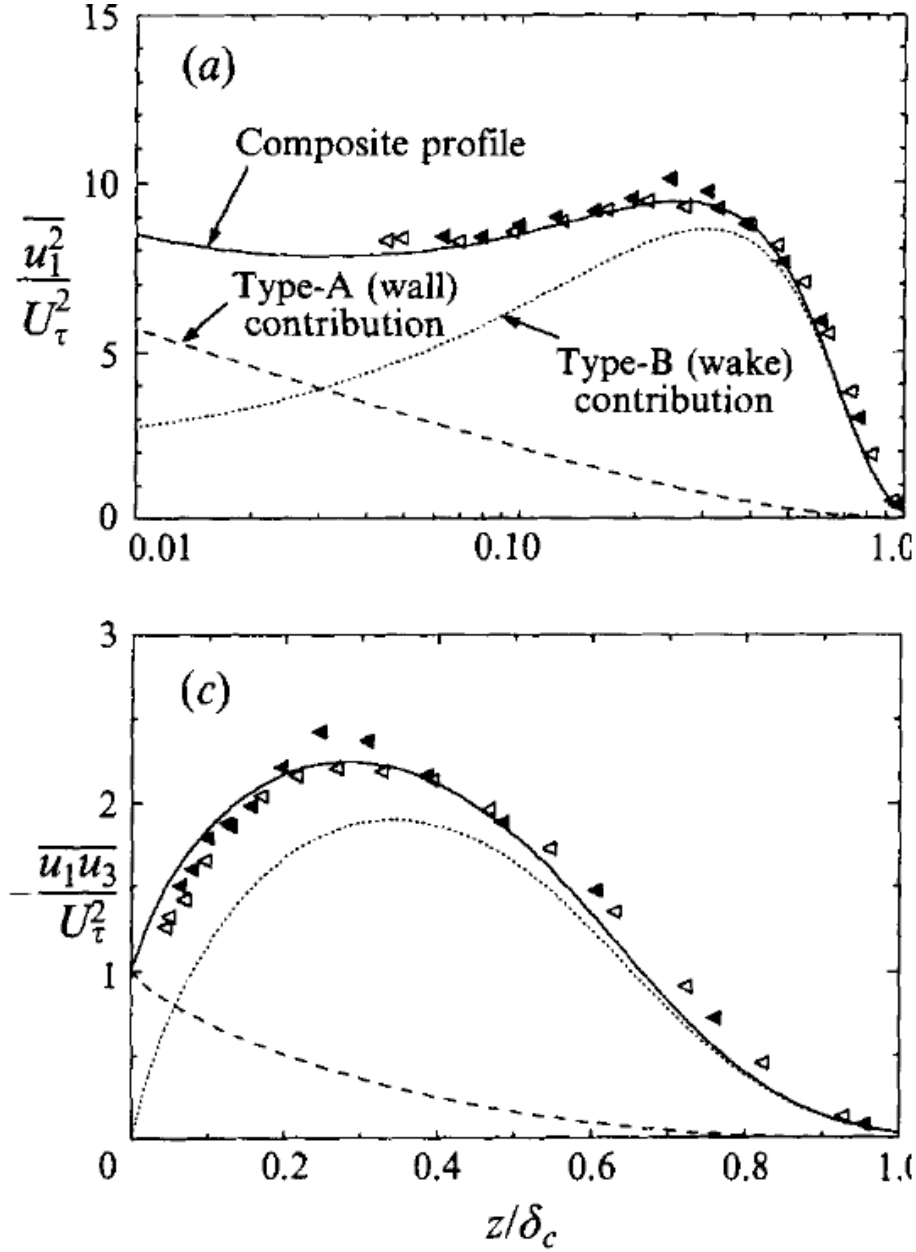

(a)
Composite profile
Type-A (wall) contribution
Type-B (wake) contribution
$\frac{\overline{u_1^2}}{U_\tau^2}$
0
5
10
15
0.01
0.10
1.0
(c)
$-\frac{\overline{u_1 u_3}}{U_\tau^2}$
0
1
2
3
0.2
0.4
0.6
0.8
1.0
z/δ_c

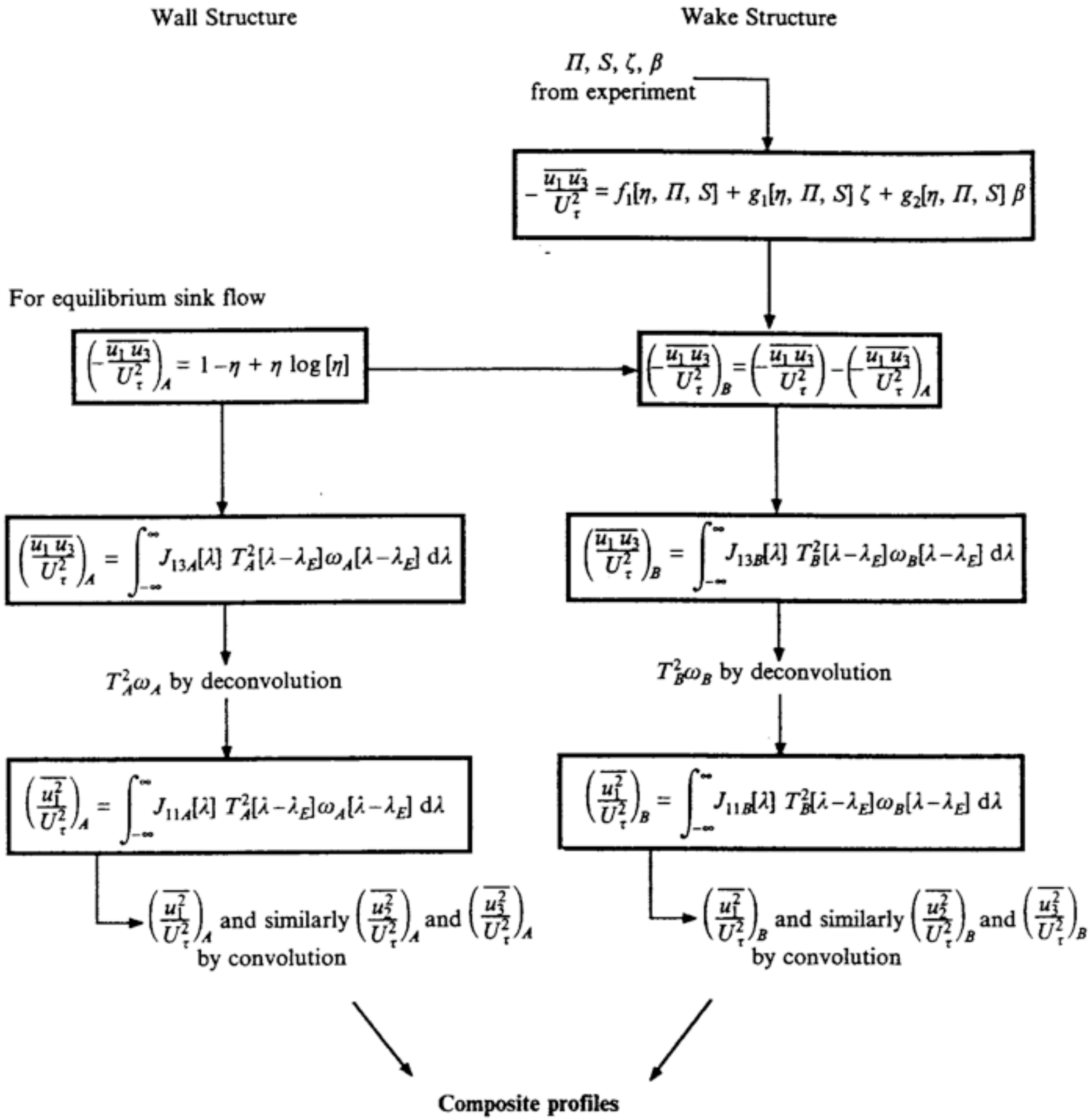

FIGURE 18. Overview of calculations for the wall-wake eddy structure model.

Attached Eddy Model: wall and wake eddies

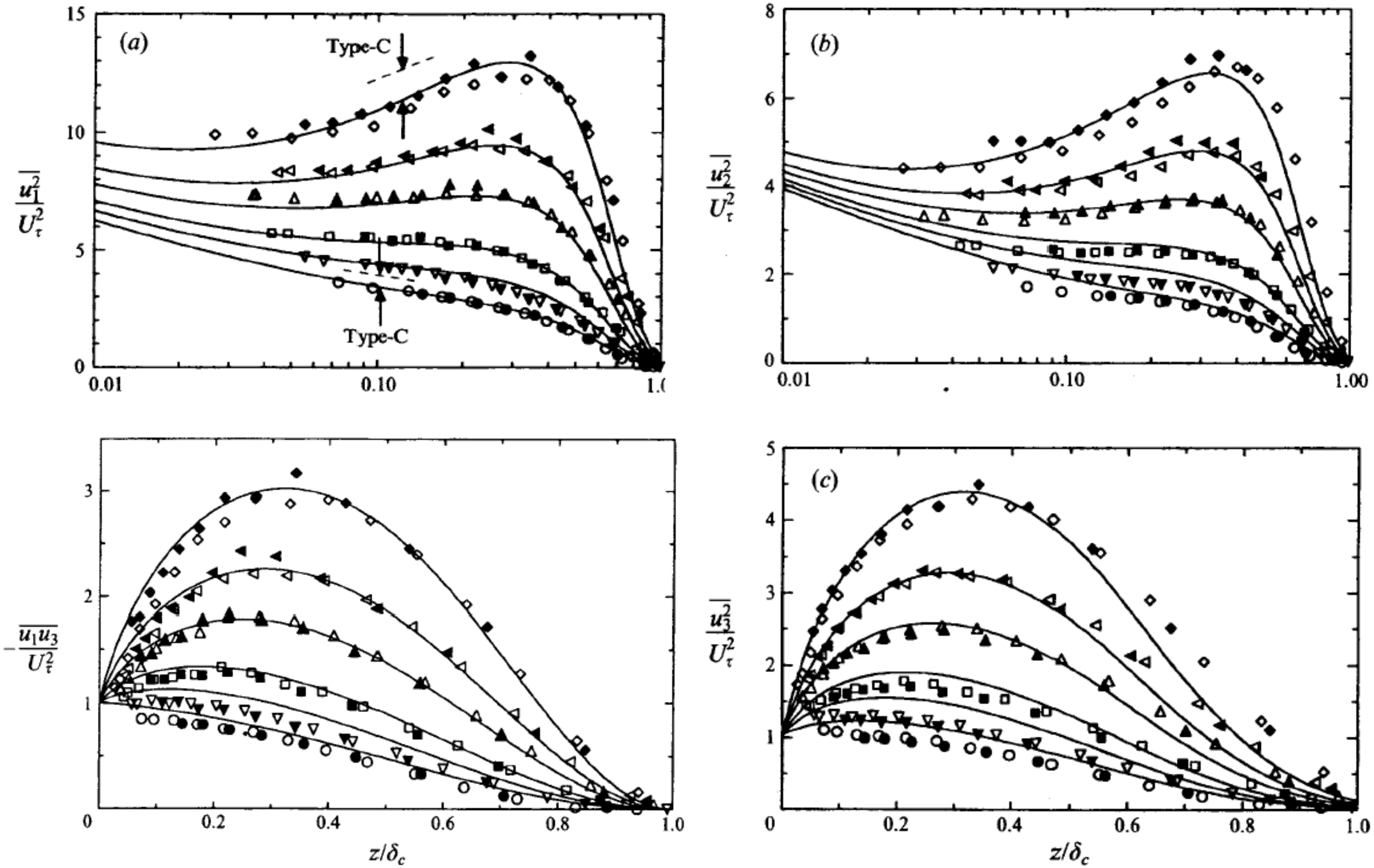

Limitations of single-uncorrelated eddy paradigm

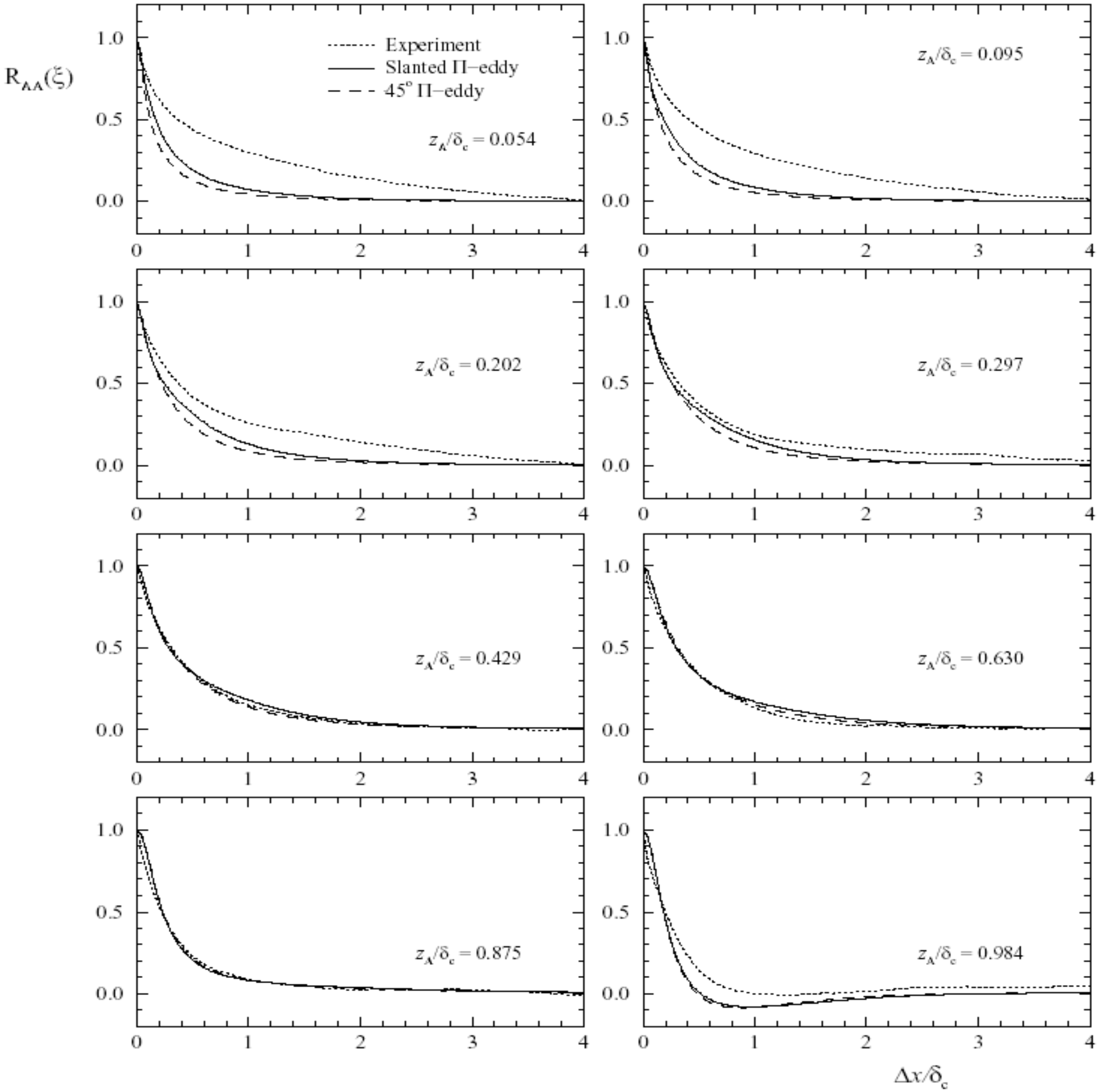

Thus far: assuming statistically uncorrelated eddies

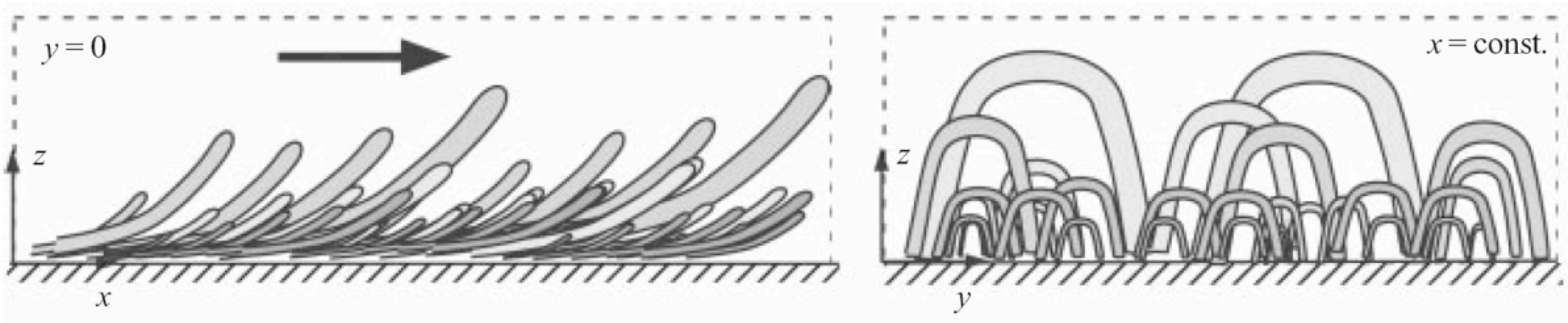

Packets: Adrian, Meinhart and Tomkins (2000)

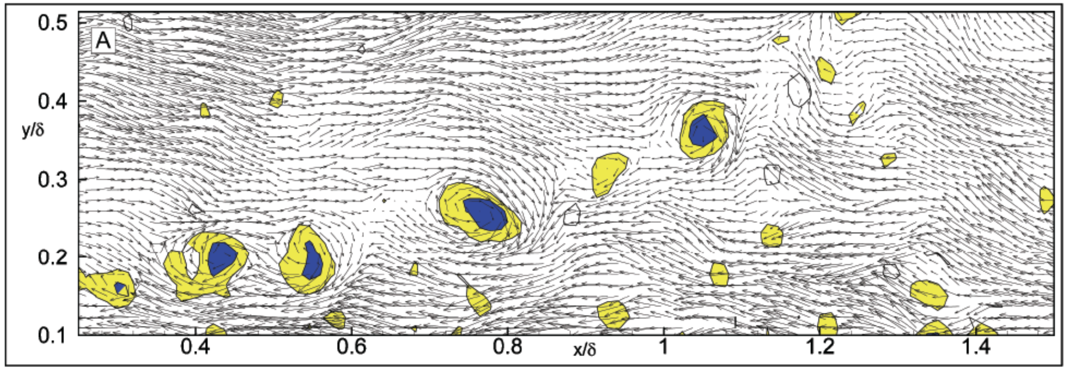

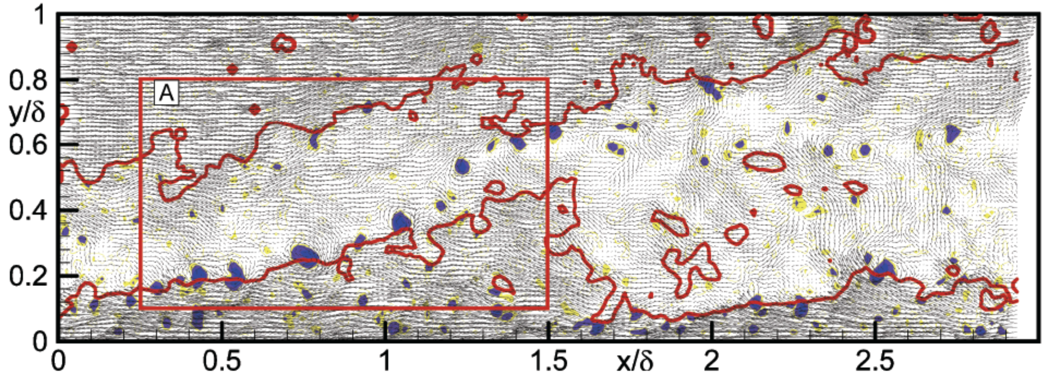

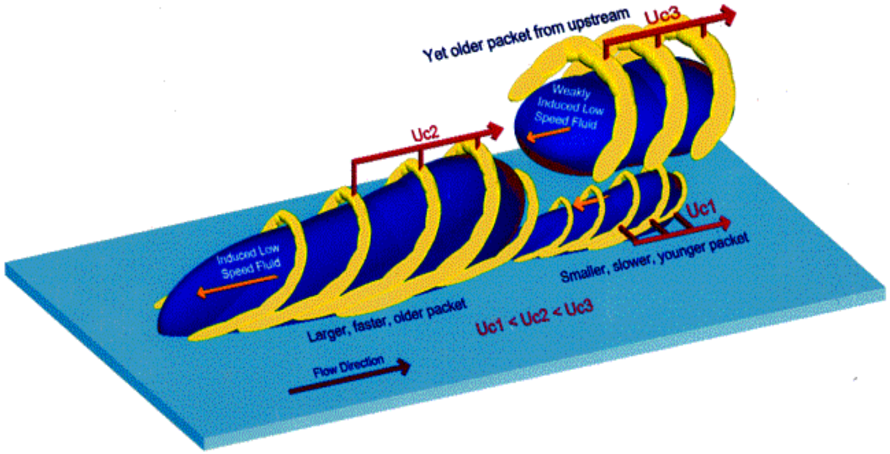

Zhou et al (1999)
Christensen & Adrian (2001)
Tomkins & Adrian (2003)

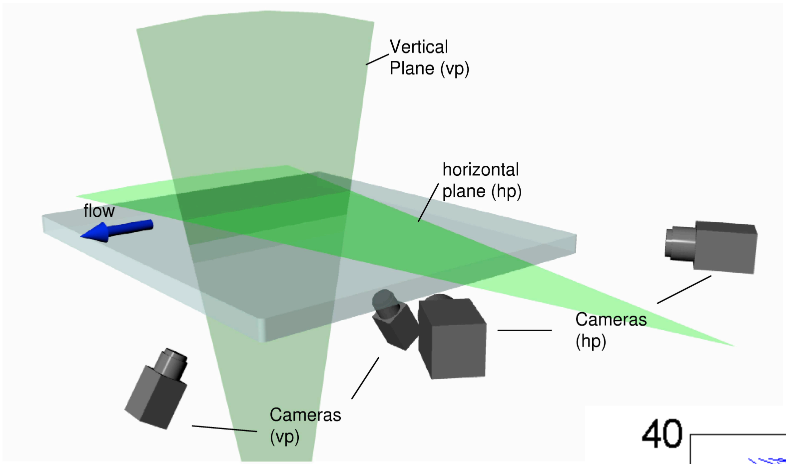

Simultaneous dual-plane PIV

Conditional Average

Conditioned on swirl event at z^+=200

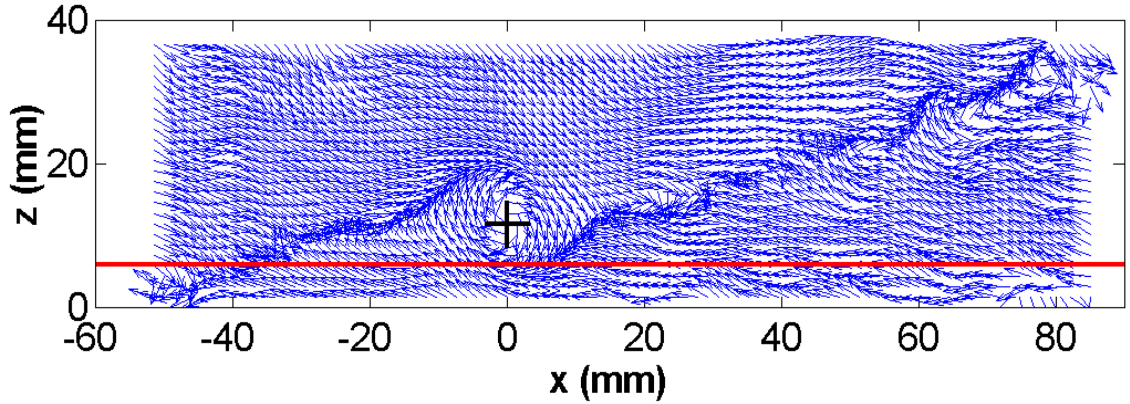

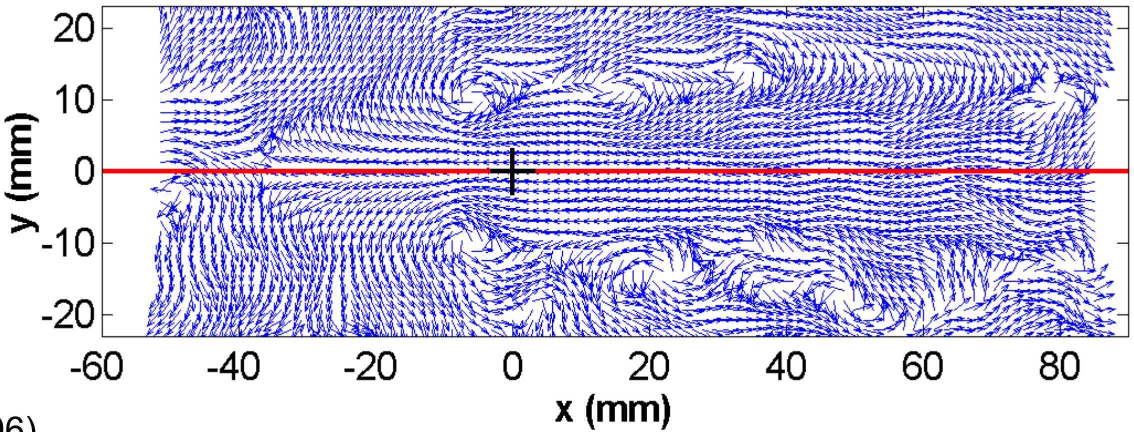

Hambleton, Hutchins & Marusic (2006)

Marusic (2001)

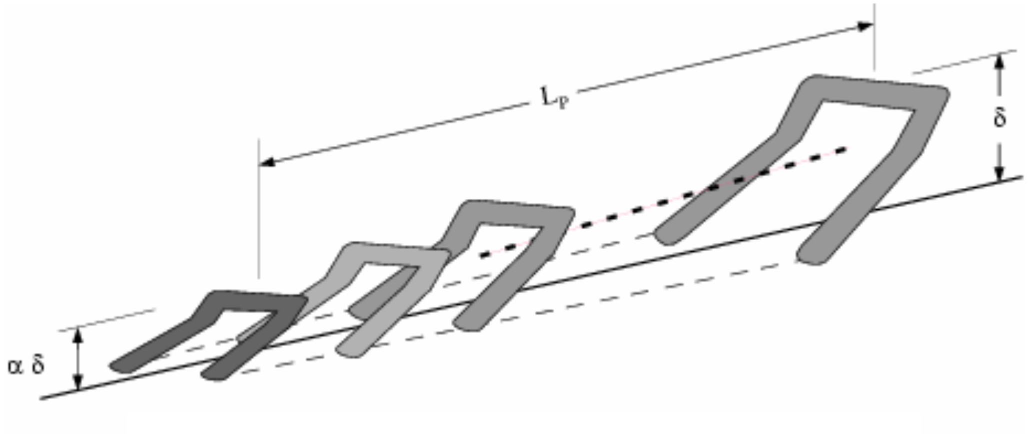

$$\frac{U_A^{(n)}}{U_0} = f_A(\frac{x}{\delta}, \frac{y}{\delta}, \frac{z_A}{\delta}), \qquad \frac{U_B^{(n)}}{U_0} = f_B(\frac{x}{\delta}, \frac{y}{\delta}, \frac{z_B}{\delta})$$

$$\psi_A(k_1\delta, \frac{y}{\delta}, \frac{z_A}{\delta}) = \frac{1}{N}\sum_{n=1}^{N}\left\{F_A^{(n)}(k_1\delta, \frac{y}{\delta}, \frac{z_A}{\delta})\mathrm{e}^{-i2\pi k_1 X_0^{(n)}}\right\}$$

$$\psi_B(k_1\delta, \frac{y}{\delta}, \frac{z_B}{\delta}) = \frac{1}{N}\sum_{n=1}^{N}\left\{F_B^{(n)}(k_1\delta, \frac{y}{\delta}, \frac{z_B}{\delta})\mathrm{e}^{-i2\pi k_1 X_0^{(n)}}\right\}$$

$$\Phi_{AB}(k_1\delta_c) = \int_{\delta_1}^{\delta_c}\left\{\frac{U_0^2}{\lambda_x\lambda_y}\int_{-\infty}^{\infty}\psi_A^*\psi_B\, d(\frac{y}{\delta})\right\} Q^2(\frac{\delta}{\delta_c})\, D(\frac{\delta}{\delta_c})\frac{1}{\delta}\, d\delta$$

$$\boxed{\mathcal{R}_{AB}(\Delta x/\delta_c) = \int_{-\infty}^{\infty}\Phi_{AB}(k_1\delta_c)\,\mathrm{e}^{ik_1\delta_c\Delta x/\delta_c}\, d(k_1\delta_c)}$$

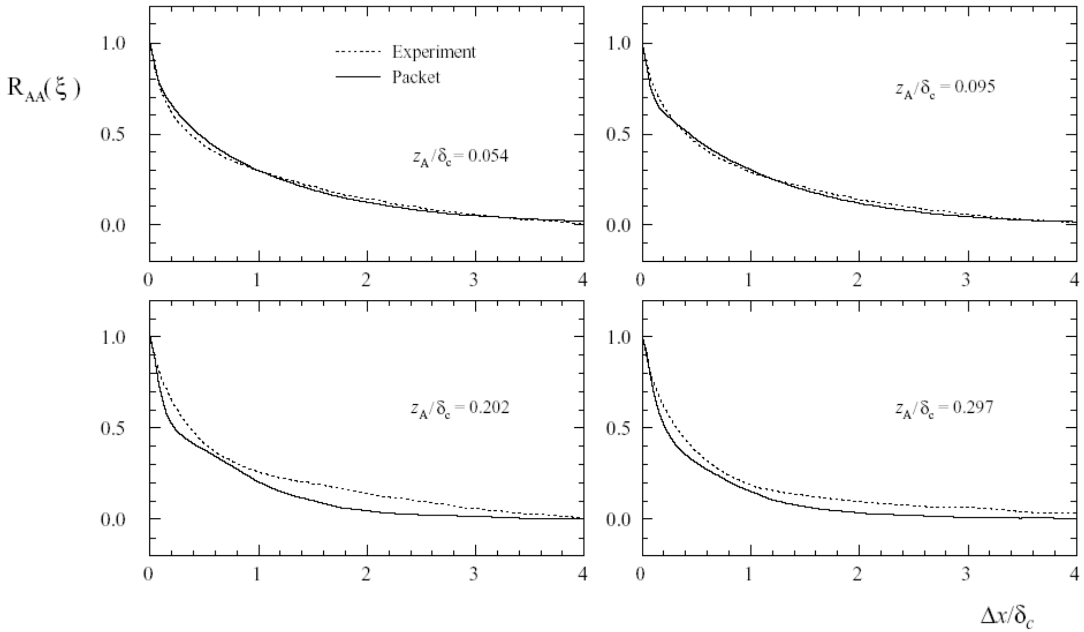

Experiment
Packet
R_AA(ξ)
z_A/δ_c = 0.054
z_A/δ_c = 0.095
z_A/δ_c = 0.202
z_A/δ_c = 0.297
Δx/δ_c

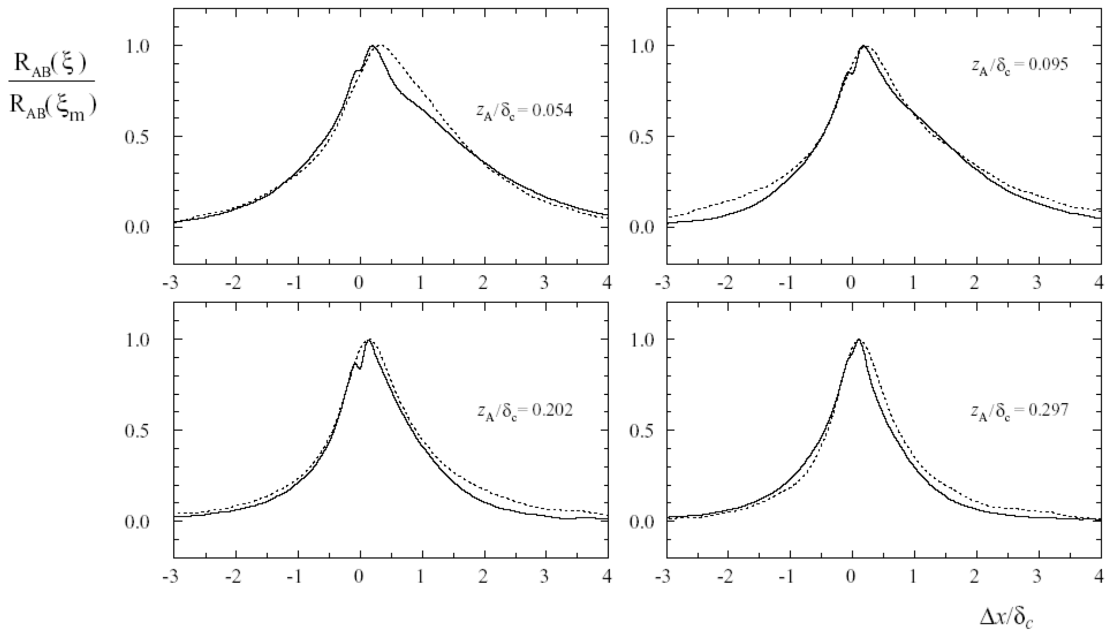

R_AB(ξ) / R_AB(ξ_m)
z_A/δ_c = 0.054
z_A/δ_c = 0.095
z_A/δ_c = 0.202
z_A/δ_c = 0.297
Δx/δ_c

Non-local effects important

- interactions beyond linear superposition

Log layer structures and interaction across the boundary layer

Superstructures/VLSM

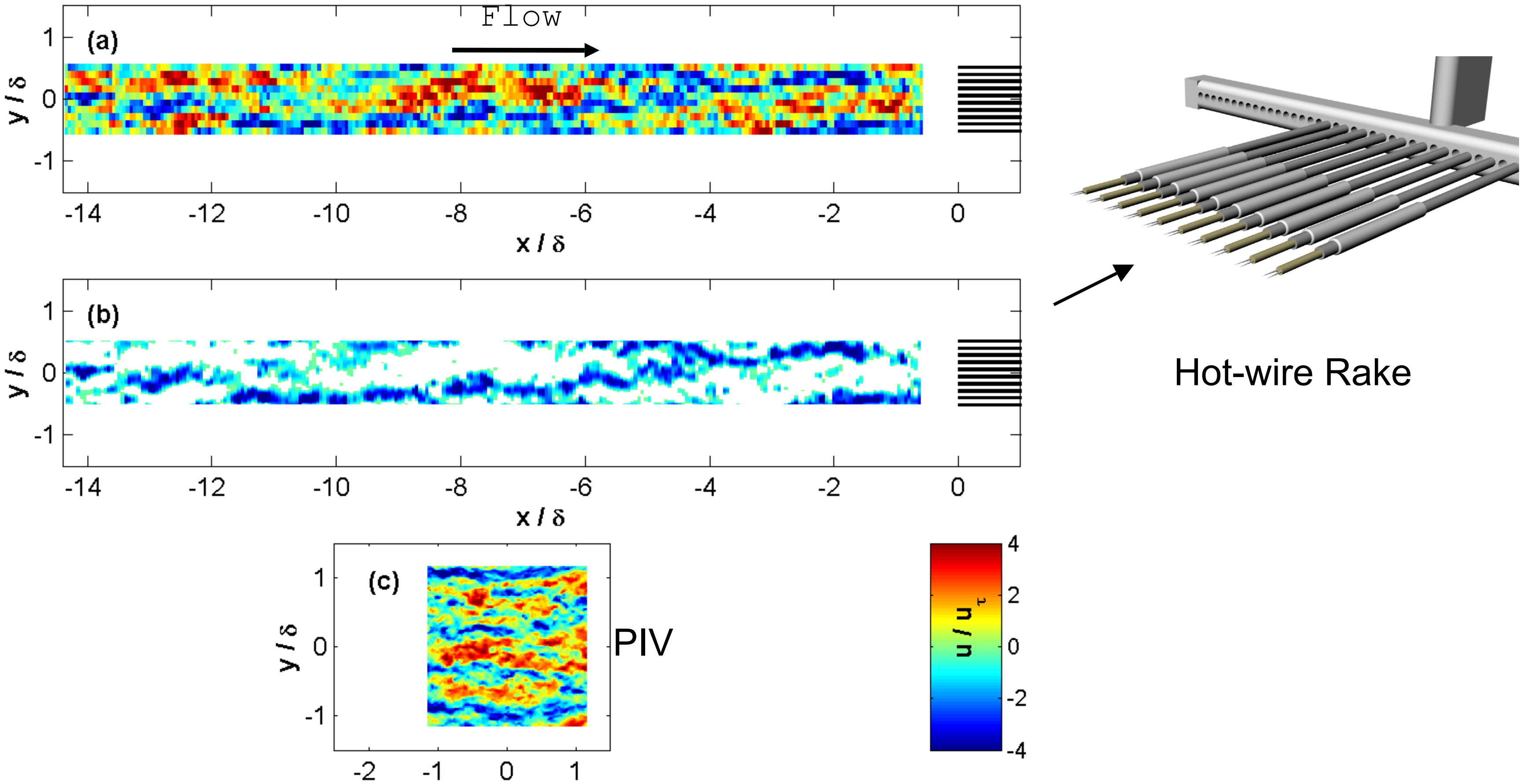

Hutchins & Marusic (2007), J. Fluid Mech. vol. 579

High frame-rate PIV
Dennis & Nickels (2011)

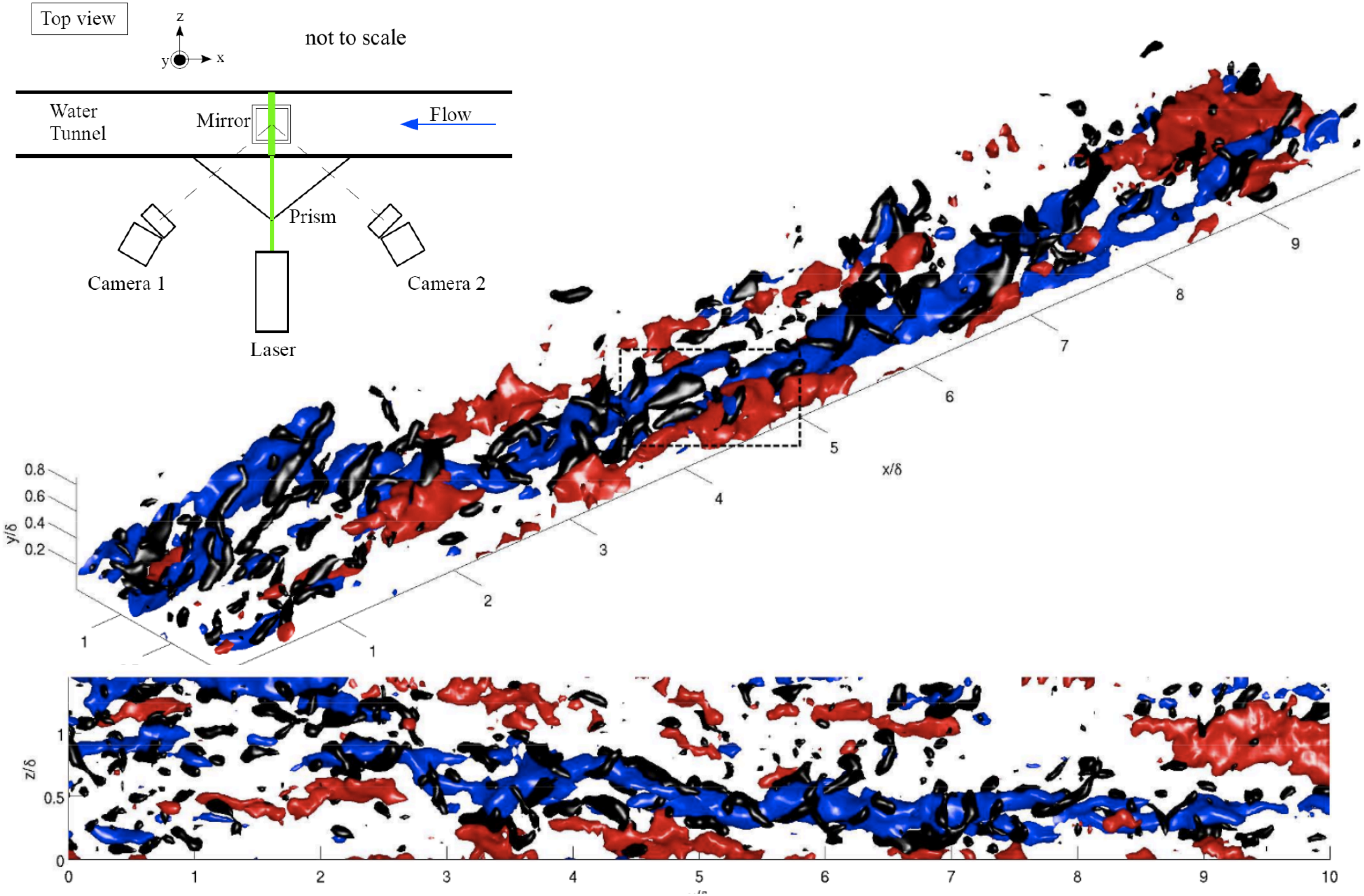

z_s
x_s
y_s

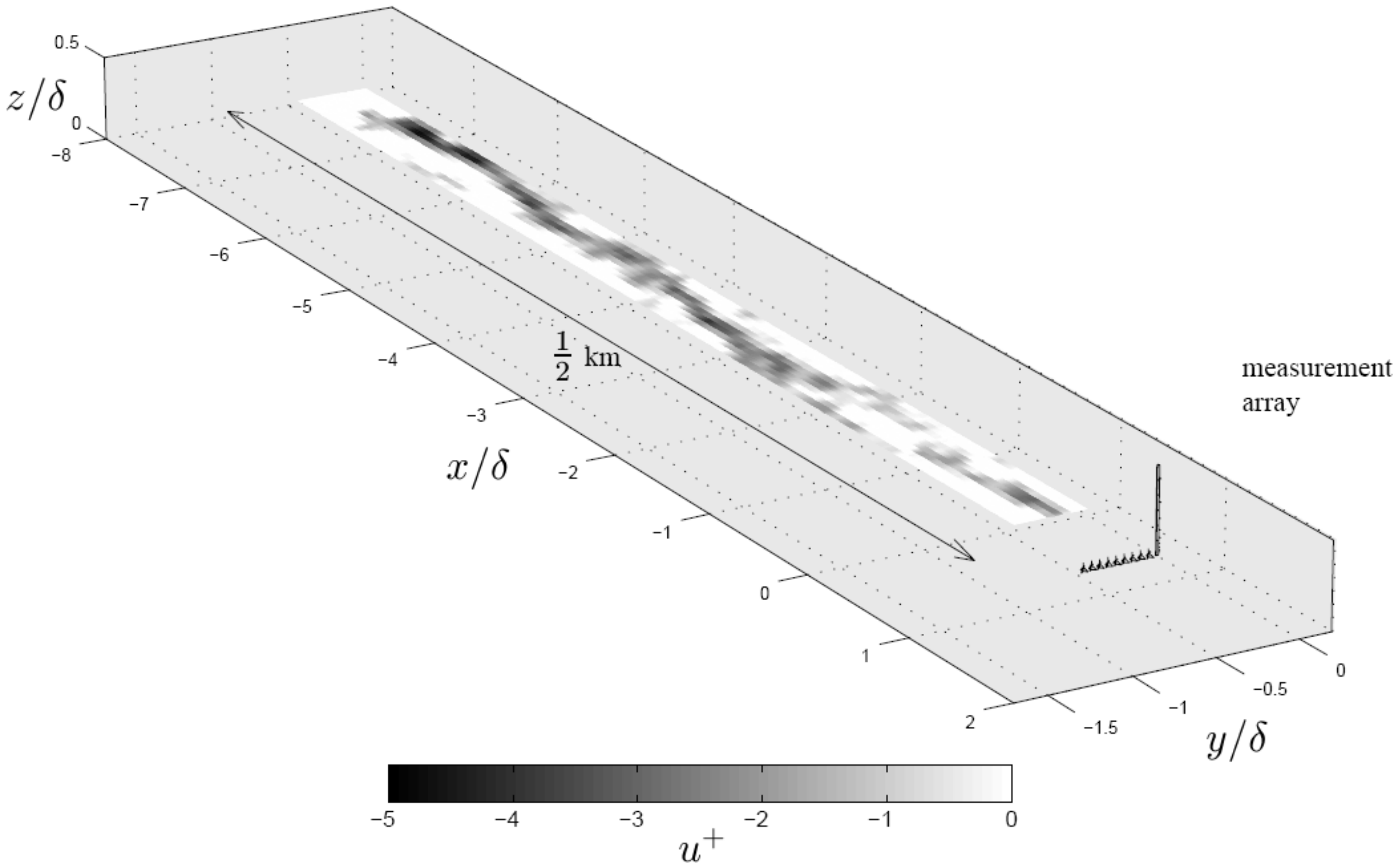

Hutchins & Marusic (2007), J. Fluid Mech. vol. 579

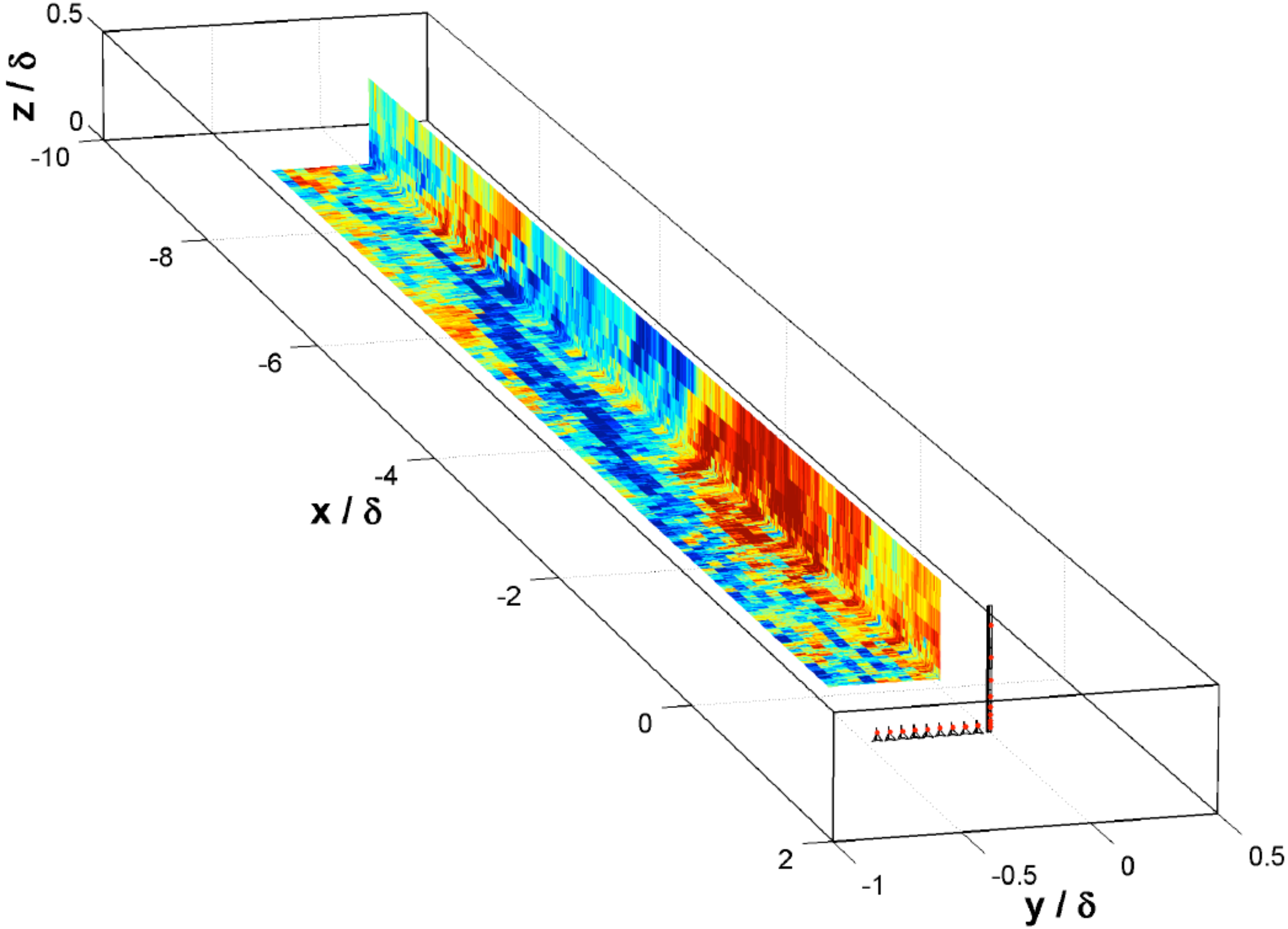

0.5
z / δ
0
-10
-8
-6
-4
x / δ
-2
0
2
-1
-0.5
0
0.5
y / δ

Conditional average on $-u$ at Δx=0, Δy=0, z/δ = 0.036

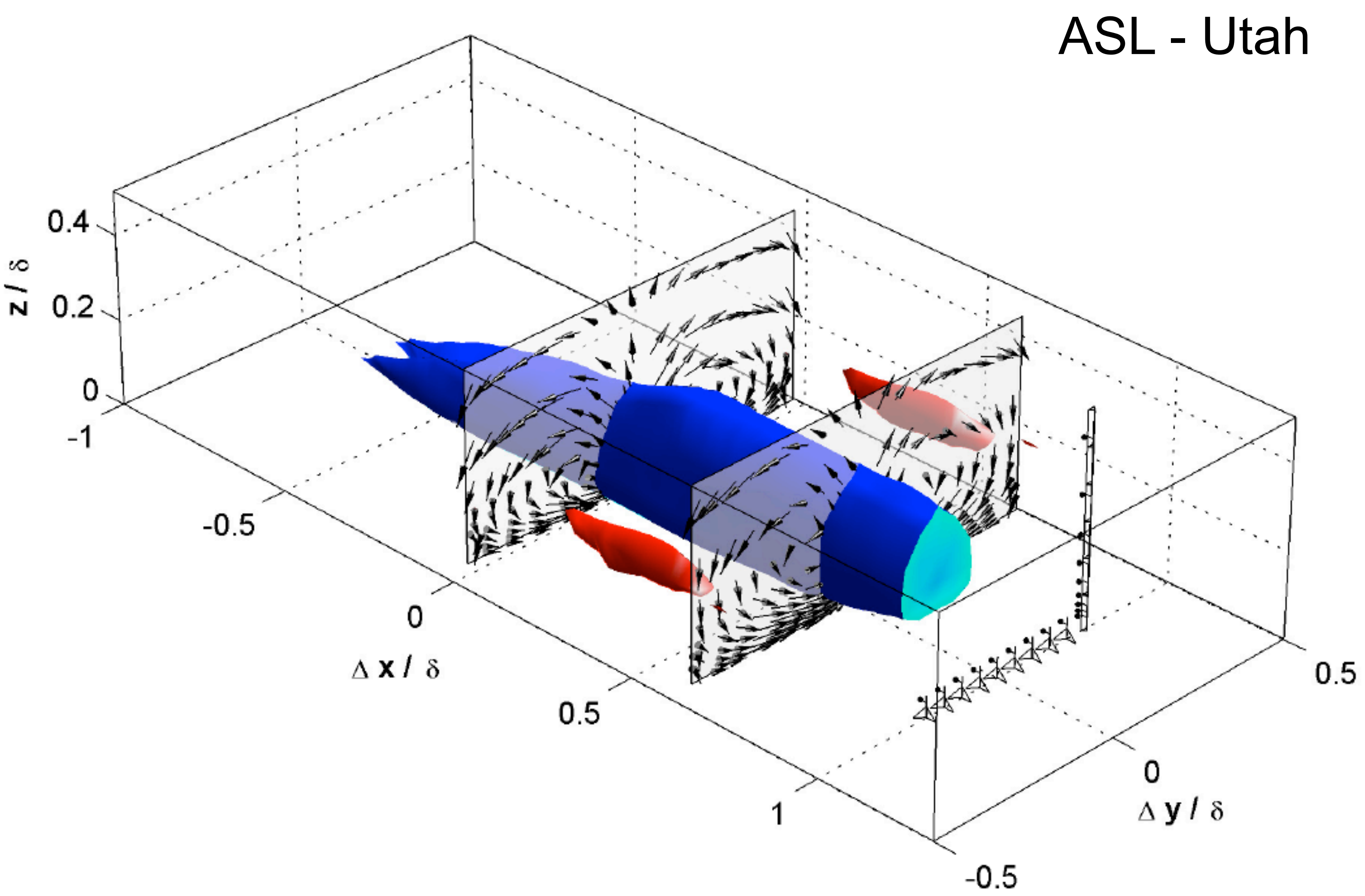

Superstructures associated with “outer-peak” in spectra

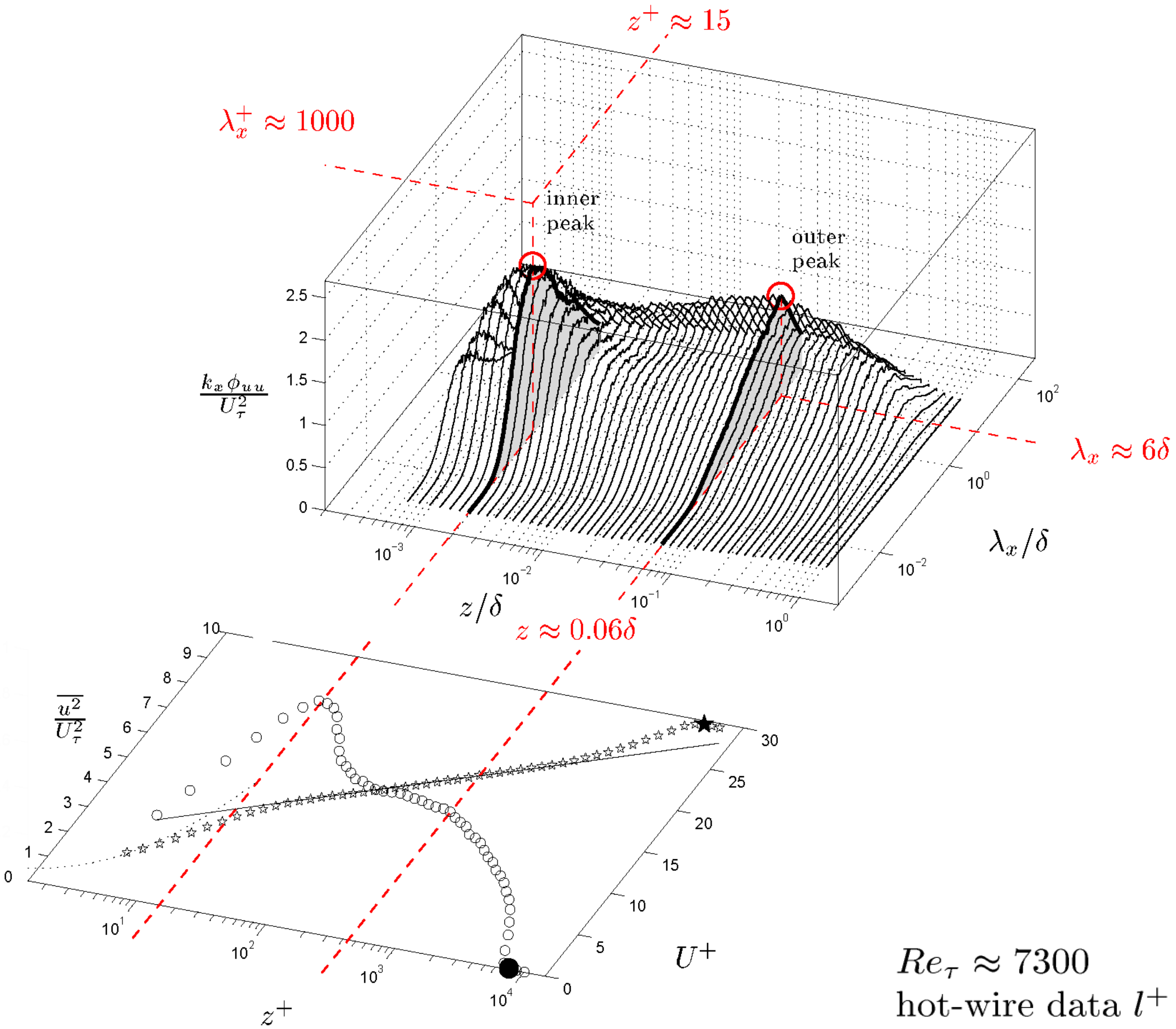

$Re_\tau \approx 7300$

hot-wire data $l^+ \approx 22$

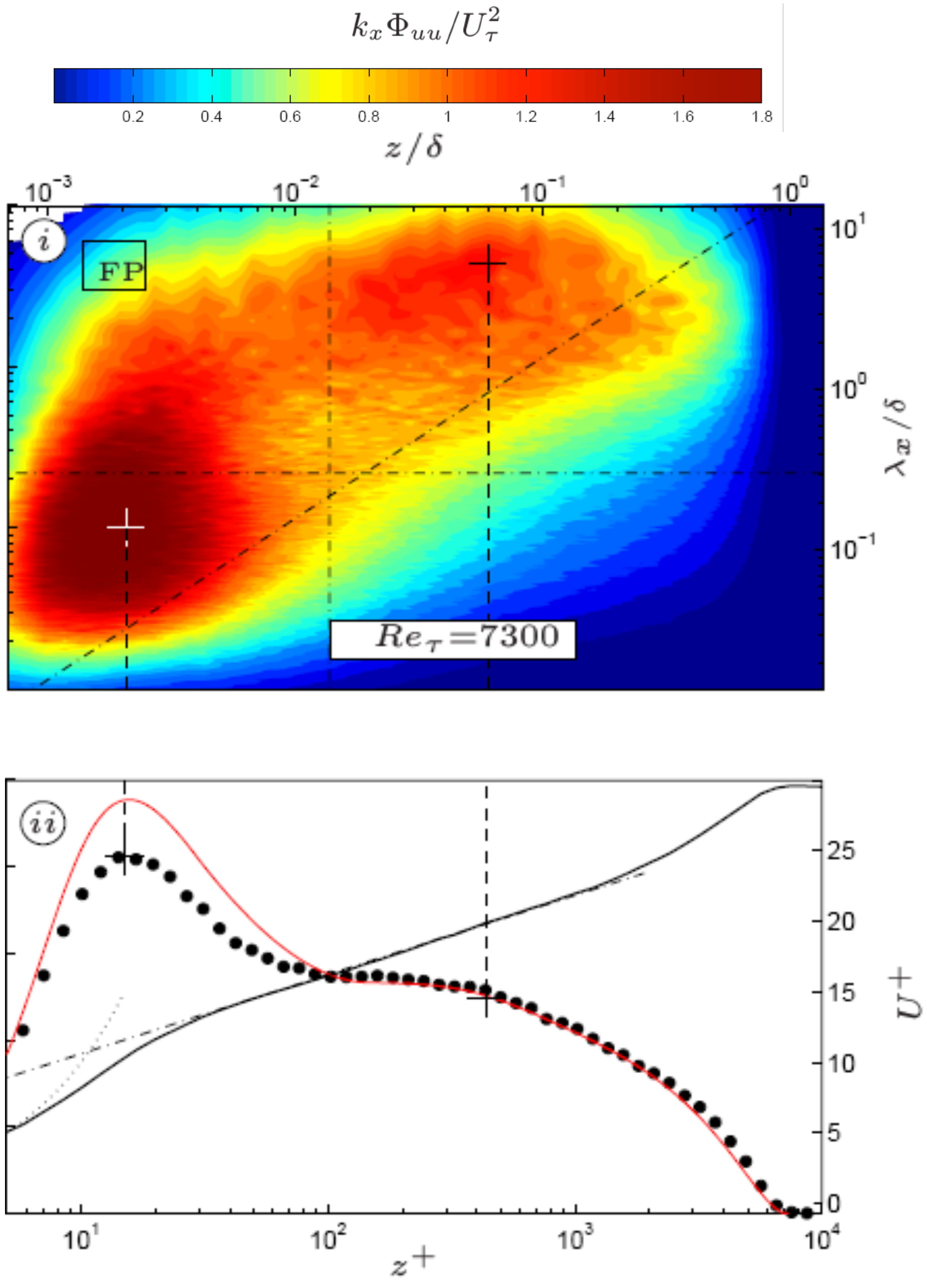

$k_x \Phi_{uu}/U_\tau^2$
0.2
0.4
0.6
0.8
1
1.2
1.4
1.6
1.8
z/δ
10^{-3}
10^{-2}
10^{-1}
10^{0}
i
FP
10^{1}
10^{0}
10^{-1}
λ_x/δ
Re_τ=7300
ii
25
20
15
10
5
0
U^+
10^{1}
10^{2}
10^{3}
10^{4}
z^+

Superstructure influence near the wall:
modulation & superposition

Simultaneous velocities at inner and outer peak locations

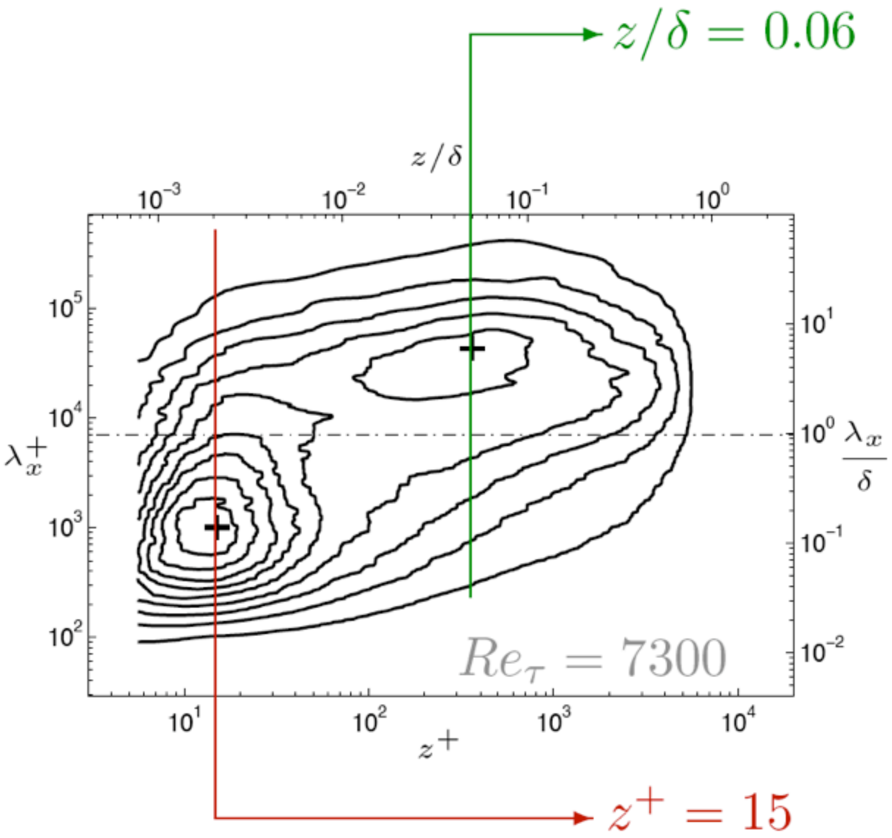

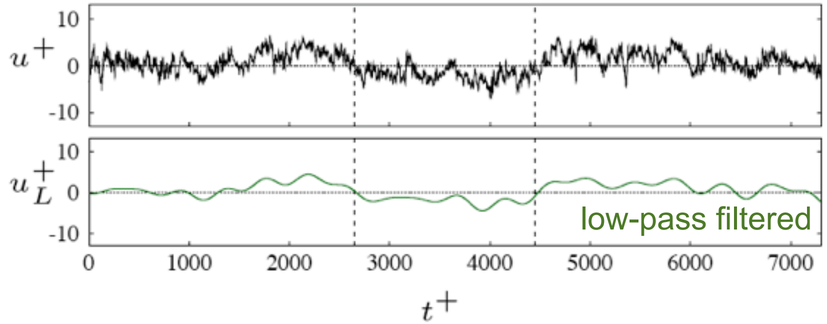

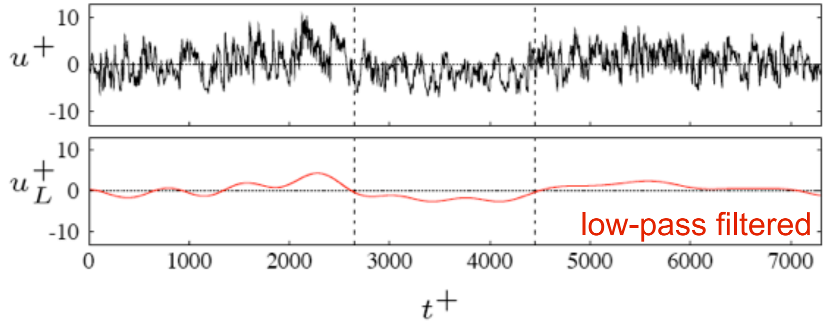

Simultaneous velocities at inner and outer peak locations

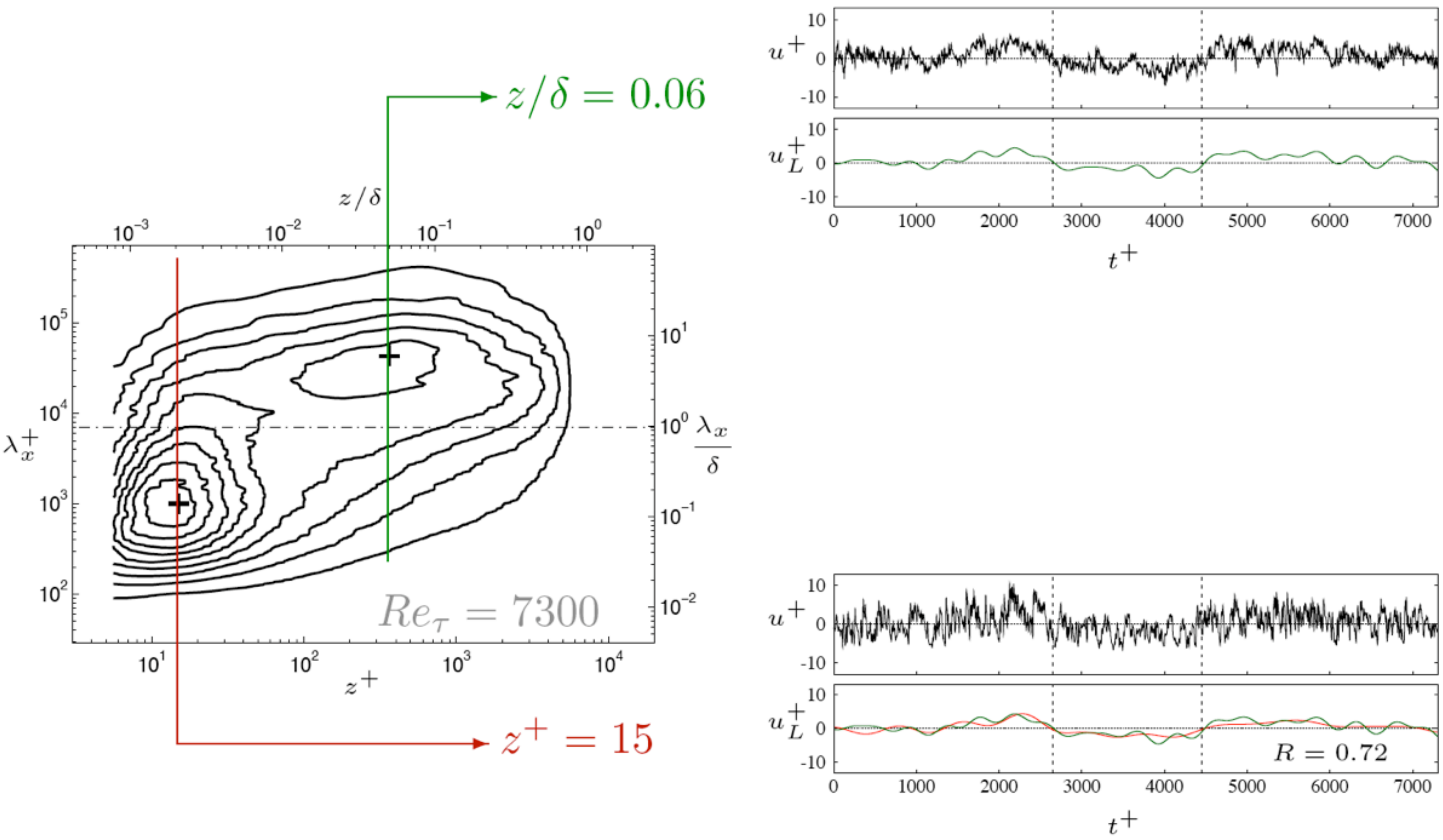

R = 0.72 with 14 deg. shift applied

Simultaneous velocities at inner and outer peak locations

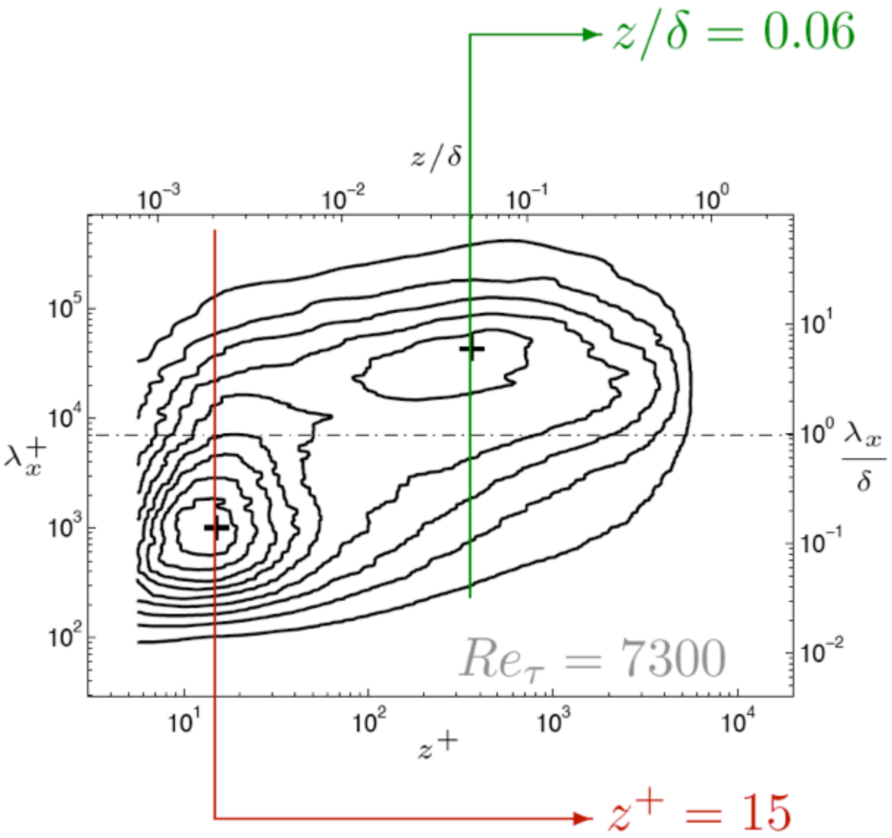

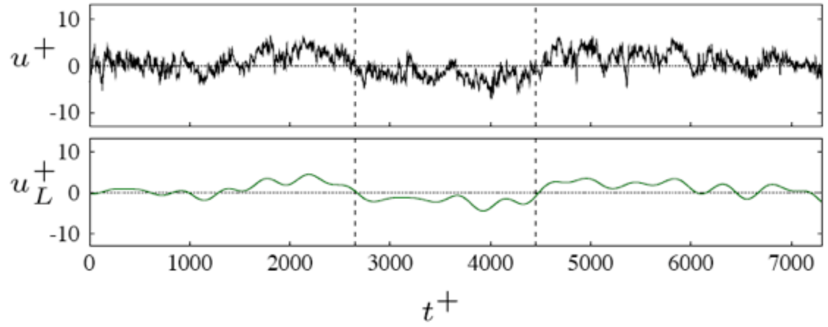

Evidence of amplitude modulation

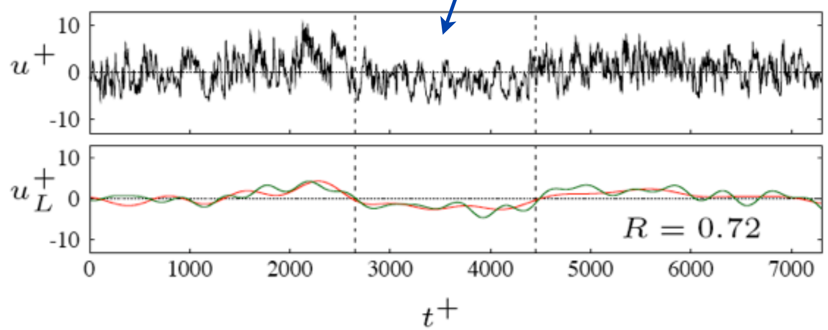

Superstructure interaction in near-wall region

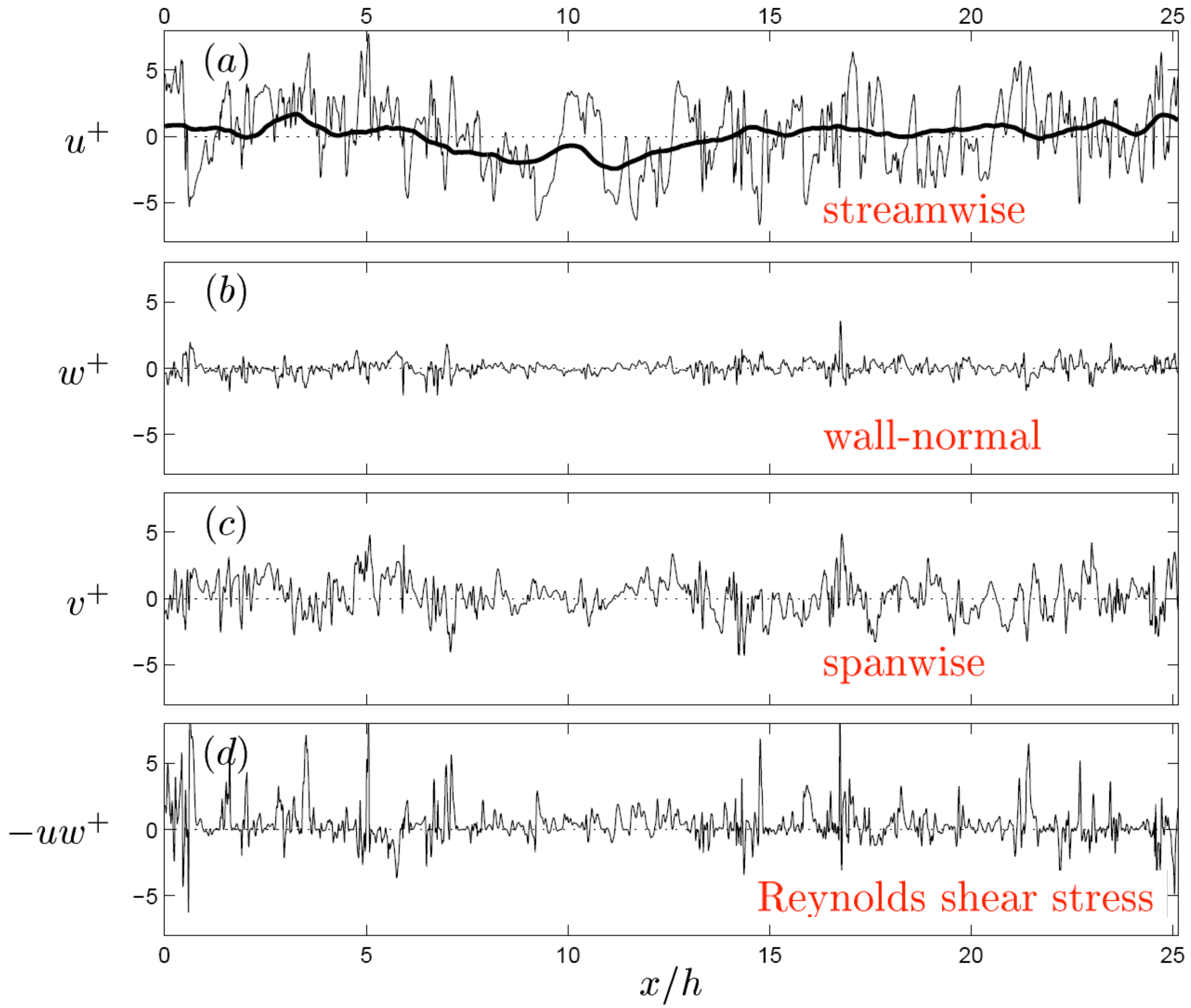

$Re_\tau = 934$ DNS data at $z^+ = 15$

Amplitude modulation in near-wall region

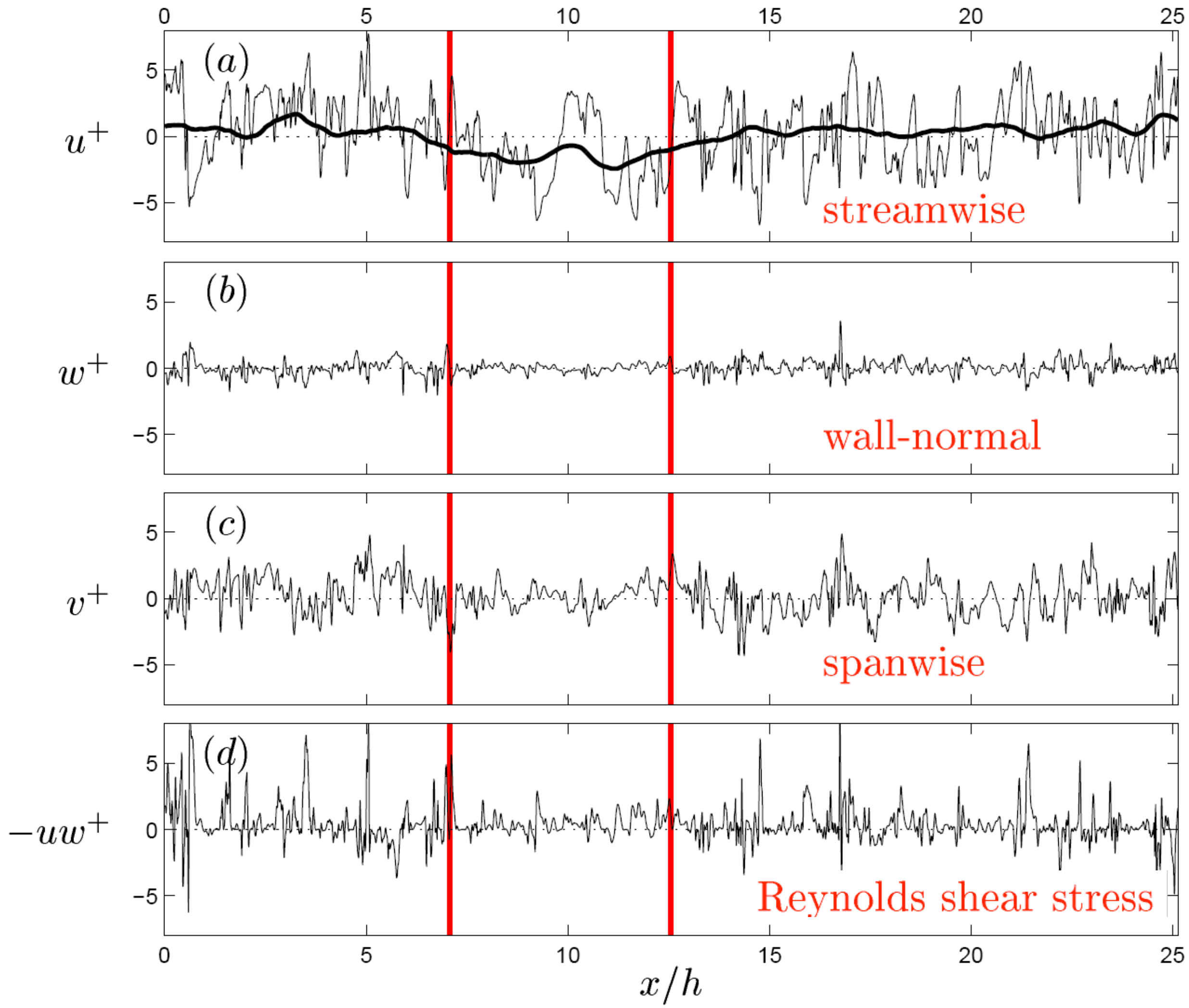

$Re_\tau = 934$ DNS data at $z^+ = 15$

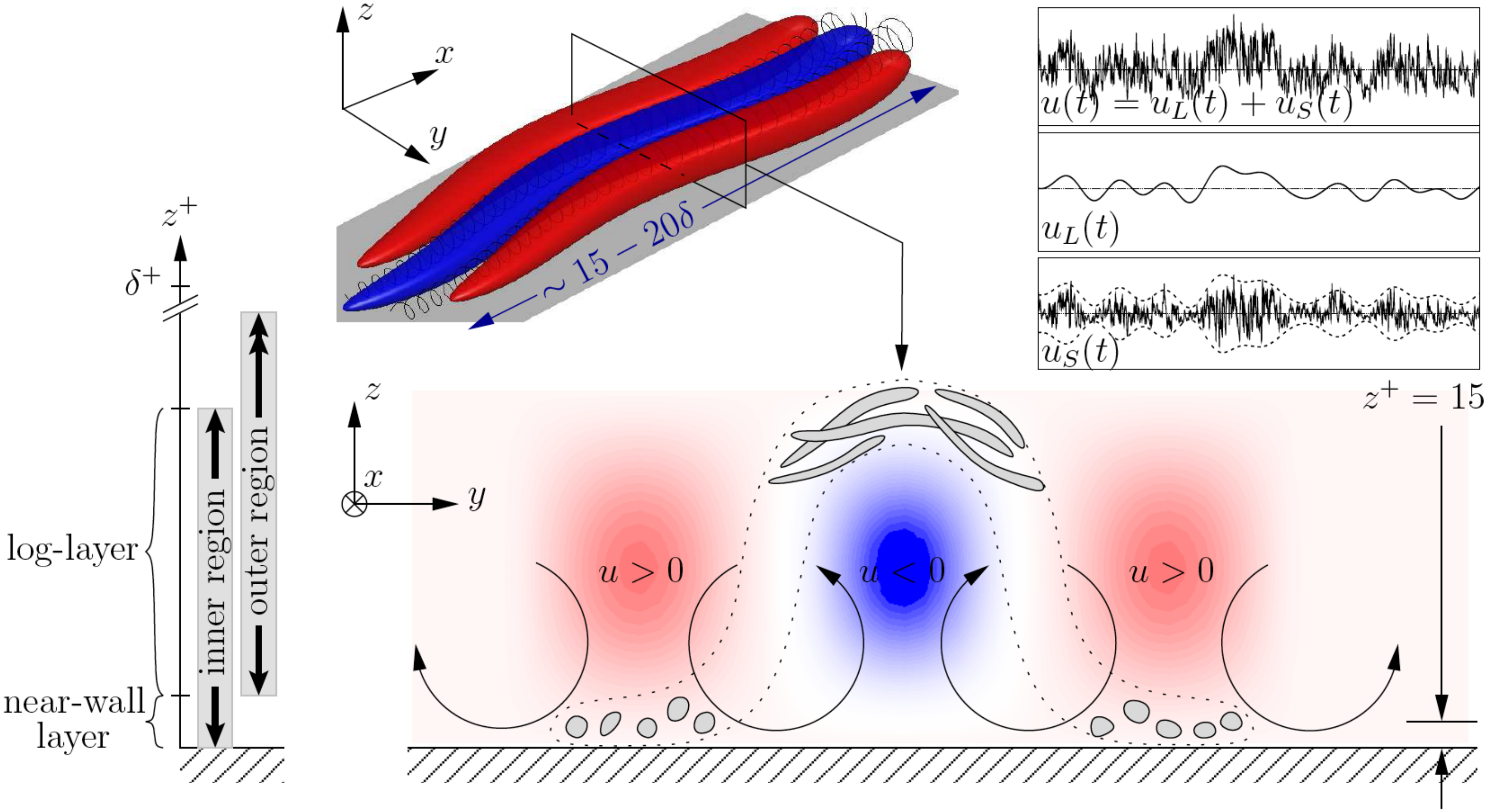

Marusic, Mathis & Hutchins (2010), *Science*. vol. 329

Quantifying superstructure interaction on near-wall region:

Can we accurately model (predict) near-wall signal from log-region signature?

Challenge of accessing near-wall region at high *Re*

Princeton superpipe measurements

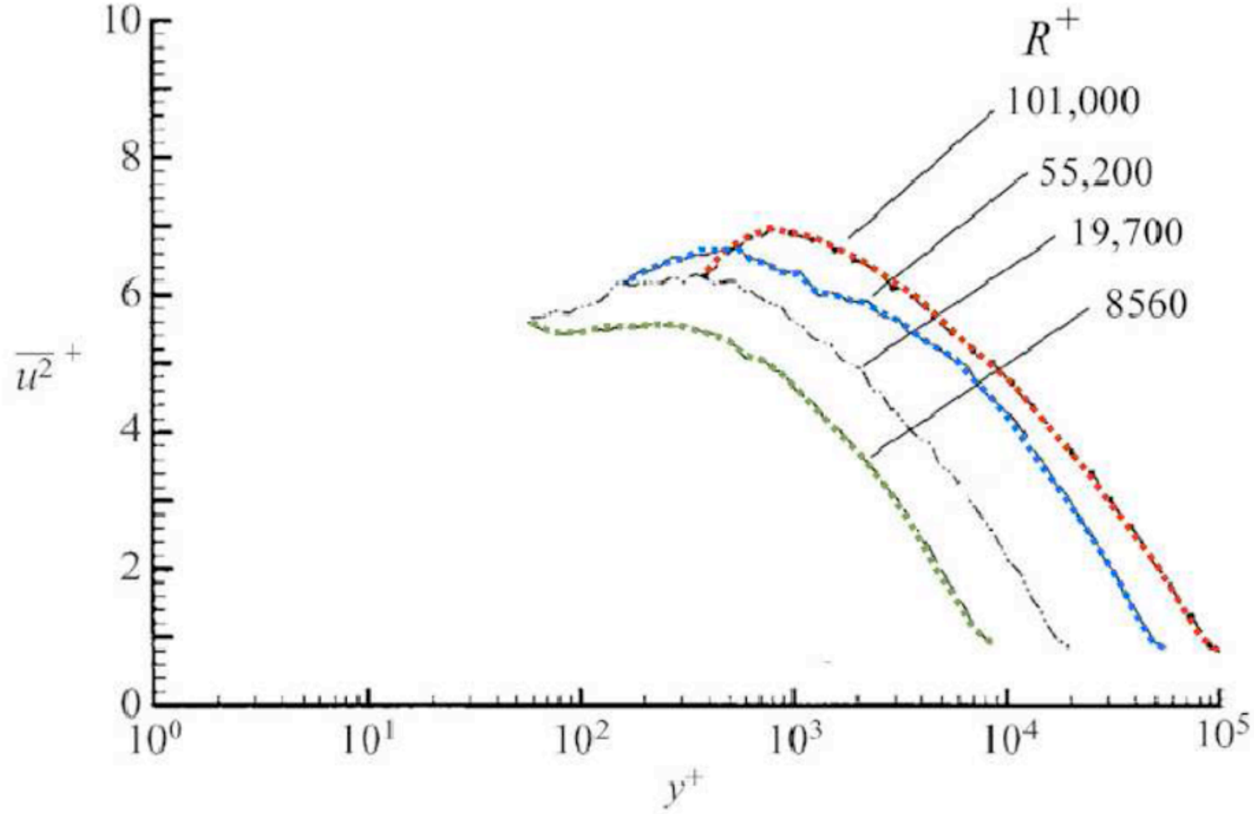

MORRISON *et al.* (2004)

Near-wall models for large-eddy simulation

Chapman (1979):

LES - outer layer resolution $\sim \mathrm{Re}^{0.4}$

- wall layer resolution $\sim \mathrm{Re}^{1.8}$

Resolved wall region in LES, typically:

$$\frac{\Delta z_{\min}}{\delta} \approx \frac{1}{\mathrm{Re}_\tau}, \qquad \frac{\Delta x}{\delta} \approx \frac{100}{\mathrm{Re}_\tau}, \qquad \frac{\Delta y}{\delta} \approx \frac{50}{\mathrm{Re}_\tau}$$

$\mathrm{Re}_\tau = 10^6$: wall-layer resolved requires 99% of grid points to resolve first 10% of boundary layer

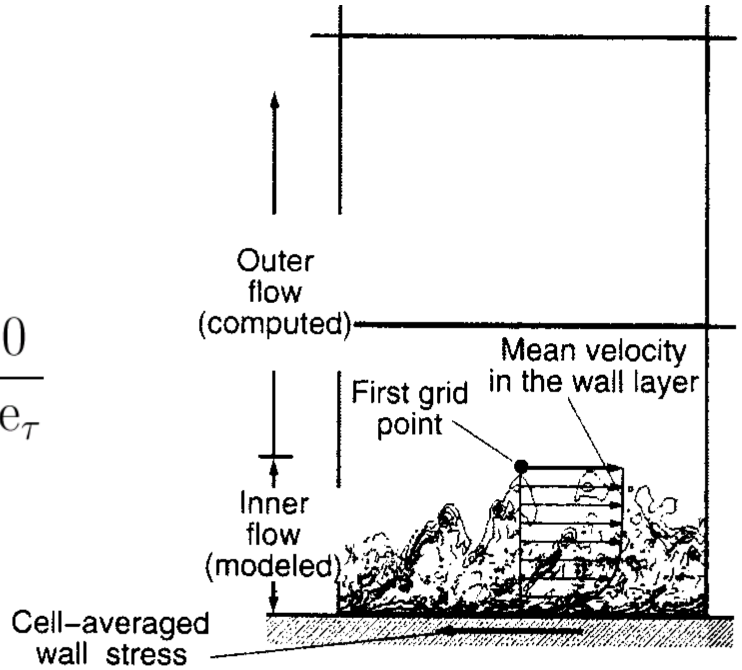

(Sketch from Piomelli 1999)

Mind the gap: a guideline for large eddy simulation

BY WILLIAM K. GEORGE[1,*] AND MURAT TUTKUN[2]

Phil. Trans. R. Soc. A (2009) **367**, 2839–2847

Based on measurements of correlations across the boundary layer:

“This suggests that it might be possible to build a near-wall model that is in sync with the outer flow (i.e. follows it), perhaps quite independent of considerations such as Reynolds number and spectral gaps. Note that this is quite the opposite of the prevailing view for the last 40 years or so that it is the wall region (with its streaks and bursts) that drives the outer flow. In fact, it assumes the opposite: namely that the inner flow is driven by the outer.”

$$\tilde{u}^{+}\left(z^{+}\right) = u^{*}\left(z^{+}\right)\left[1 + \beta u_{LS}^{+}\left(z_{O}^{+}, \theta_{LS}\right)\right] + \alpha u_{LS}^{+}\left(z_{O}^{+}, \theta_{LS}\right)$$

with *LS* for Large-Scale

keep energy $\lambda_x^+ > 7000$

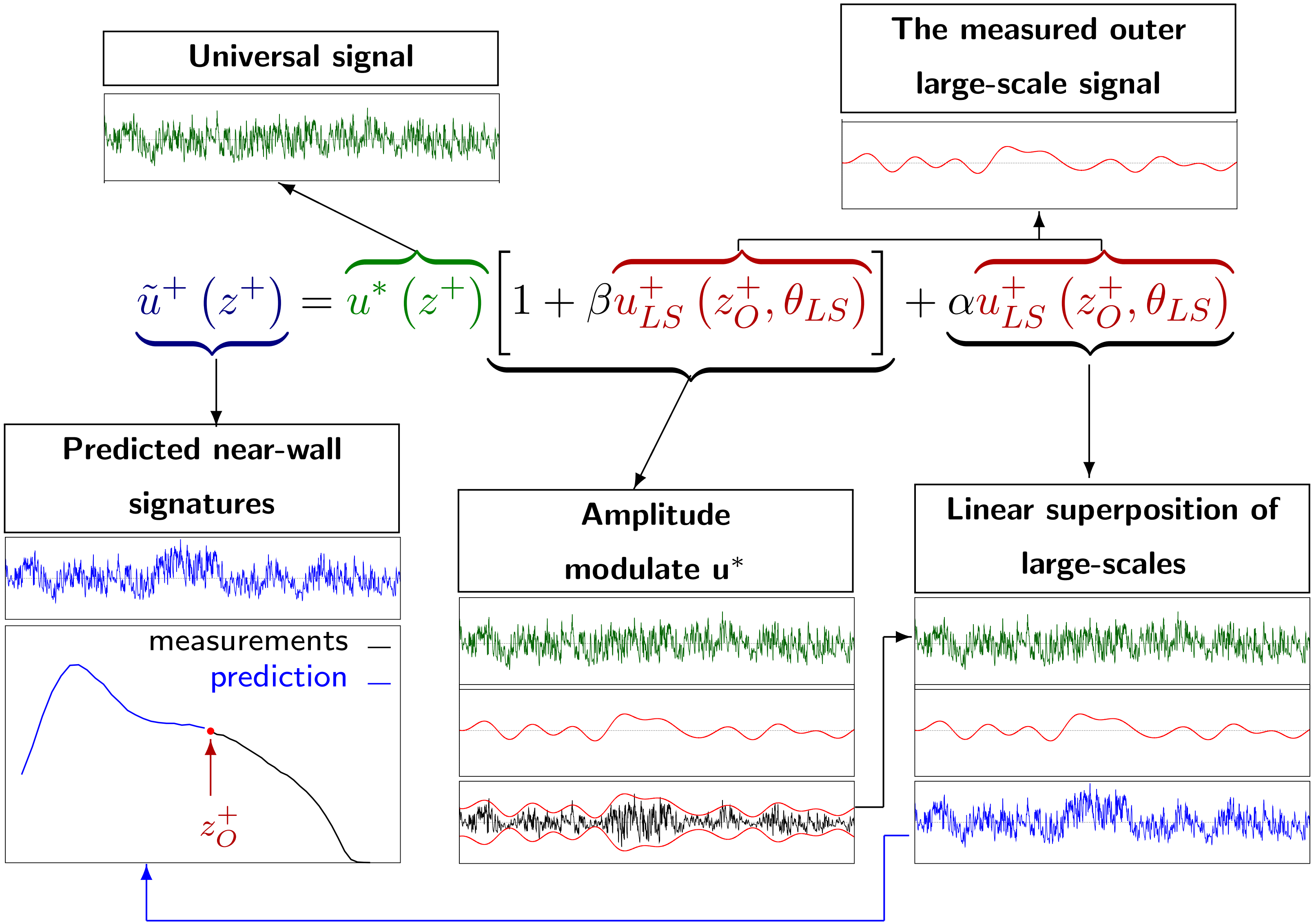
Universal signal
The measured outer large-scale signal
$\tilde{u}^+(z^+) = u^*(z^+)\left[1 + \beta u^+_{LS}(z^+_O, \theta_{LS})\right] + \alpha u^+_{LS}(z^+_O, \theta_{LS})$
Predicted near-wall signatures
Amplitude modulate u*
Linear superposition of large-scales
measurements
prediction
z^+_O

Experimental setup for calibration of the model

Two-point hot-wire simultaneous measurements:
$Re_\tau = 7300$ (arbitrary chosen Reynolds number)
$U_\infty = 10.02$ m/s
$U_\tau = 0.34$ m/s
$\delta = 0.33$
$l^+ = 22$

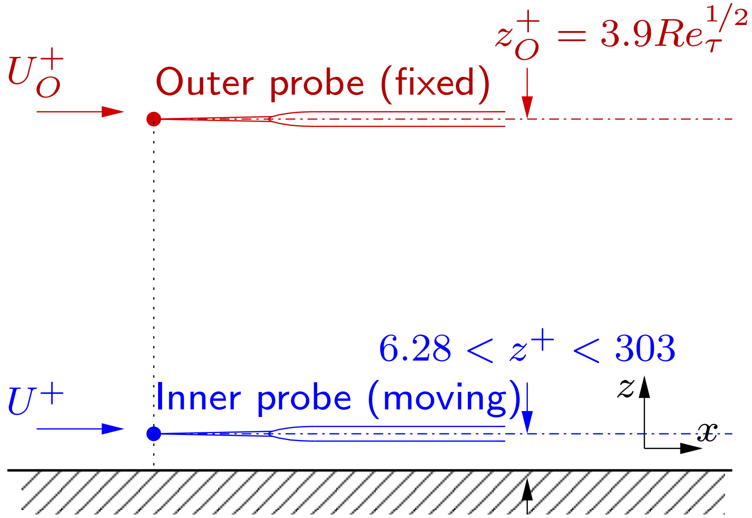

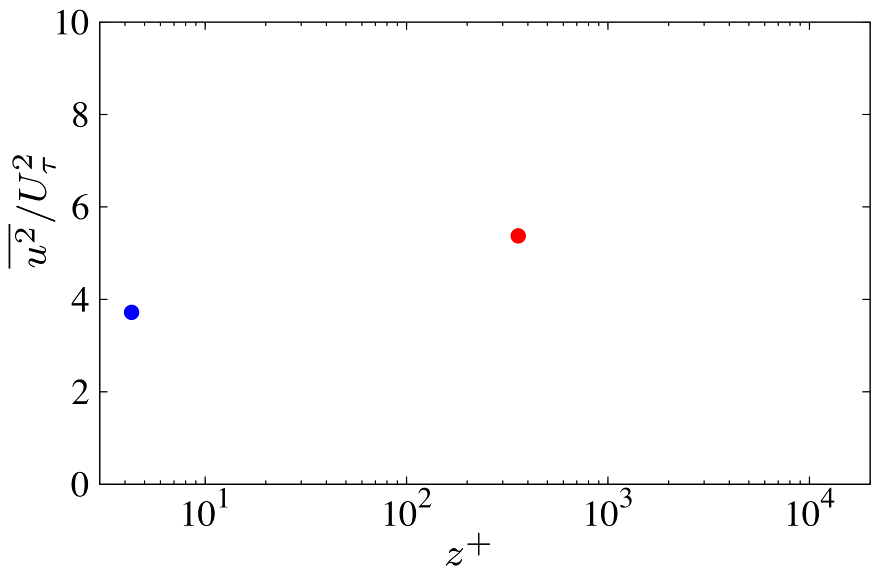

Experimental setup for calibration of the model

Two-point hot-wire simultaneous measurements:
$Re_\tau = 7300$ (arbitrary chosen Reynolds number)
$U_\infty = 10.02$ m/s
$U_\tau = 0.34$ m/s
$\delta = 0.33$
$l^+ = 22$

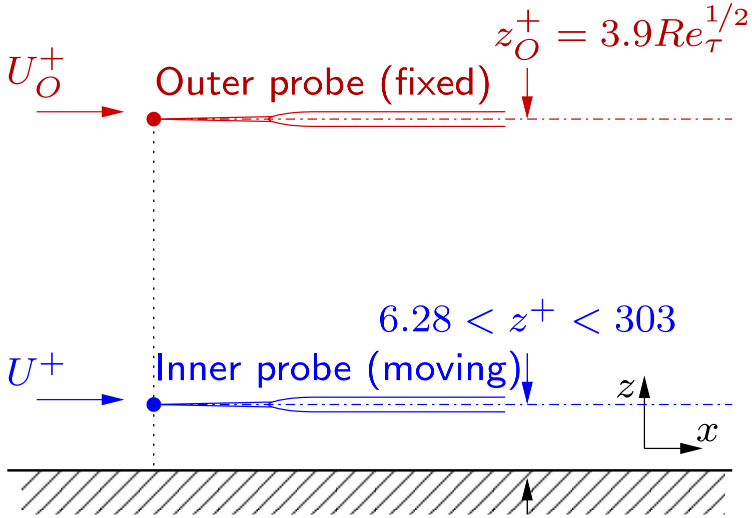

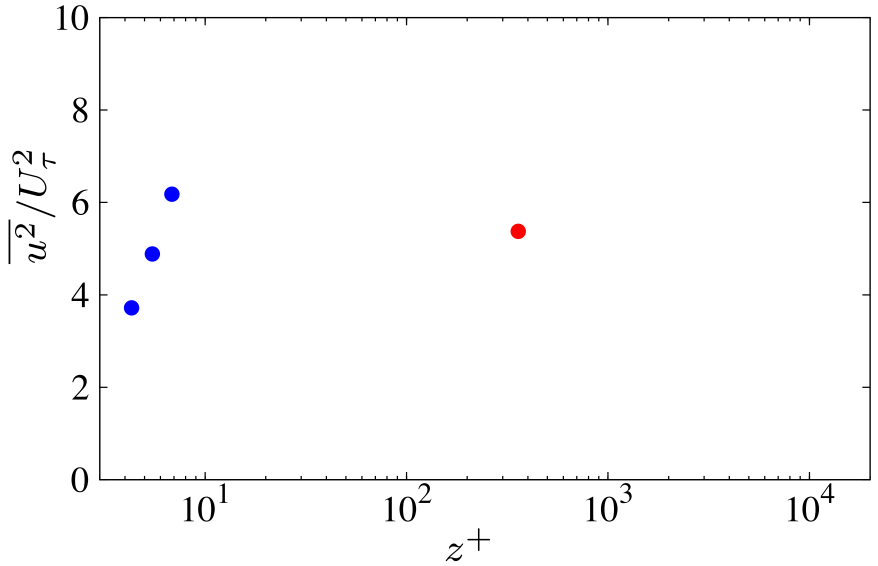

Experimental setup for calibration of the model

Two-point hot-wire simultaneous measurements:
$Re_\tau = 7300$ (arbitrary chosen Reynolds number)
$U_\infty = 10.02$ m/s
$U_\tau = 0.34$ m/s
$\delta = 0.33$
$l^+ = 22$

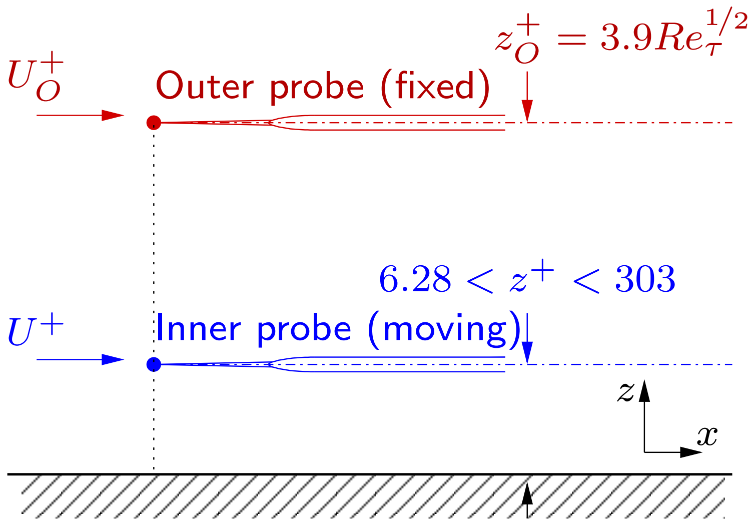

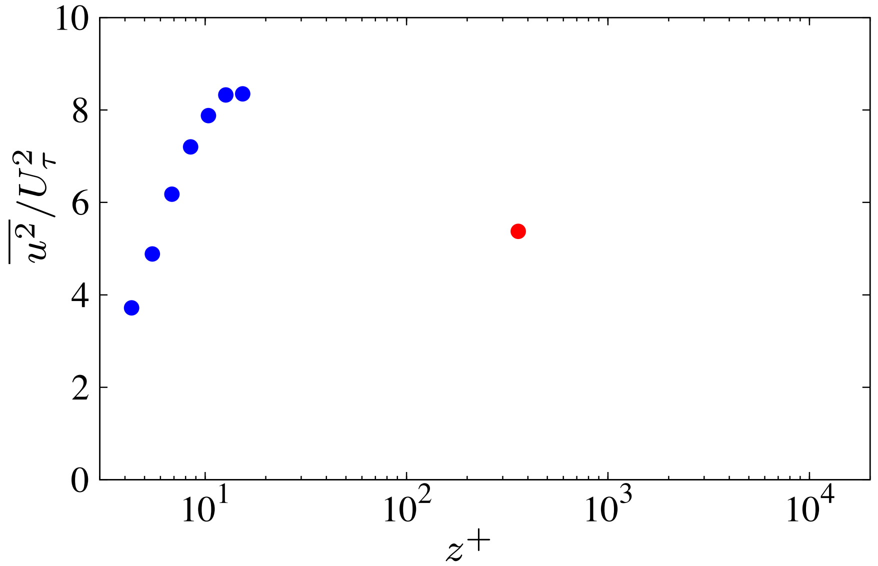

Experimental setup for calibration of the model

Two-point hot-wire simultaneous measurements:
$Re_\tau = 7300$ (arbitrary chosen Reynolds number)
$U_\infty = 10.02$ m/s
$U_\tau = 0.34$ m/s
$\delta = 0.33$
$l^+ = 22$

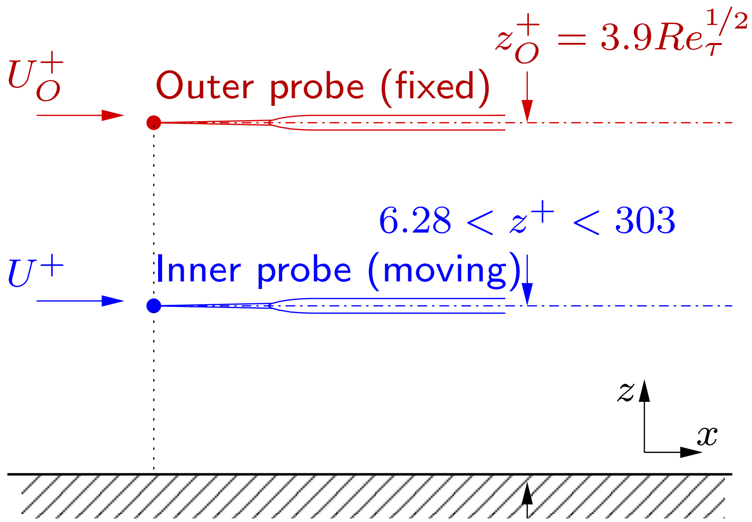

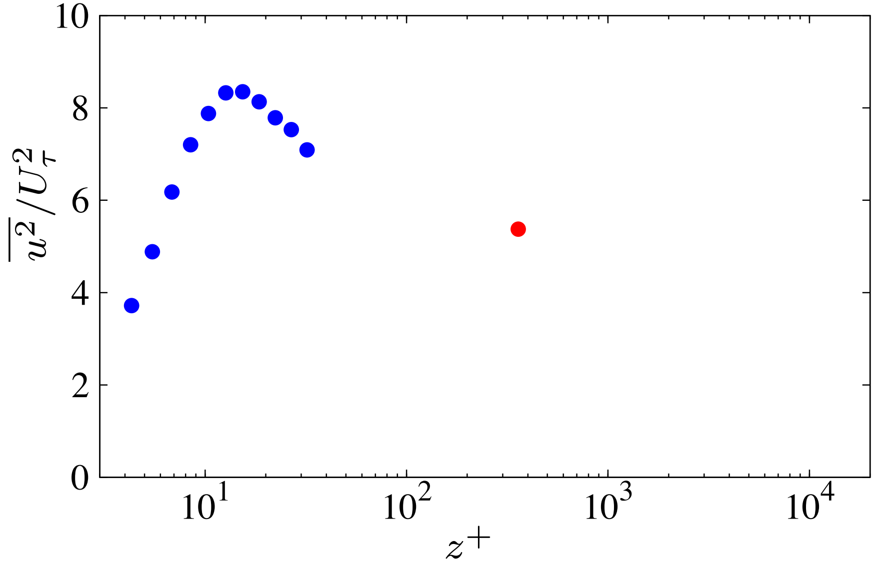

Experimental setup for calibration of the model

Two-point hot-wire simultaneous measurements:
$Re_\tau = 7300$ (arbitrary chosen Reynolds number)
$U_\infty = 10.02$ m/s
$U_\tau = 0.34$ m/s
$\delta = 0.33$
$l^+ = 22$

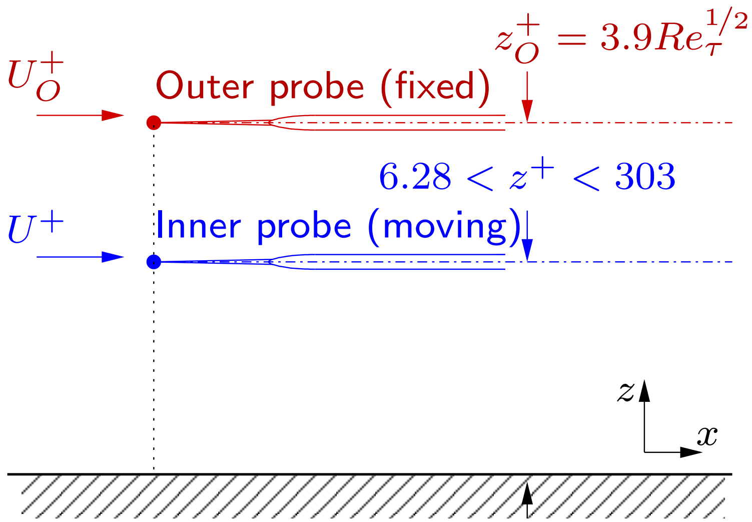

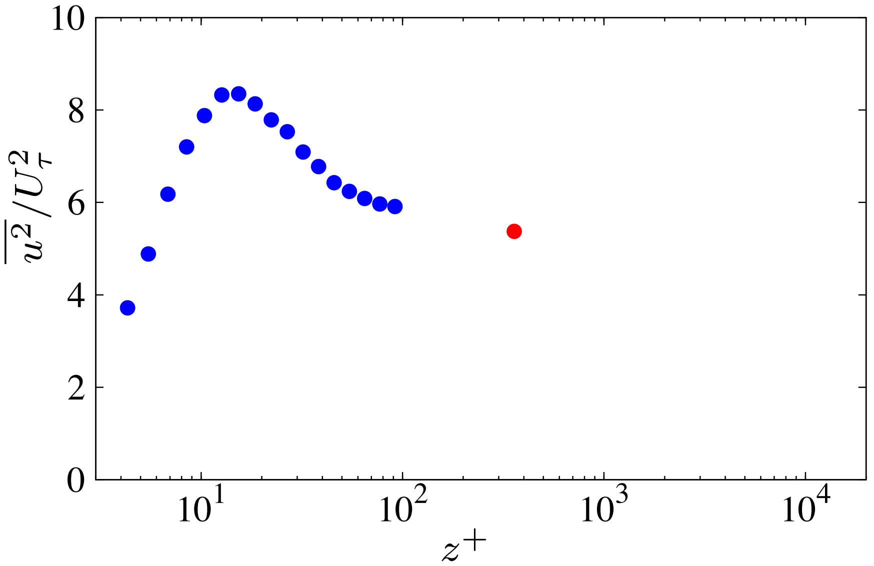

Experimental setup for calibration of the model

Two-point hot-wire simultaneous measurements:
$Re_\tau = 7300$ (arbitrary chosen Reynolds number)
$U_\infty = 10.02$ m/s
$U_\tau = 0.34$ m/s
$\delta = 0.33$
$l^+ = 22$

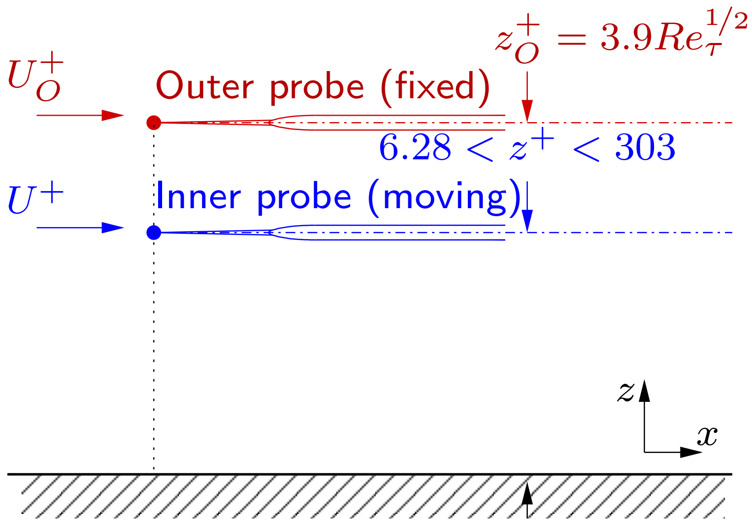

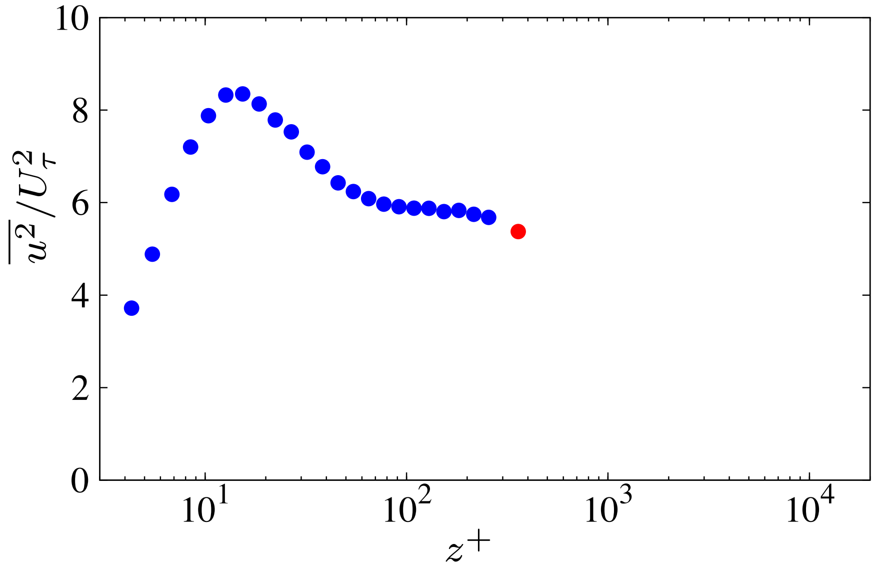

Determination of the model's parameters

$$u^+(z^+) \;=\; u^*(z^+)\;\left[1 + \;\beta\;\; u^+_{LS}\;(z^+_O,\,\theta_{LS}\;)\right] + \;\alpha\;\; u^+_{LS}\;(z^+_O,\,\theta_{LS}\;)$$

calibration measurement

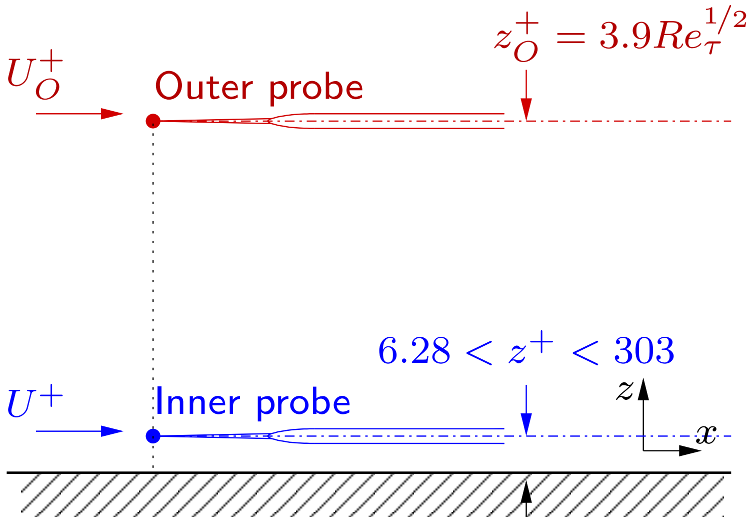

Determination of the model's parameters

$$\boxed{u^+(z^+)} = u^*(z^+) \left[1 + \beta \boxed{u^+_{LS}}(z^+_O, \theta_{LS})\right] + \alpha \boxed{u^+_{LS}}(z^+_O, \theta_{LS})$$

$u^+(z^+)$ and $u^+_{LS}(z^+_O)$ known from the 2 points measurements

calibration measurement

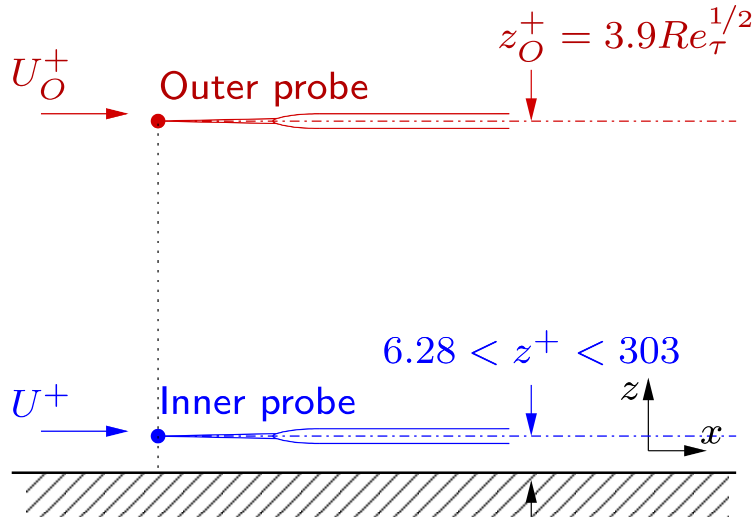

Determination of the model's parameters

$$u^+(z^+) = \boxed{u^*(z^+)} \left[1 + \boxed{\beta}\; u^+_{LS}\left(z^+_O, \boxed{\theta_{LS}}\right)\right] + \boxed{\alpha}\; u^+_{LS}\left(z^+_O, \boxed{\theta_{LS}}\right)$$

$u^+(z^+)$ and $u^+_{LS}(z^+_O)$ known from the 2 points measurements

$u^*(z^+)$, $\alpha(z^+)$, $\beta(z^+)$ and $\theta_{LS}(z^+)$ need to be determined

calibration measurement

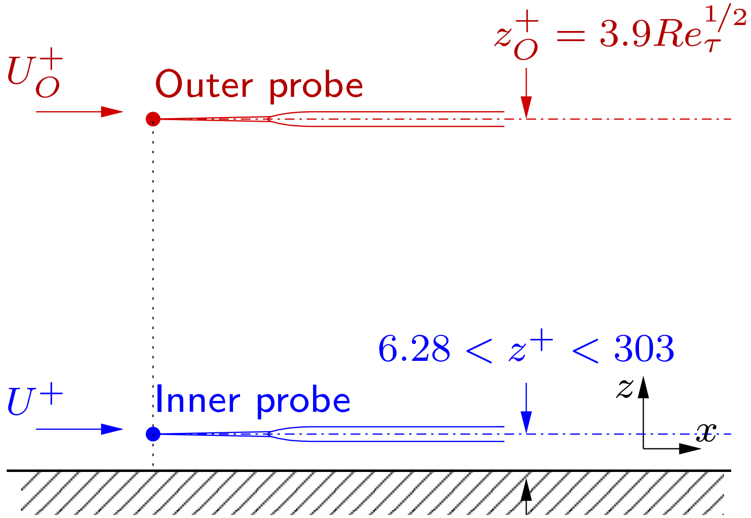

Determination of the model's parameters

$$u^+(z^+) = u^*(z^+)\left[1 + \beta \; u^+_{LS}\left(z^+_O, \theta_{LS}\right)\right] + \alpha \; u^+_{LS}\left(z^+_O, \theta_{LS}\right)$$

$$\alpha(z^+) = \max\left(R_{u^+_{LS}(z^+)u^+_{LS}(z^+_O)}\right)$$ and corresponding $\theta_{LS}(z^+)$

calibration measurement

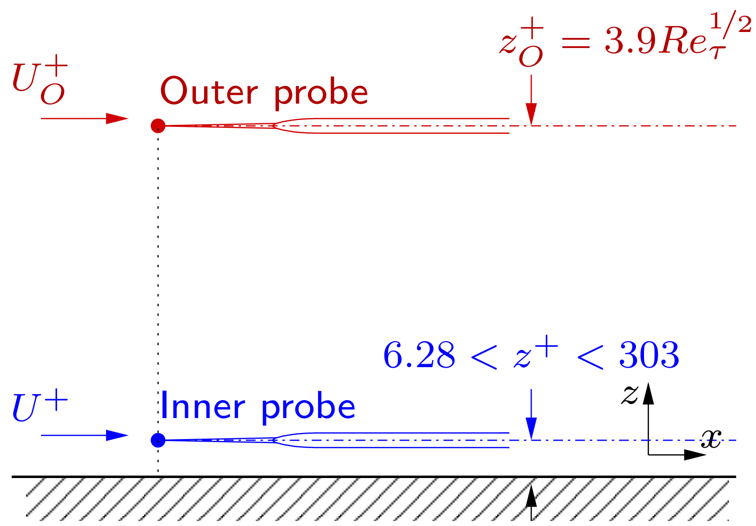

Determination of the model's parameters

$$u^+(z^+) = u^*(z^+)\left[1 + \beta\ u^+_{LS}\left(z^+_O, \boxed{\theta_{LS}}\right)\right] + \boxed{\alpha}\ u^+_{LS}\left(z^+_O, \boxed{\theta_{LS}}\right)$$

$$\alpha(z^+) = \max\left(R_{u^+_{LS}(z^+)u^+_{LS}(z^+_O)}\right)$$ and corresponding $\theta_{LS}(z^+)$

calibration measurement

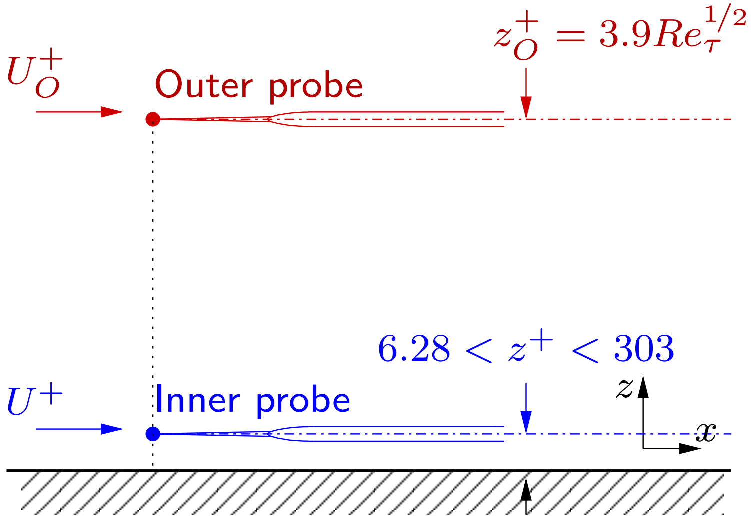

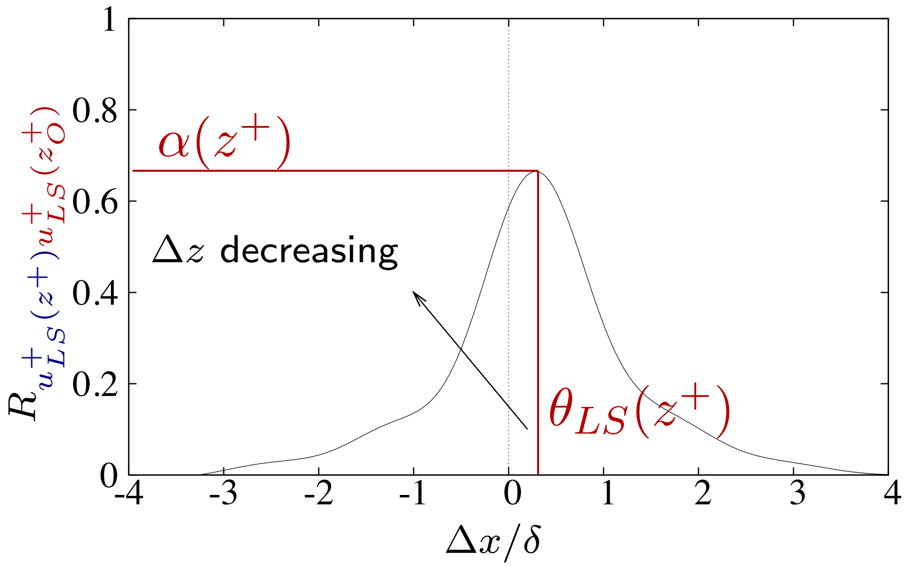

Determination of the model's parameters

$$u^+(z^+) = u^*(z^+)\left[1 + \beta\ u^+_{LS}\left(z^+_O, \theta_{LS}\right)\right] + \alpha\ u^+_{LS}\left(z^+_O, \theta_{LS}\right)$$

$$\alpha(z^+) = \max\left(R_{u^+_{LS}(z^+)u^+_{LS}(z^+_O)}\right)$$ and corresponding $\theta_{LS}(z^+)$

calibration measurement

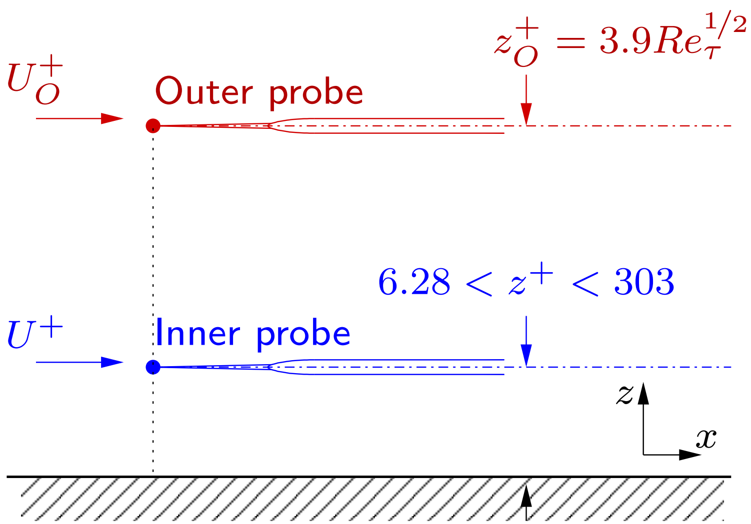

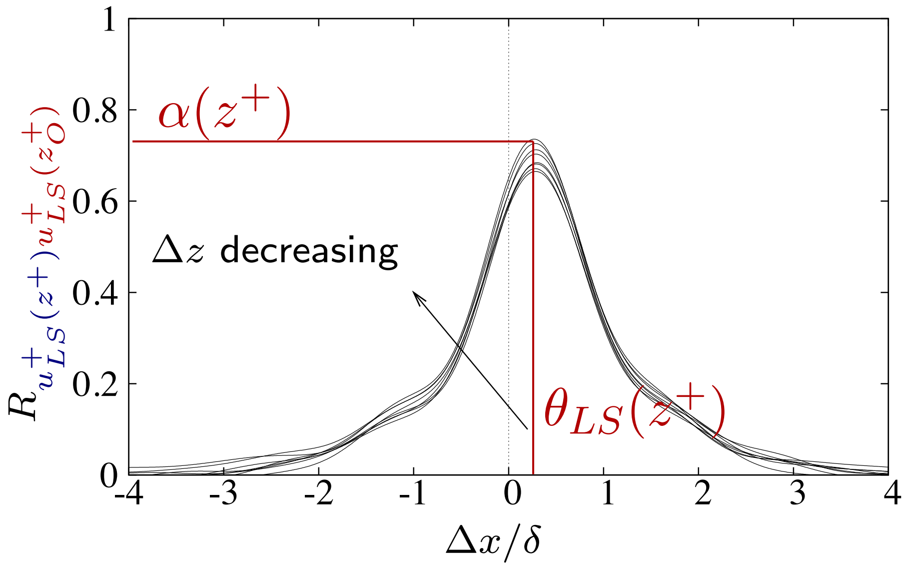

Determination of the model's parameters

$$u^+(z^+) = u^*(z^+)\left[1 + \beta\ u^+_{LS}\left(z^+_O, \theta_{LS}\right)\right] + \alpha\ u^+_{LS}\left(z^+_O, \theta_{LS}\right)$$

$$\alpha(z^+) = \max\left(R_{u^+_{LS}(z^+)u^+_{LS}(z^+_O)}\right)$$ and corresponding $\theta_{LS}(z^+)$

calibration measurement

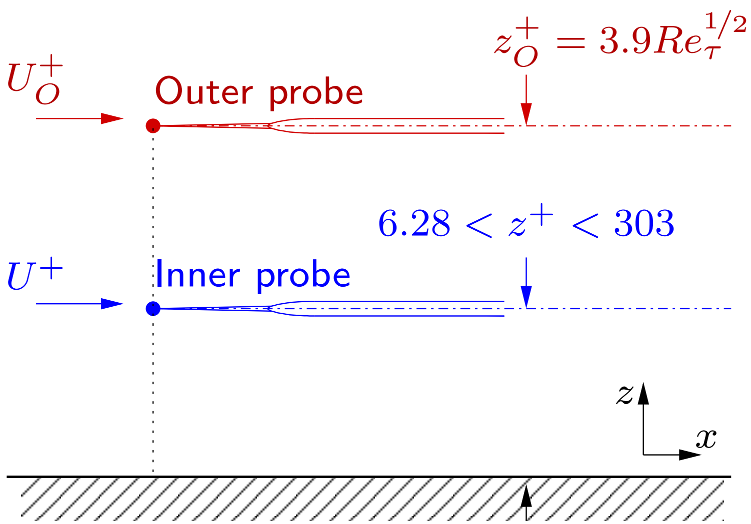

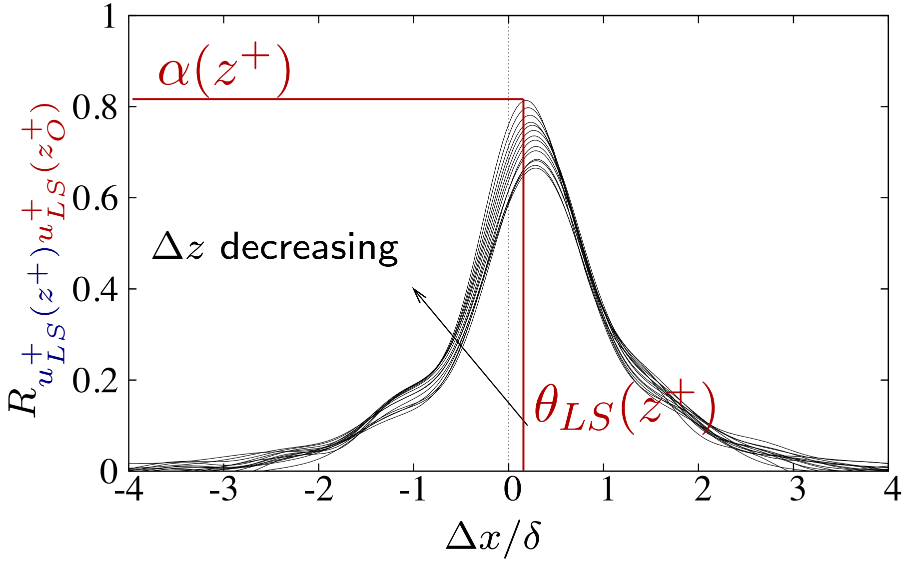

Determination of the model's parameters

$$u^+(z^+) = u^*(z^+)\left[1 + \beta\ u_{LS}^+\left(z_O^+, \boxed{\theta_{LS}}\right)\right] + \boxed{\alpha}\ u_{LS}^+\left(z_O^+, \boxed{\theta_{LS}}\right)$$

$$\alpha(z^+) = \max\left(R_{u_{LS}^+(z^+)u_{LS}^+(z_O^+)}\right)$$ and corresponding $\theta_{LS}(z^+)$

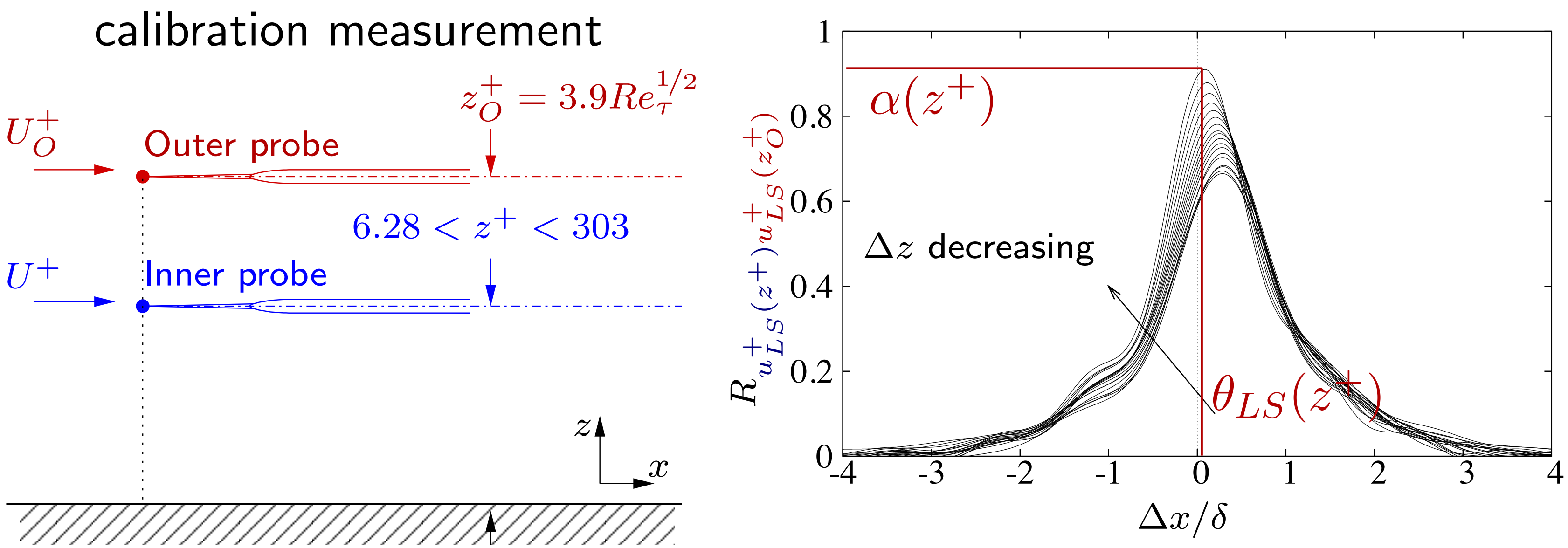

Determination of the model's parameters

$$u^+(z^+) = \boxed{u^*(z^+)}\left[1 + \boxed{\beta}\ u^+_{LS}\left(z^+_O,\ \theta_{LS}\right)\right] + \alpha\ u^+_{LS}\left(z^+_O,\ \theta_{LS}\right)$$

$$u^*\left(z^+\right) = \frac{u^+\left(z^+\right) - \alpha u^+_{LS}\left(z^+_O, \theta_{LS}\right)}{1 + \beta u^+_{LS}\left(z^+_O, \theta_{LS}\right)}, \qquad \beta \text{ such as } \mathrm{AM}(u^*) = 0$$

calibration measurement

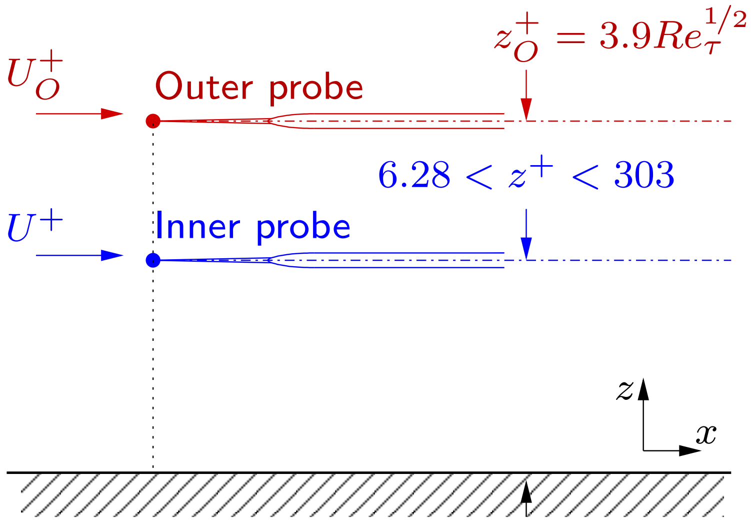

Pre-multiplied energy spectra map reconstruction

$$\tilde{u}^+(z^+) = u^*(z^+)\left[1 + \beta u^+_{LS}\left(z^+_O, \theta_{LS}\right)\right] + \alpha u^+_{LS}(z^+_O, \theta_{LS})$$

Single-point hot-wire measurements:
$Re_\tau = 2800$
$U_\infty = 11.97$ m/s
$U_\tau = 0.44$ m/s
$\delta = 0.01$ m
$l^+ = 22$

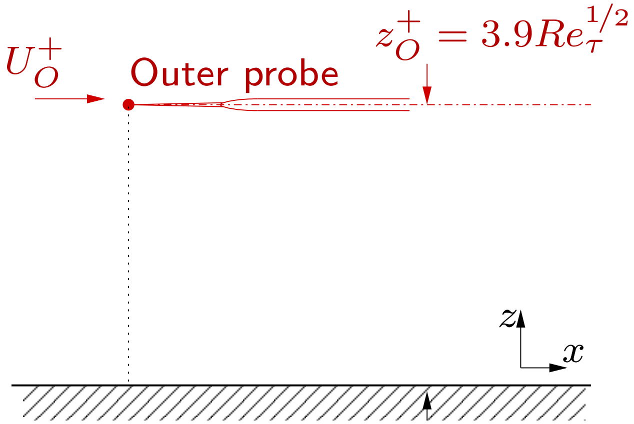

Pre-multiplied energy spectra map reconstruction

$$\tilde{u}^+(z^+) = u^*(z^+)\left[1 + \beta u_{LS}^+\left(z_O^+, \theta_{LS}\right)\right] + \alpha u_{LS}^+(z_O^+, \theta_{LS})$$

Single-point hot-wire measurements:
$Re_\tau = 2800$
$U_\infty = 11.97$ m/s
$U_\tau = 0.44$ m/s
$\delta = 0.01$ m
$l^+ = 22$

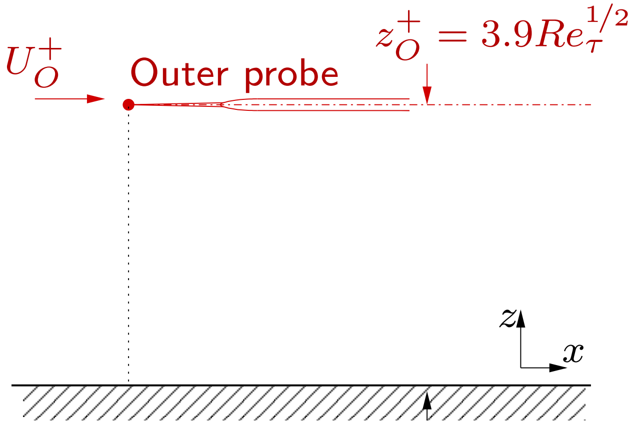

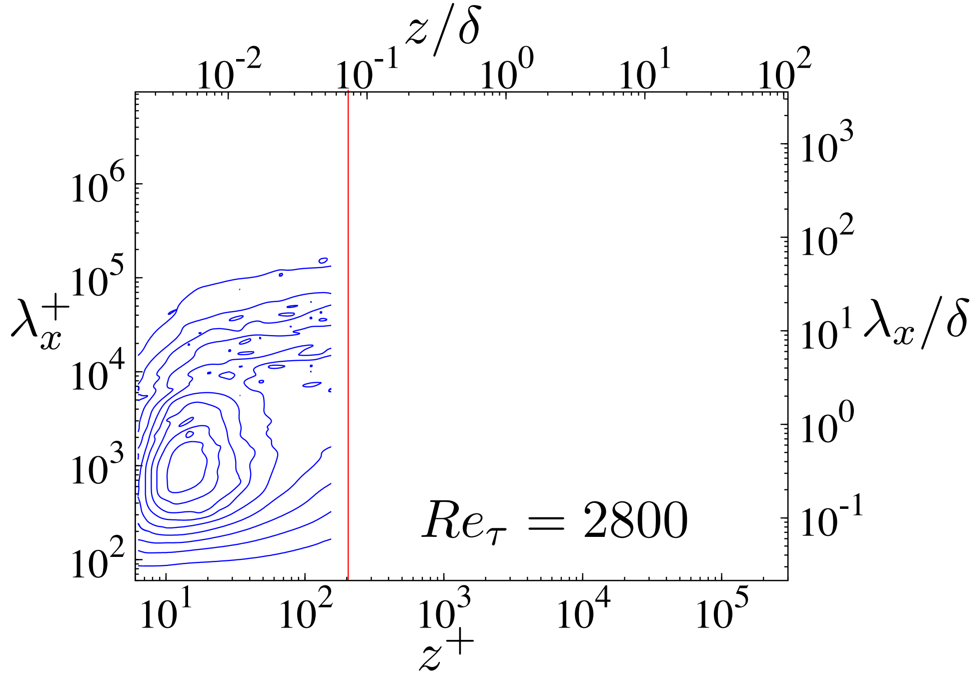

Pre-multiplied energy spectra map reconstruction

$$\tilde{u}^+(z^+) = u^*(z^+)\left[1 + \beta u^+_{LS}\left(z^+_O, \theta_{LS}\right)\right] + \alpha u^+_{LS}(z^+_O, \theta_{LS})$$

Single-point hot-wire measurements:
$Re_\tau = 2800$
$U_\infty = 11.97$ m/s
$U_\tau = 0.44$ m/s
$\delta = 0.01$ m
$l^+ = 22$

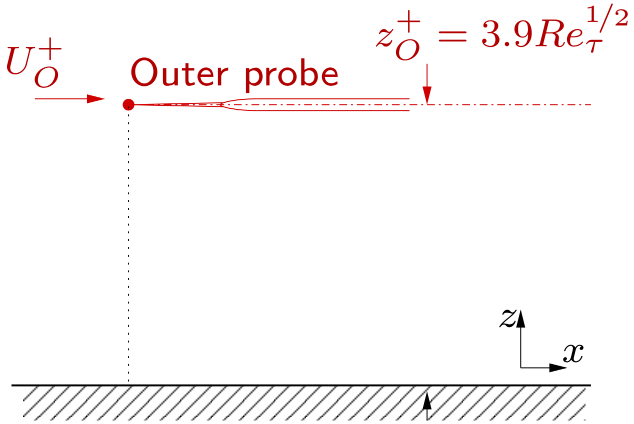

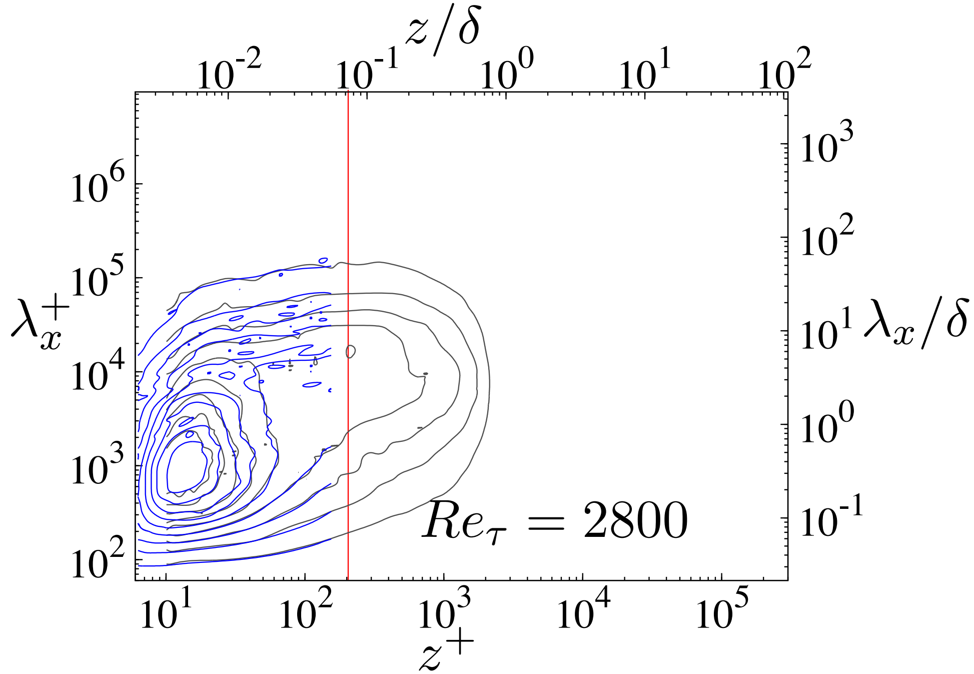

Pre-multiplied energy spectra map reconstruction

$$\tilde{u}^+(z^+) = u^*(z^+)\left[1 + \beta u^+_{LS}\left(z^+_O, \theta_{LS}\right)\right] + \alpha u^+_{LS}(z^+_O, \theta_{LS})$$

Single-point hot-wire measurements:
$Re_\tau = 3900$
$U_\infty = 11.87$ m/s
$U_\tau = 0.43$ m/s
$\delta = 0.14$ m
$l^+ = 21$

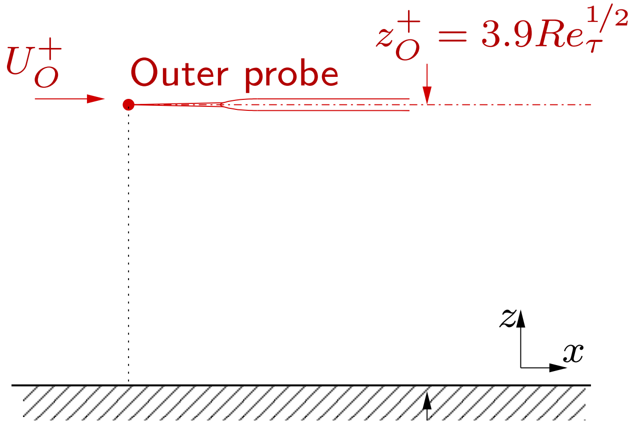

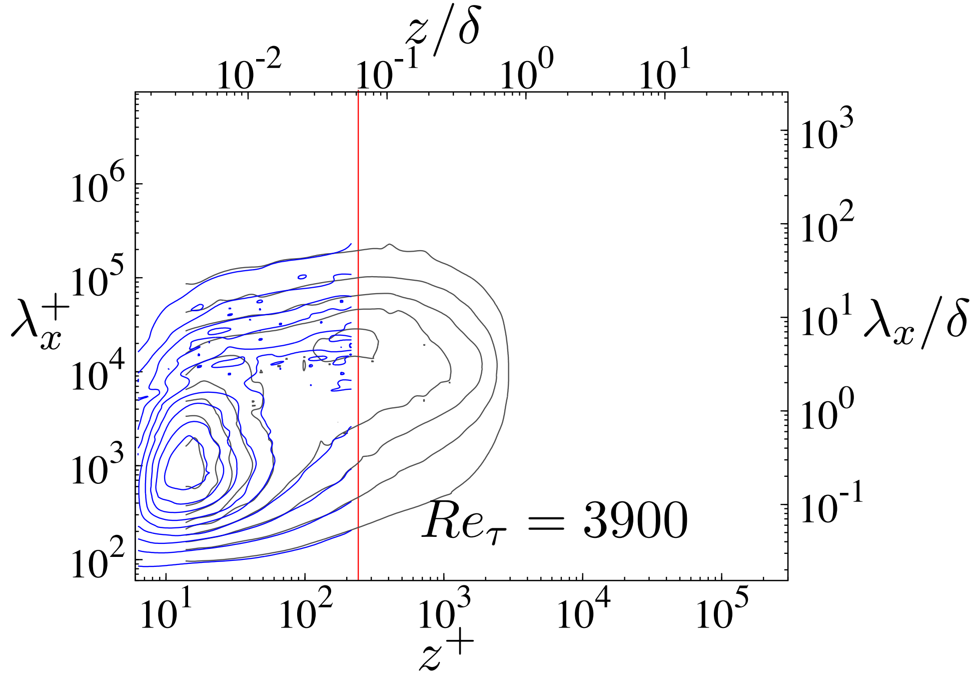

Pre-multiplied energy spectra map reconstruction

$$\tilde{u}^+(z^+) = u^*(z^+)\left[1 + \beta u_{LS}^+\left(z_O^+, \theta_{LS}\right)\right] + \alpha u_{LS}^+(z_O^+, \theta_{LS})$$

Single-point hot-wire measurements:
$Re_\tau = 7350$
$U_\infty = 10.03$ m/s
$U_\tau = 0.32$ m/s
$\delta = 0.33$ m
$l^+ = 23$

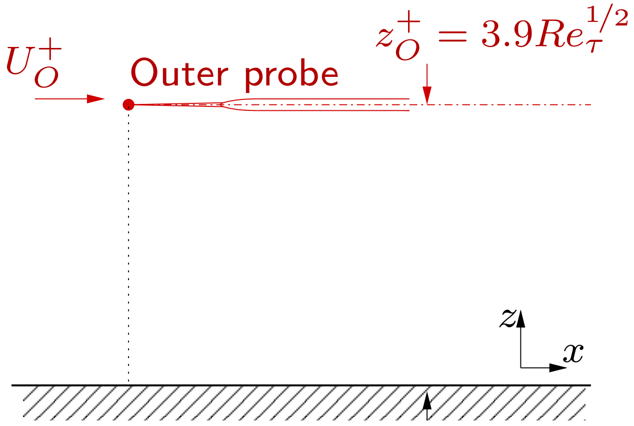

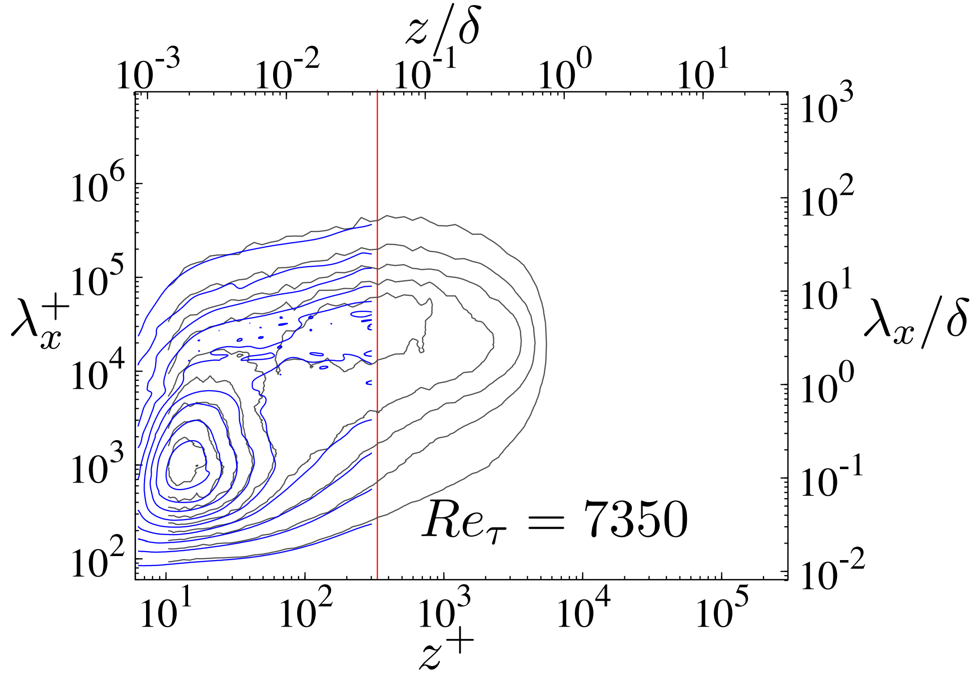

Pre-multiplied energy spectra map reconstruction

$$\tilde{u}^+(z^+) = u^*(z^+)\left[1 + \beta u^+_{LS}\left(z^+_O, \theta_{LS}\right)\right] + \alpha u^+_{LS}(z^+_O, \theta_{LS})$$

Single-point hot-wire measurements:
$Re_\tau = 13600$
$U_\infty = 20.63$ m/s
$U_\tau = 0.67$ m/s
$\delta = 0.31$ m
$l^+ = 22$

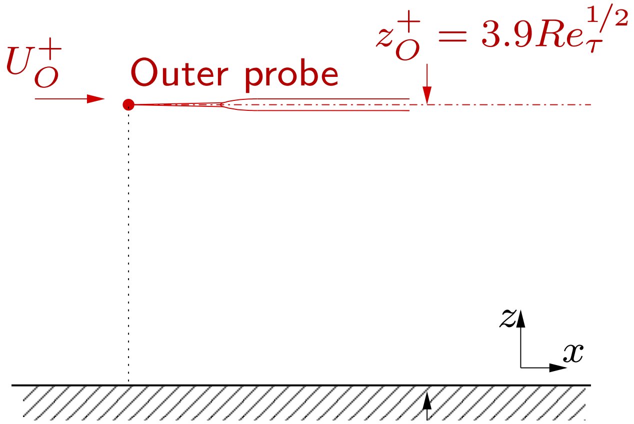

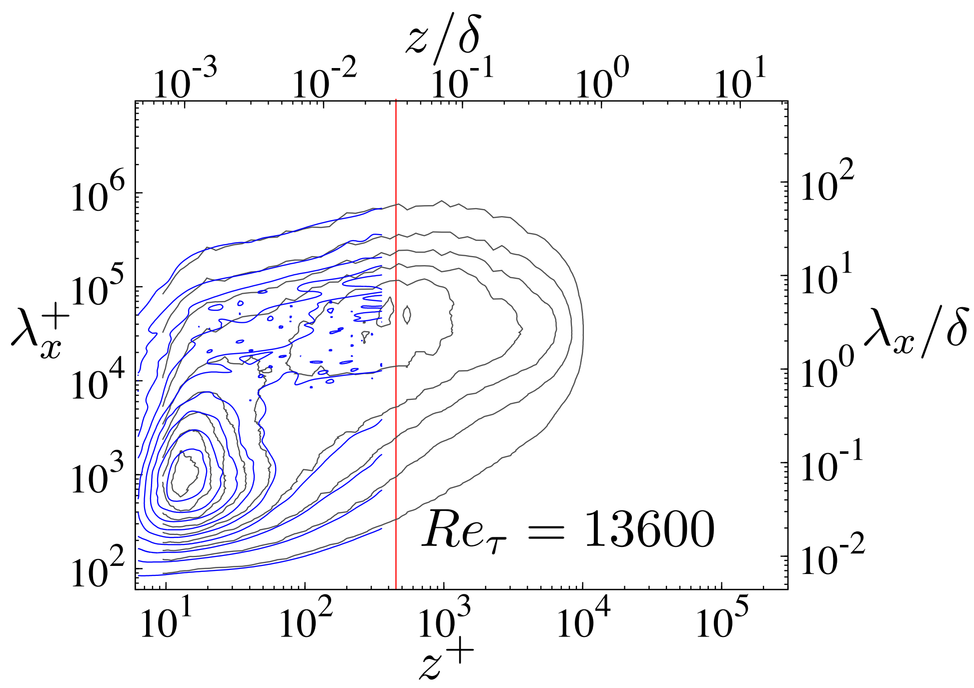

Pre-multiplied energy spectra map reconstruction

$$\tilde{u}^+(z^+) = u^*(z^+)\left[1 + \beta u^+_{LS}\left(z^+_O, \theta_{LS}\right)\right] + \alpha u^+_{LS}(z^+_O, \theta_{LS})$$

Single-point hot-wire measurements:
$Re_\tau = 19000$
$U_\infty = 30.20$ m/s
$U_\tau = 0.96$ m/s
$\delta = 0.30$ m
$l^+ = 22$

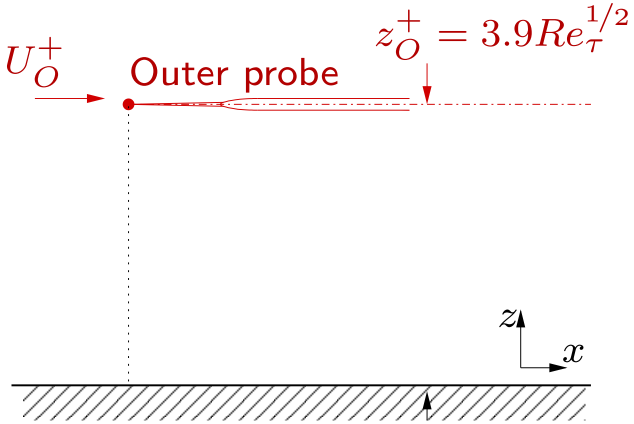

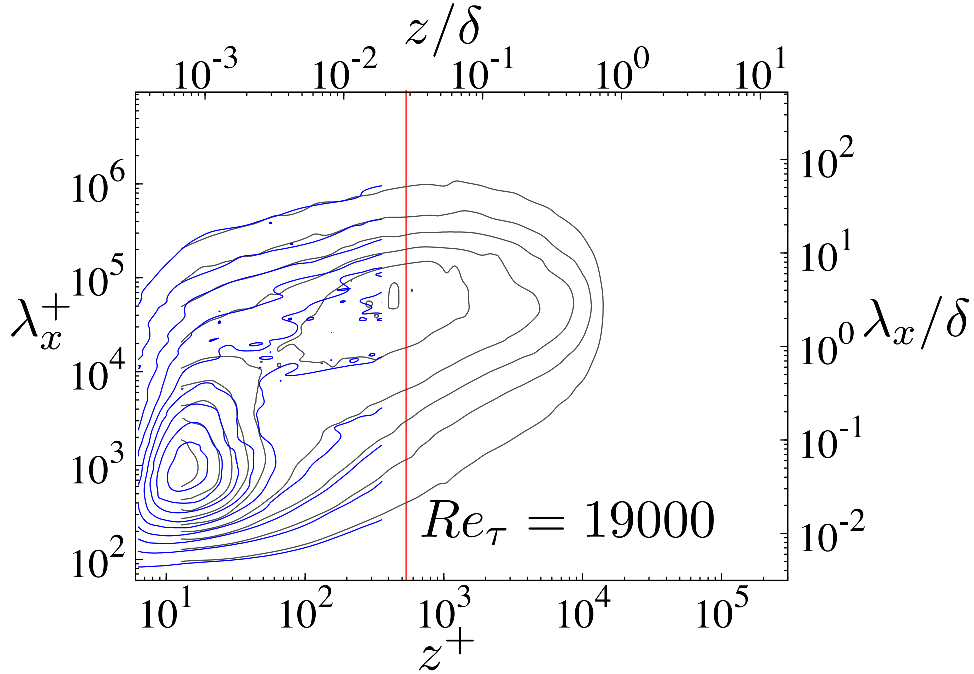

Pre-multiplied energy spectra map reconstruction

$$\tilde{u}^+(z^+) = u^*(z^+)\left[1 + \beta u^+_{LS}\left(z^+_O, \theta_{LS}\right)\right] + \alpha u^+_{LS}(z^+_O, \theta_{LS})$$

Single-point sonic anemometer measurements:
$Re_\tau = 1.4 \times 10^6$
U_∞ unknown
$U_\tau = 0.26$ m/s
$\delta \simeq 100$ m

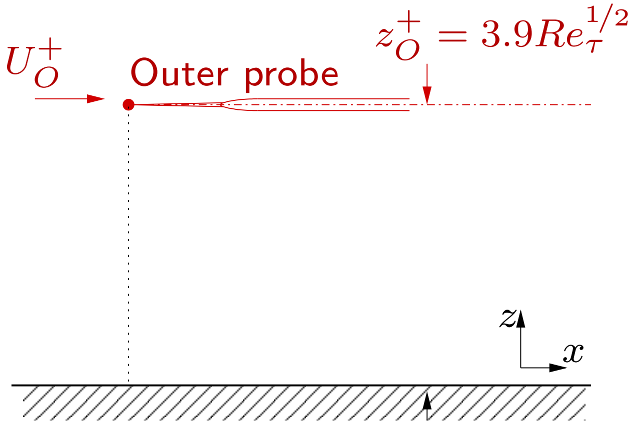

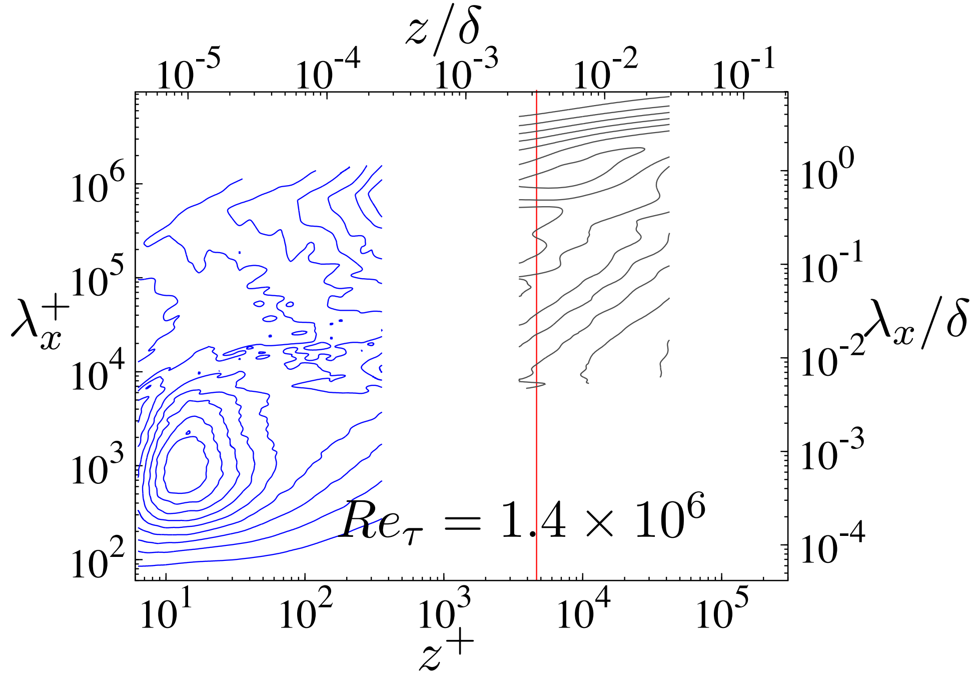

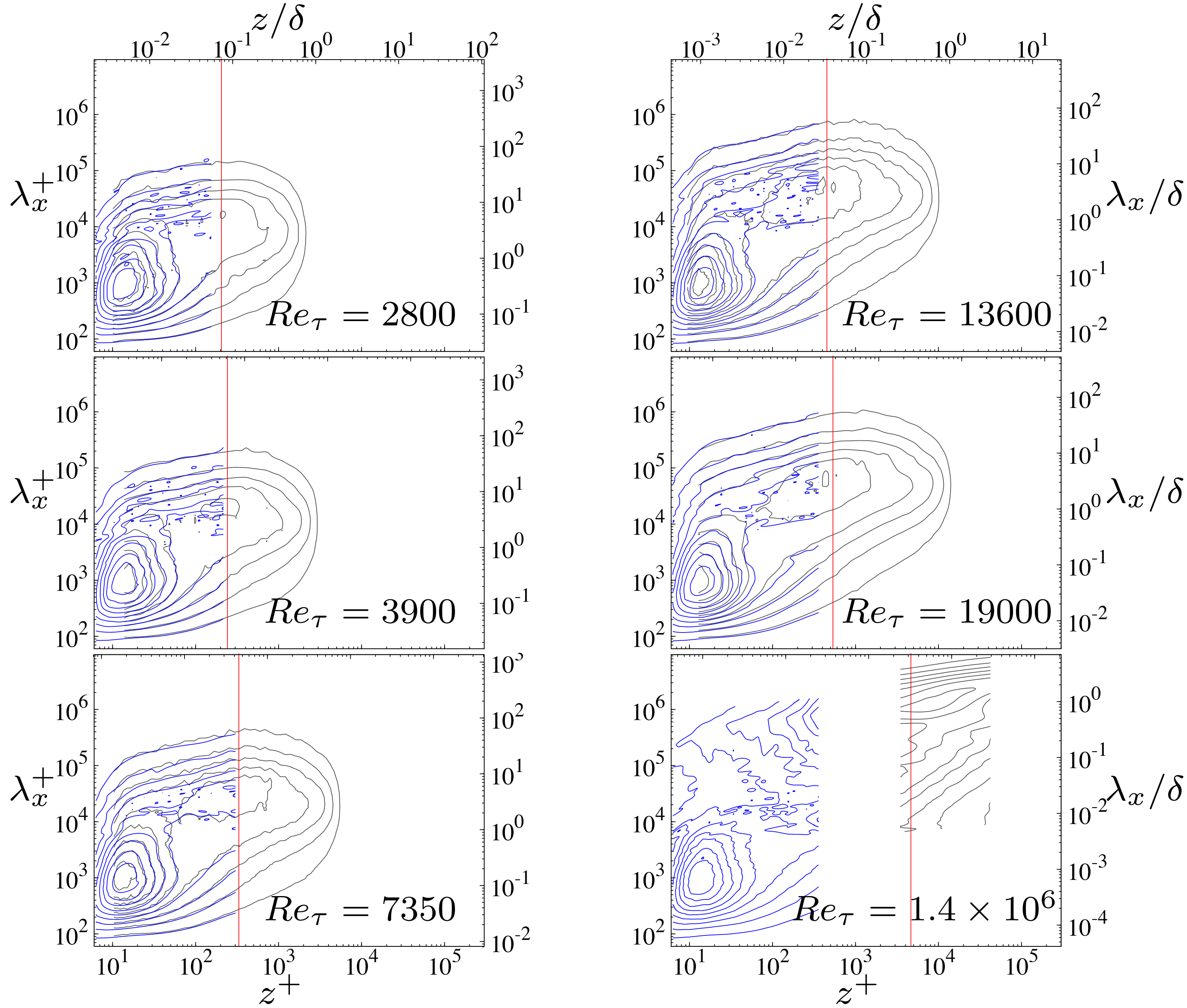

z/δ
λ_x^+
λ_x/δ
$Re_\tau = 2800$
$Re_\tau = 13600$
$Re_\tau = 3900$
$Re_\tau = 19000$
$Re_\tau = 7350$
$Re_\tau = 1.4 \times 10^6$
z^+

Statistics

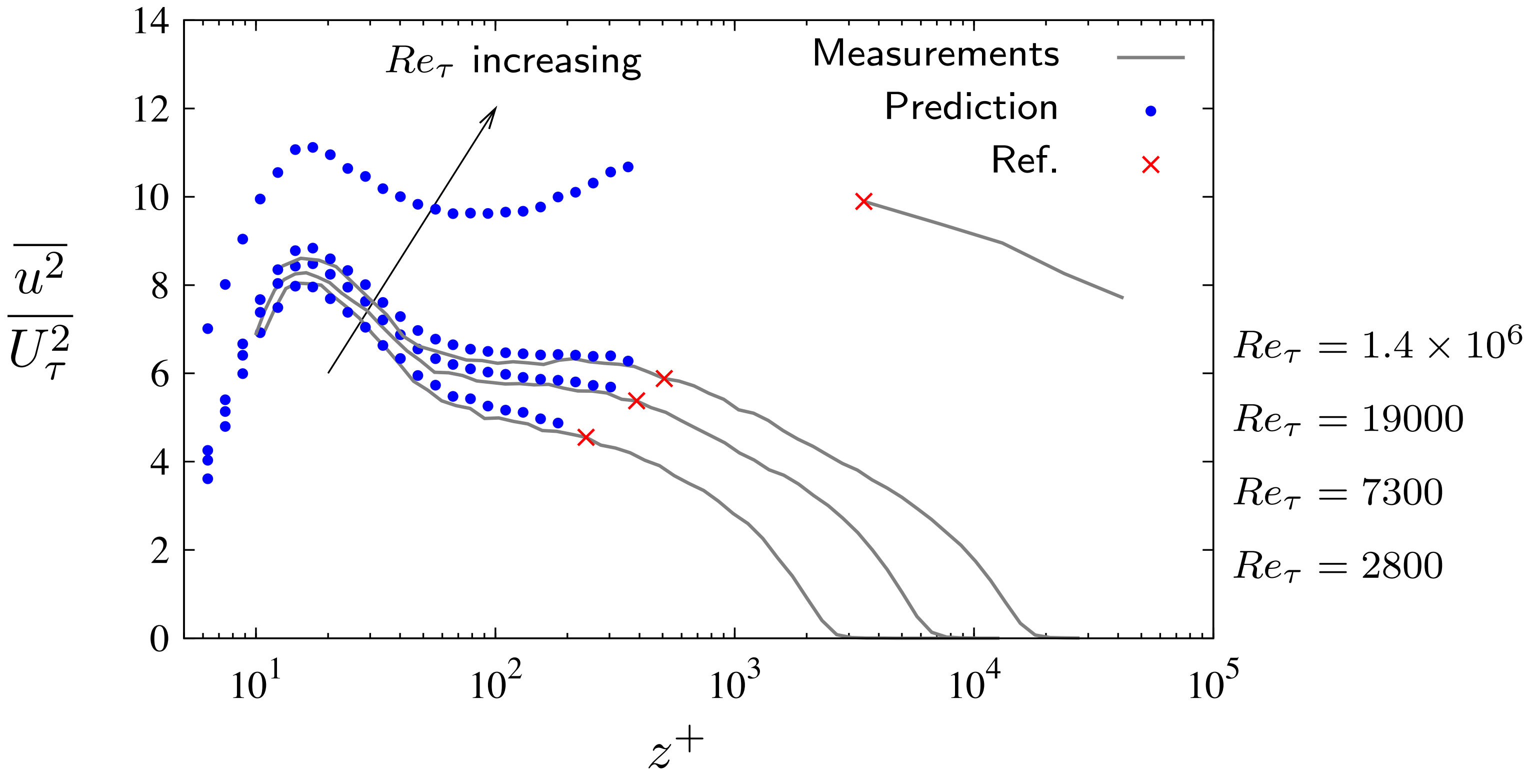

Re_τ increasing
Measurements
Prediction
Ref.
$\frac{\overline{u^2}}{\overline{U_\tau^2}}$
z^+
$Re_\tau = 1.4 \times 10^6$
$Re_\tau = 19000$
$Re_\tau = 7300$
$Re_\tau = 2800$

Statistics

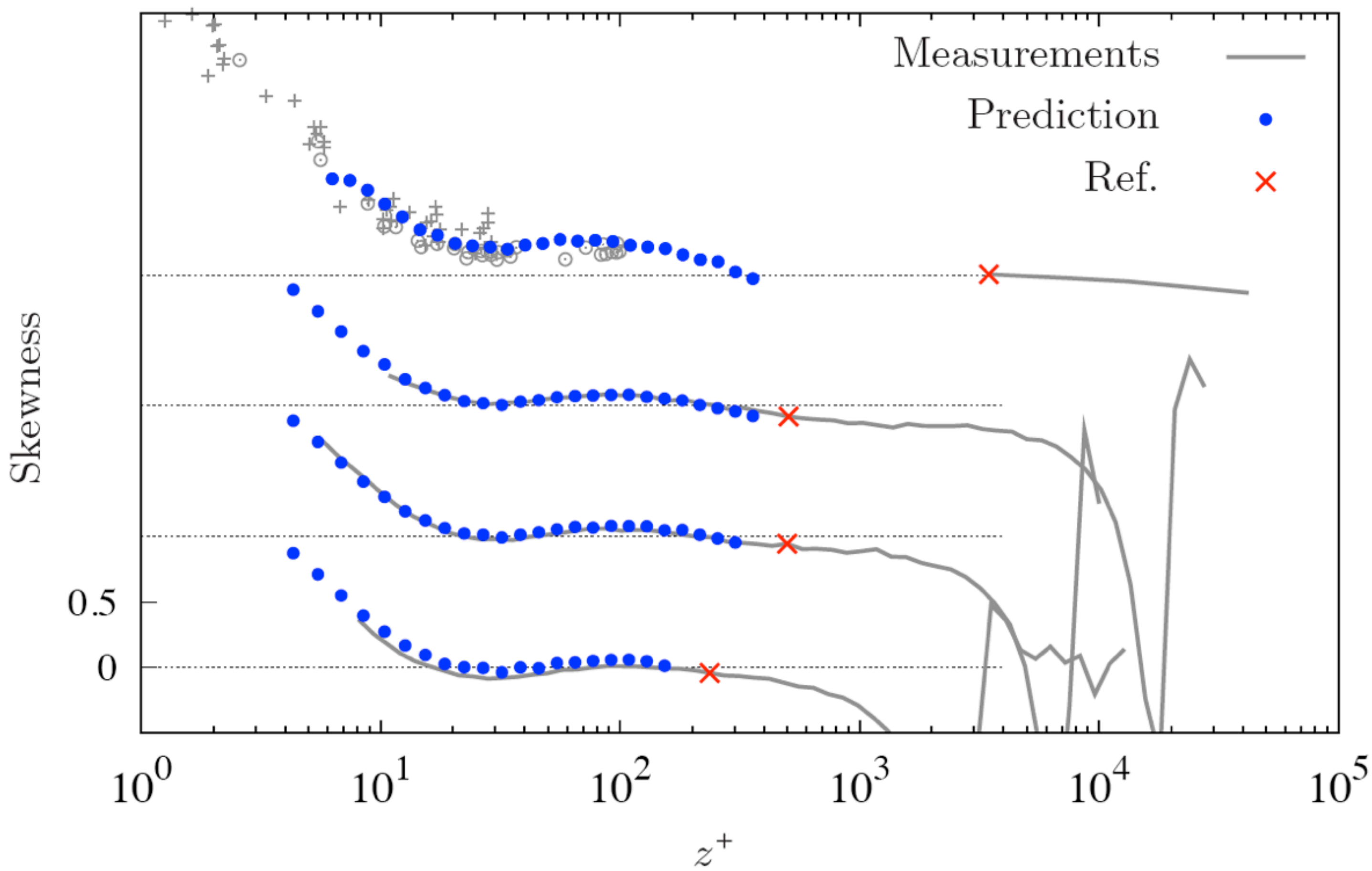

Measurements
Prediction
Ref.
Skewness
0.5
0
10^0
10^1
10^2
10^3
10^4
10^5
z^+

Statistics

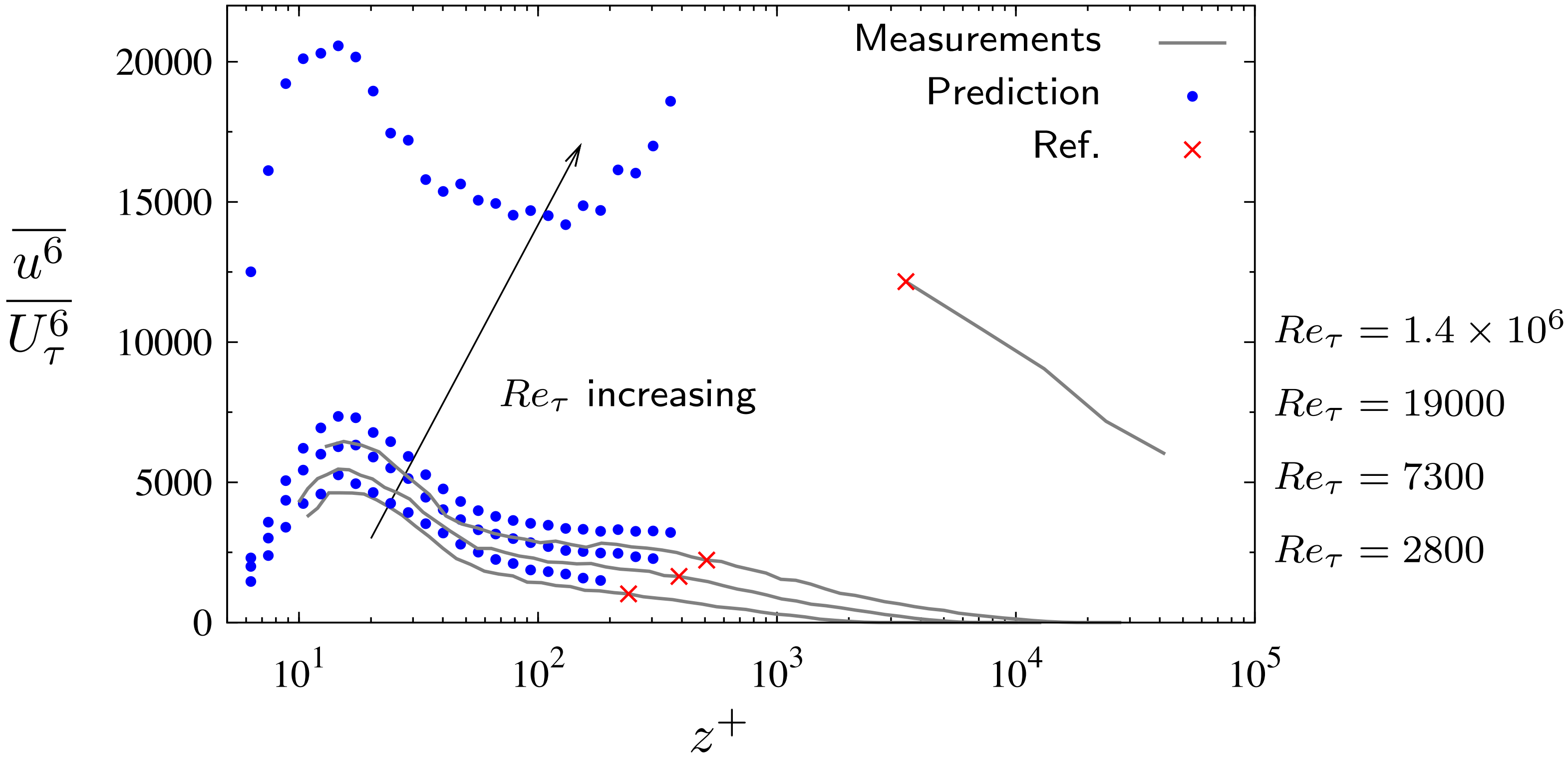

Measurements
Prediction
Ref.
20000
15000
10000
5000
0
$\frac{\overline{u^6}}{U_\tau^6}$
Re_τ increasing
10^1
10^2
10^3
10^4
10^5
z^+
$Re_\tau = 1.4 \times 10^6$
$Re_\tau = 19000$
$Re_\tau = 7300$
$Re_\tau = 2800$

Prediction for other wall-bounded flows

Channel, Pipe, APG-TBL and ZPG-TBL comparison

- Four different flow geometries (all in Melbourne)
  - Zero-Pressure-Gradient Turbulent Boundary Layer (ZPG-TBL)
  - Adverse-Pressure-Gradient Turbulent Boundary Layer (APG-TBL)
  - Channel
  - Pipe
- Kármán number $Re_\tau \simeq 3000 - 3500$

Facility	Re_τ	U_∞ (m/s)	δ (m)	ν/U_τ (μm)	l^+
ZPG-TBL	3020	12.5	0.10	33.2	30
APG-TBL	3510	17.1	0.10	32.1	16
Channel	3015	23.1	0.05	16.7	30
Pipe	3005	24.3	0.05	16.4	30

Prediction for other wall-bounded flows

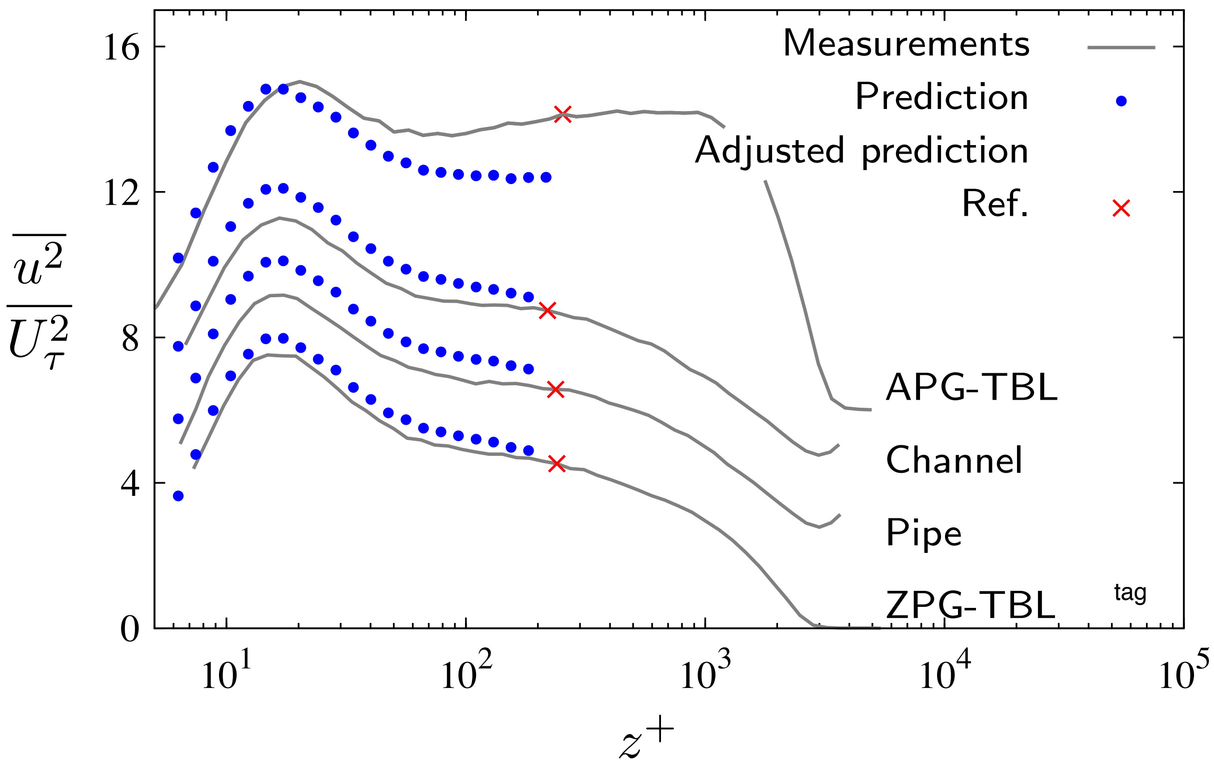

Prediction for other wall-bounded flows

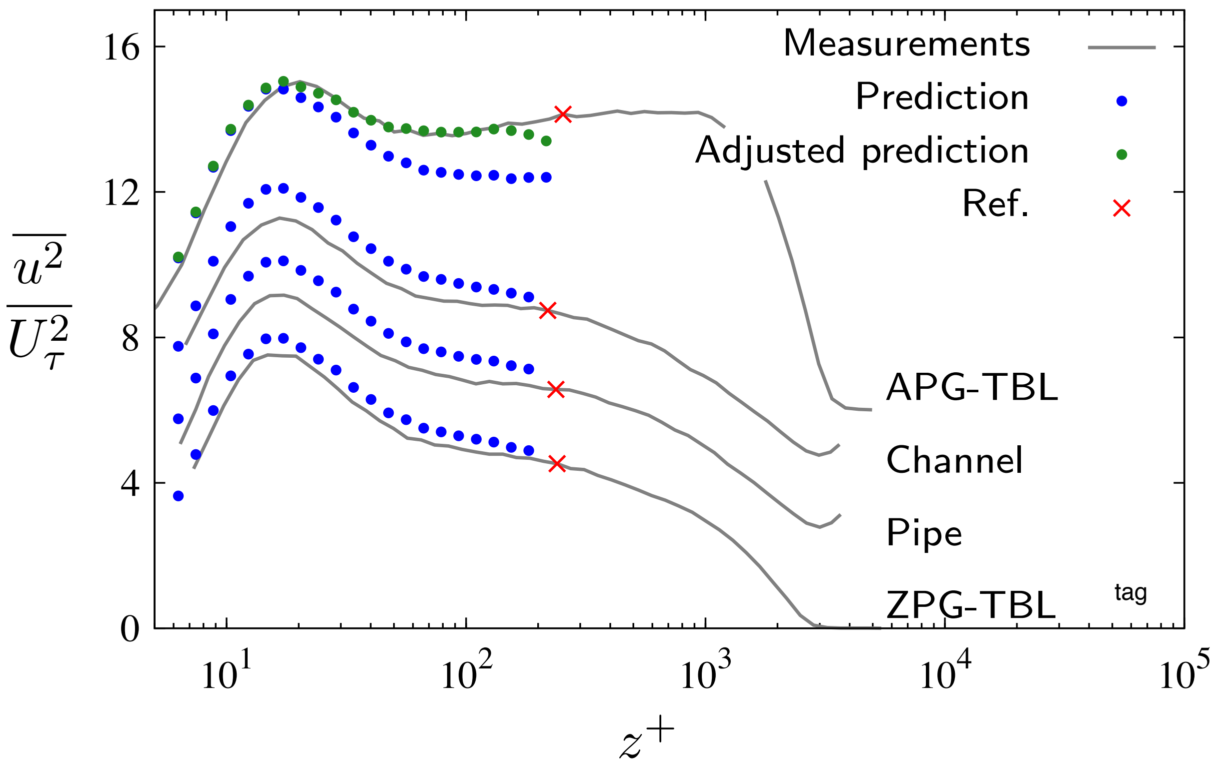

Adjustment of β and α:

$$\tilde{u}^+(z^+) = u^*(z^+)\left[1 + \beta u^+_{LS}\left(z^+_O, \theta_{LS}\right)\right] + \alpha u^+_{LS}(z^+_O, \theta_{LS})$$

Prediction for other wall-bounded flows

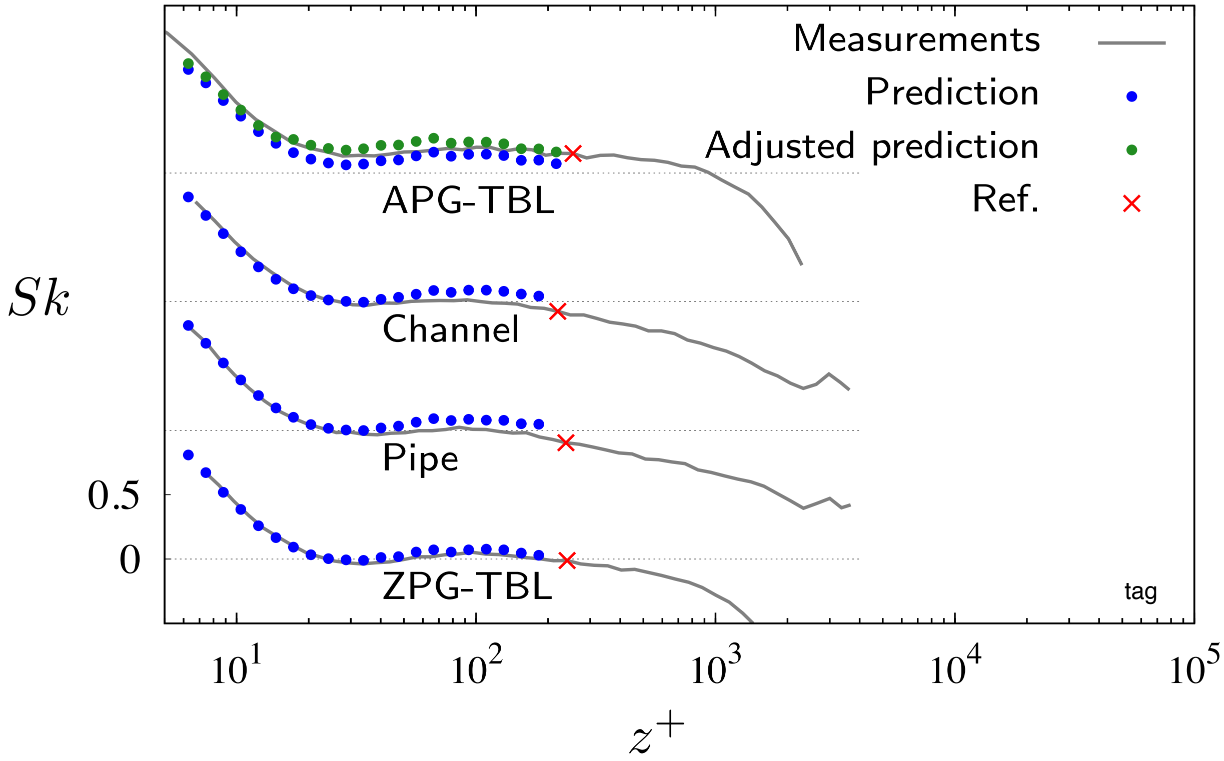

Adjustment of β and α:

$$\tilde{u}^+(z^+) = u^*(z^+)\left[1 + \beta u^+_{LS}\left(z^+_O, \theta_{LS}\right)\right] + \alpha u^+_{LS}(z^+_O, \theta_{LS})$$

Prediction for other wall-bounded flows

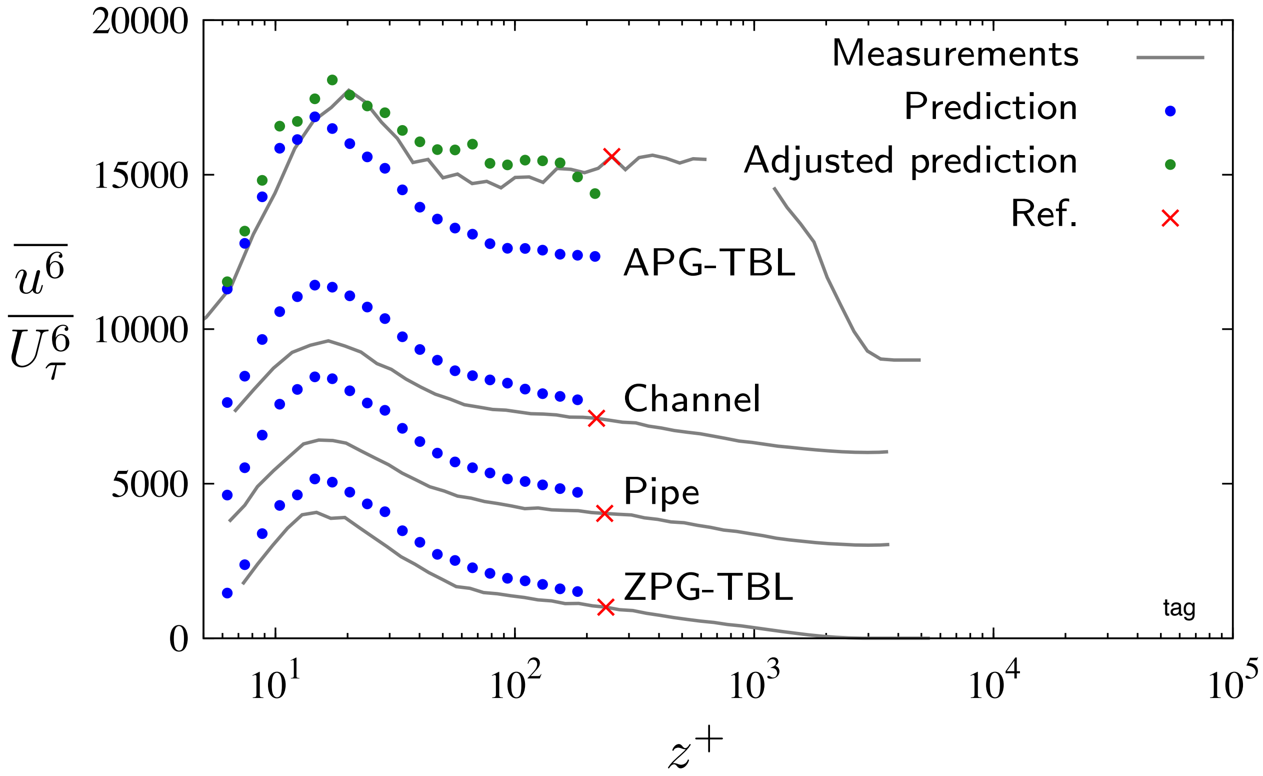

Adjustment of β and α:

$$\tilde{u}^+(z^+) = u^*(z^+)\left[1 + \beta u^+_{LS}\left(z^+_O, \theta_{LS}\right)\right] + \alpha u^+_{LS}(z^+_O, \theta_{LS})$$

Other considerations / future directions

Uniform momentum zones in wall turbulence (consistent with packets of eddies)

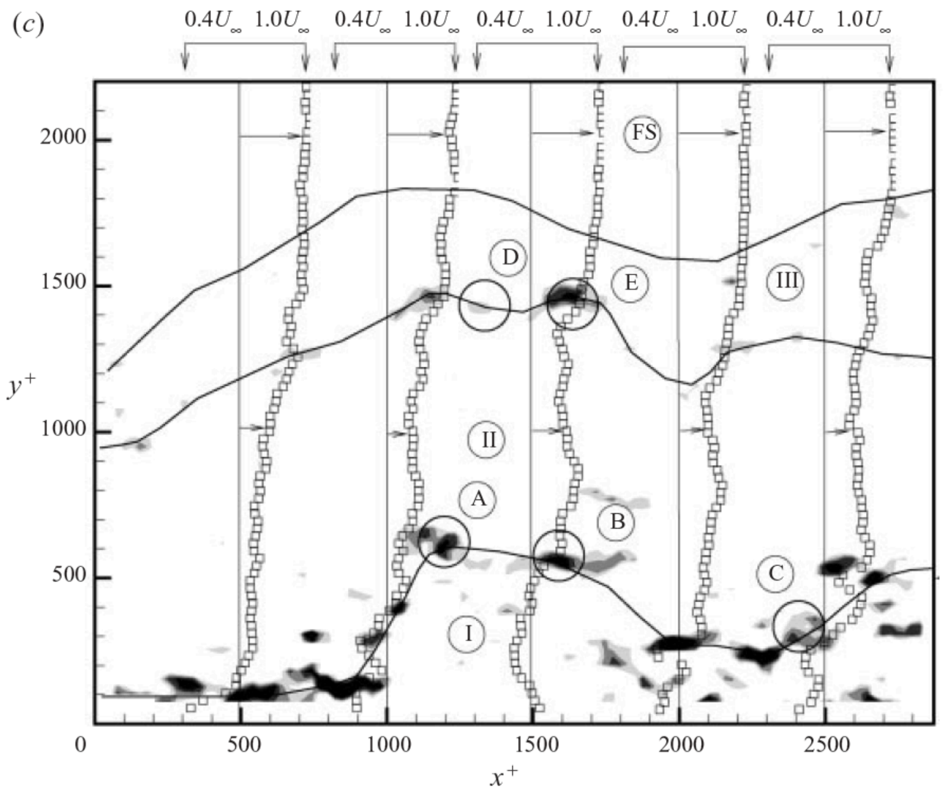

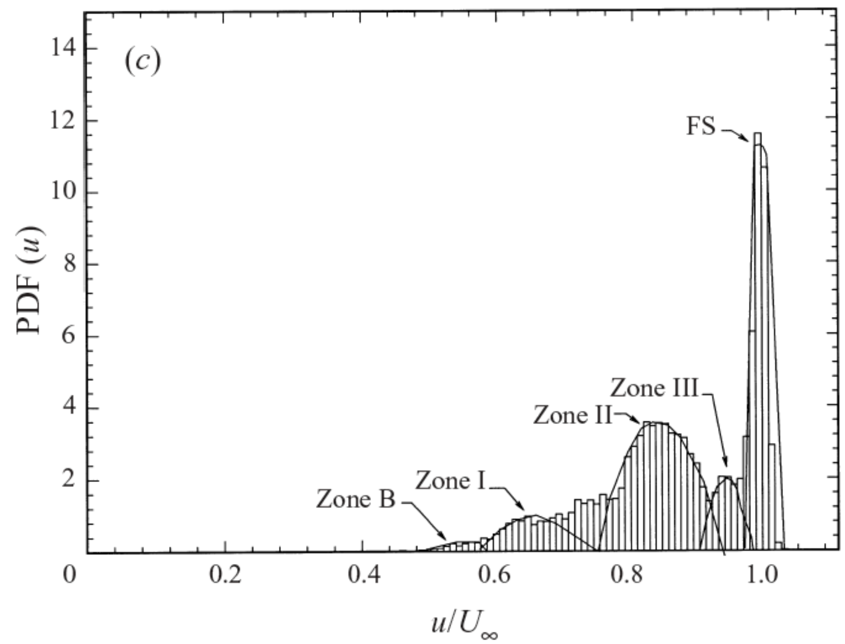

Modelling approaches beyond Reynolds decomposition?

Conclusions / Comments

- Coherent eddy structure concepts helpful for modelling the energy-containing, heterogeneous, motions in turbulence. But, this is still at a rudimentary stage and recent experiments (looking at 2D/3D fields) have been important in shaping our view of the what the important eddies are and how they interact across the flow.

- Superstructures or very-large-scale motions play a key role in the dynamics of wall turbulence.

- The results support the concept of a universal inner-region that is modified through a modulation and superposition of the large-scale outer motions, which are specific to the geometry or imposed streamwise pressure gradient acting on the flow. Predictive (non-linear) model based on these observations is seen to work well.

- Next step is to integrate a dynamical causality to the kinematics. Evidence of modulation is felt to be an important clue towards this aim.

- Is it worthwhile rethinking Reynolds decomposition (cf something between RANS and LES) ?